

Dear Editor and Reviewers,

Please find below our response to reviewers' comments, followed by the revised versions of the manuscript, with the first showing the final text and the second version containing track changes. We would like to thank the reviewers for the constructive suggestions and we sincerely hope they will find our reply satisfactory.

Sincerely,

M. Tedesco and co-authors.

Anonymous Referee #1

Received and published: 7 December 2015

This study explores observed and modeled trends in albedo of the Greenland Ice Sheet. Significant darkening is observed during the last 30+ years, though the trends are confined to the ablation and melt zones of the ice sheet. Modeling studies are applied to attribute causes of the observed trends. One of the chief causes was determined, largely through elimination of other potential causes, to be exposure of buried impurities, a process that is not represented in the model that was applied (MAR). Overall, this is an informative and comprehensive study that pursues multiple lines of reasoning and analysis to narrow down possible causes of the darkening. The paper is very well-written and logically organized. The comments included below are generally minor, and I see no major hurdles for publication in The Cryosphere.

Major comments:

A closely related study that explores recent (2001-2013) albedo change in the dry snow zone of Greenland was recently published in Geophysical Research Letters (Polashenski et al, doi: 10.1002/2015GL065912). Consistent with this study, Polashenski et al concluded that recent changes in deposition of dust or black carbon could not be causing substantial surface darkening trends in the dry snow zone, and furthermore that a substantial portion of the trend in dry zone albedo seen in MODIS data is actually an artifact associated with degradation of the MODIS Terra sensor. It would be helpful to cite this study in the context of (e.g.,) discussions in section 3.4.1, section 5 paragraph 1, and perhaps in Conclusions.

R: Thanks for the suggestion. We included the reference as requested and added the text in the Discussion section.

The description of AEROCOM model results (section 3.4.1 and Figure 6) and application of these results to exclude a significant aerosol deposition trend, need improvement. Specifically:

- **The description beginning on p.5609, line 12 describes AEROCOM outputs from 14 global models, but text later in this paragraph suggests that only one model (the GISS ModelE) was actually used in the analysis. Is this correct? Similarly, the Figure 6 caption indicates "AEROCOM standardized deposition fluxes", but it is**

not clear if all 14 AEROCOM models were used here or only the GISS model. Results from 1 model are obviously less robust than results from 14 models. If only one model was used in this analysis, the description should be amended to refer to the GISS ModelE, rather than AEROCOM suite of models.

R: Thanks. We indeed used only the outputs of the NASA GISS ModelE. We modified the text and the caption accordingly.

- p.5609: Please mention the range of years that were simulated in these runs, whether or not interannually-varying aerosol emission inventories were used for the simulations, and whether or not interannually-varying sea surface temperatures were used to drive the model(s). All of these details influence the usefulness of this model analysis for determining whether or not real trends in aerosol deposition have occurred on the ice sheet.

R: Detailed information about the simulations is reported in the many publications associated with the AeroComm project, some of which cited in the text. We think that it is better for the reader to refer to those for gathering a more complete information on the details of those simulations.

- section 3.4.2: As the authors note, the lack of trends in MODIS fire counts is not necessarily an indication of trends in fire-derived aerosol emissions. For example, fires could have become more intense, larger, and/or more persistent (longer duration), despite exhibiting no trend in count. The authors also state "Notably, we were not able to find studies specifically looking at trends in boreal forest fire emissions". To derive a more meaningful assessment of boreal fire emission trends, the authors could analyze satellite-derived black carbon emissions data from either the Global Fire Emissions Database (GFED) (<http://www.globalfiredata.org/>), and/or the Fire Inventory from NCAR (FINN) (<http://bai.acom.ucar.edu/Data/fire/>), both of which are gridded datasets that are freely available for download via the URLs listed above.

R: Thanks for the suggestion. We have indeed inserted a new figure (and relative text) containing the analysis of the BC emissions from the GFED dataset. In view of this, we have also re-organized the corresponding sections.

Finally, it is somewhat unusual for a co-author to post a comment asking for clarification on his or her own paper. This may indicate that more communication between the co-authors is needed.

R: Thanks for this comment. The co-author is new to the mechanism. I agree that more communication should have happened. The co-author has been removed from the authors' list as his contribution has been removed from the text, following the suggestions from both reviewers.

Minor comments:

abstract, line 21: "known underestimates in projected melting": I suggest inserting "past" before "projected", or changing "projected" to "hindcasted".

R: thanks. We changed 'projected' to 'hindcasted'.

5599,10: "... recent work assessing simulated albedo over Greenland..." - It would be helpful to provide a clue to the reader here that a discussion of this evaluation is presented later in the manuscript.

R: Done, thanks.

5600,26: "between" -> "Between"

R: that sentence appears truncated in the final pdf but the word 'between' should not be capitalized as it is part of the previous sentence. We found the presence of a Tab in the Word document that suggested the Copernicus system to jump to a new line.

5601,2: "In MAR these values of albedo are set to 0.65 and 0.55" - If any observational studies were used to justify these choices, please cite them.

R: The original values were suggested by Lefebvre and others cited in the references. No observational study has been used though work is underway to do so.

Equation 6: This implies that an infinitely thick melt pond would have an albedo of 0.40. Should the albedo instead asymptote towards something more like 0.07, the albedo of open water?

R: Yes, that is correct. Currently, the MAR model does not handle melt ponds based on their depth but it distributes the surface water evenly within the area of the pixel. This aspect needs to be addressed and it has been part of a recently proposed project to the National Science Foundation by the lead author.

5601,22: "... the albedo in MAR is a weighted, vertically-averaged value of snow albedo and ice albedo" - Please provide an equation or reference that describes this weighting. In particular, the meaning of "vertically-averaged", in the context of surface albedo, is unclear to me.

R: The weighting is performed by averaging the snow and ice albedo proportionally to the thickness of the snow and ice layer within the top 10 cm (e.g., if snow depth is 3 cm then albedo is obtained by multiplying the snow albedo by 0.3 and adding the ice albedo multiplied by 0.7). We added the sentence in the parenthesis in the text.

5602,1: "in which case the albedos of snow and ice are adjusted based on the cloud fraction modelled by MAR." - This implies that the spectral weights shown in Equation 1 are adjusted for cloudiness (correct?). If so, I suggest clarifying precisely how this is achieved, perhaps earlier in the text where Equation 1 is described. If the technique is described in another paper it may be adequate to simply reference that paper.

R: We added the reference to the paper. Thanks for pointing this out.

5602,16: Is "GLASS-MODIS" any different than "MODIS" albedo (e.g., product MCD43C)? If so, how is it different? If not, I suggest simply referring to this as "MODIS". Either way, please list the MODIS albedo or reflectance product and version/collection from which GLASS is derived.

1 *R: We would rather to keep the naming of 'MODIS-GLASS' albedo to remain consistent with*
2 *the terminology. We also added two new referencse (Zhao et al., 2013and Ying et al., 2014) in*
3 *which the GLASS processing system and products are described.*

4 **5603,9: "MODIS and GLASS" -> "MODIS and GLASS albedo"**

5 *R: changed, thanks.*

6 **5604,20: "Notably, strong negative summer snowfall anomalies from 2010 to 2012 are**
7 **simulated by MAR..." - Are these strong anomalies also present in station data and/or re-**
8 **analysis data?**

9 *R: We did not check for this but we will be doing so shortly. Still, we don't plan to include such*
10 *analysis in the current version of the manuscript as it is not a major point of our paper.*

11 **5606,10: "summer albedo from GLASS decreased..." - And by how much did MAR albedo**
12 **decrease over this time period? It would be helpful to include this in the paper.**

13 *R: We added this information in the text.*

14 **5606,17: "This hypothesis is supported..." - Did Wientjes (2011) argue that *recent***
15 **increases in dust deposition to this region of the ice sheet have led to significantly decreased**
16 **albedo, or that exposure of dust deposits buried long ago have led to the albedo decrease? It**
17 **seems that only the latter would be consistent with the main explanation put forth in this**
18 **paper. Please clarify.**

19 *R: Thanks, we removed this sentence following the request from the other reviewer.*

20 **5612,7: "info" -> "in"**

21 *R: Done.*

22 **5614,14: "oft he" -> "of the"**

23 *R: Done.*

24 **5616,8: "The MACC model shows no significant trend..." - And does the GOCART model**
25 **show a significant trend?**

26 *R: We revised the sentence to include the statistical significance of both.*

27 **5616,11: "Neither model captures trends in exposed silt/dust" - In fact, neither model even**
28 **represents this process, much less captures the trend.**

29 *R: We modified the sentence to point to the fact that the processes are not captured.*

30 **5617,22-29: The relevance of these results is a bit unclear to me. In fact, I think the whole**
31 **discussion contained in this paragraph could be shortened, as readers may get bogged down**

1 in this discussion and it does not appear to be critically relevant for the main results of the
2 study.

3 *R: Thanks for the suggestion. We decided to remove this section, in agreement with the*
4 *suggestion from the other reviewer as well.*

5 **Figure 2 caption: Please indicate that figures (b-d) show MAR-simulated results (whereas**
6 **figure (a) shows an observed trend).**

7 *R: Done, thanks.*

8 **Figure 3 caption: Please clarify (and double check) whether these maps depict MAR -**
9 **GLASS, or GLASS - MAR trends. "... positive values indicating those regions where MAR**
10 **trend is smaller in magnitude..." - I suspect this is incorrect. The map show sharply**
11 ***negative* values in southern Greenland.**

12 *R: Thanks for pointing this out. It should, indeed, be GLASS – MAR. We modified the caption*
13 *accordingly.*

14 **Figure 5: Please use larger axis labels. Please also list the spectral ranges used to define**
15 **"visible", "near-infrared", and "shortwave-infrared".**

16 *R: We modified the figure as requested.*

17 **Figure 6: As commented above, please clarify whether this depicts all AEROCOM models,**
18 **or just the GISS model.**

19 *R: Done, thanks.*

20 **Figure 8: Does "RU" (legend) refer to Eurasia or Russia, and is this consistent with the**
21 **caption? Are these annual, or summer-only fire counts? An alternative approach for this**
22 **figure would be to include separate panels for North America and Eurasia, and show**
23 **absolute fire counts instead of standardized quantities. By standardizing both, the relative**
24 **magnitudes of Eurasia and North America fire counts becomes lost.**

25 *R: We thanks the reviewer for the suggestion but we made a typo and the legend 'RU' was*
26 *supposed to be 'EU' as it is now explained in the caption and it was originally reported in the*
27 *text. The data refers to the cumulative fires between April and August. This is now specifically*
28 *mentioned in the text.*

29 **Figure 9 caption: In the next to last sentence "(bottom)" and "(top)" appear to be re-**
30 **versed. More melt under RCP85 should lead to a larger drop in albedo, so I would expect**
31 **RCP85 to define the bottom of the envelope. Also, "GIS" should be "GrIS" for consistency**
32 **with the rest of the paper.**

33 *R: Thanks, We modified the GrIS from GIS. We also corrected the position of the 'bottom' and*
34 *'top' words in the last sentence.*

1 **Figure 10: The caption refers to shades of grey, whereas the figure shows colors. Please**
2 **clarify. Also, the red lines (GLASS albedo) are not readily apparent in this figure.**

3 *R: thanks for pointing this out. We modified the caption.*

4 **Figure 11: It would be helpful to note or indicate whether or not these trends are**
5 **statistically significant.**

6 *R: We added text in the caption to report the statistical significance of the trends.*

7

1

2 **Anonymous Referee #2**

3 Received and published: 7 December 2015

4 This work extends prior efforts to evaluate trends in Greenland ice sheet albedo by incorporating
5 earlier AVHRR data as well as MODIS data. The results show a trend in declining albedo since
6 1996. Further discussion attributes this decline mostly to melt processes, with a modest portion of
7 the decline, which is not matched by modeled albedo, attributed to exposure of light absorbing
8 impurities, largely by process of elimination.

9 This discussion of potential causes of decline is valuable, and I believe the authors are correct in
10 their assessment that LAI exposure must play some role. The line of support for the conclusions
11 has a few weak points, however, which need to be patched up prior to publication. Most
12 importantly, I find that the uncertainties in the modeled albedo are likely too large to firmly
13 attribute any discrepancy to another mechanism. **I think the authors must at least evaluate and**
14 **discuss the alternate hypotheses – namely that 1. the discrepancy between modeled and**
15 **observed albedo decline is simply due to modeling error or inaccurate parameterization of**
16 **the melt processes in the model and not due to any melt-exposure of light absorbing**
17 **impurities. 2. Error in sensing albedo may exceed the discrepancy.** Since the conclusions are
18 based on a test site within the ‘dark band’ I think it should be possible to clarify #2 (see also
19 specific comment on this below). #1 will require more thorough evaluation of the model’s ability
20 to represent melt processes, particularly its simulation of bare ice albedo. I found the ice sheet –
21 wide comparison between MAR and station data inadequate to understand specifically whether
22 the model is properly handling the very large albedo declines due to melt and exposure of bare
23 ice.

24 *R: Hypothesis #1 is plausible, and likely plays a role but difficult to evaluate in the manner*
25 *suggested by the reviewer. Observations of melt, runoff and bare-ice exposure are quite limited,*
26 *and non-existent over the time period used here. As far as we are aware, there has not been an*
27 *attempt to estimate bare ice albedo independent of any impurities that it contains. Moreover,*
28 *there is no satellite dataset currently available that defines bare-ice extent over the ice sheet. An*
29 *evaluation against in situ measurements by Colgan et al. (2015) suggests that MAR v3.5.2, which*
30 *is similar to MAR v3.5.1 used here, agrees with available measurements of SMB in the ablation*
31 *area of the ice sheet, but this evaluation was limited to a small number of locations in one region*
32 *of the GrIS ablation area. It is also impossible to independently evaluate MAR’s estimate of melt*
33 *generated in the absence of impurities, as the real world includes impurities, and any evaluation*
34 *would therefore be comparing melt generated in the presence of impurities with the impurity-free*
35 *melt simulated by MAR. We would be very glad to hear from the reviewer whether he/she has*
36 *suggestions in this regard.*

37 *Nevertheless, we believe that Hypothesis #1 has been addressed to some degree already. The*
38 *study of Alexander et al. (2014) showed that albedo within negative SMB areas of the GrIS*
39 *exhibits a bimodal distribution, likely due to the presence of two surface types, ice and snow.*
40 *Moustafa et al. (2015) find similar results on a local scale. As shown by Alexander et al. (2014),*
41 *MAR also produces a bimodal distribution of low elevation albedo, suggesting that it effectively*
42 *captures the two surface types. Moreover Alexander et al. (2014) showed that the MAR version*
43 *used here tends to overestimate albedo primarily in low elevation areas where bare ice is*
44 *exposed, and especially along the west coast ablation area where impurities concentrations are*

known to be high, and that this overestimation primarily occurs in the lower peak of the albedo distribution, i.e. albedo is overestimated here primarily because bare ice albedo is overestimated.

Specifically I request the authors show that the discrepancy between modeled and observed albedo can be rigorously differentiated from agreement between the two albedo values in the ‘dark band’ by placing error bars on the model values (and remote sensing values, though these are likely smaller) and defending these error bars. My suspicion is that this will be challenging, based on the disagreement with in-situ albedo values RMSE about 0.04-0.05 and few in situ observations in the ablation zone, but I think it must be addressed.

R: Because of the lack of observations, it is difficult, if not impossible at this stage, for us to place error estimates on the albedo values from MAR, considering, among other things, that any observation of albedo include the effect of impurities. Moreover, in the ablation zone, surface heterogeneity leads to high spatial variability in albedo that ultimately affects the comparison between modelled (at 25 km) and measured (AWS) albedo. This is manifested in the relatively poor agreement between MODIS and MAR trends at in situ stations in the ablation zone, as shown in Alexander et al., 2014). Moreover, below the "dark band" at the S4 and S5 stations of the k-transect, the bare ice albedo is higher (0.5) than the one at relatively higher elevations where bare ice contaminated with impurities appears. Therefore, there are areas where MAR overestimates/underestimates bare ice albedo and integrated over the whole bare ice area, we can reasonably assume that there are compensations errors and that the mean albedo/melt value over bare ice is accounting for this effect at the MAR spatial horizontal scale (25 km). Moreover, all available in-situ measurements are collected by sensors that provide only the integrated albedo (e.g., pyranometers) and it is not possible, therefore, to address the differences between modeled and observed values to grain size metamorphism (NIR region) and impurities (visible). This is one of the reasons we are advocating for hyperspectral measurements over the Greenland ice sheet in our conclusions. One option we are currently evaluating to start including error bars on modeled albedo is to ‘perturb’ the inputs to the model (e.g., altering the albedo in the snow model by known quantities). This would provide an assessment of the sensitivity of the model to the albedo value rather than error bars but it is a first step in this direction, which we agree with reviewers needs to be explored and addressed. This approach, though, requires additional work that is computationally expensive and would require several months for the models outputs to be ready. Over this past summer, we have also collected helicopter-based hyperspectral albedo measurements over the bare ice zone for the purpose of quantifying MAR uncertainty. But, again, this is a work in progress.

I also think it would be valuable for the authors to more clearly quantify what fraction of the albedo change is likely due to enhanced melt, vs. the fraction (residual) that is being attributed to impurities. The other anonymous reviewer appears to have interpreted that impurities dominate – and this does not appear to me to be true.

R: We agree with the reviewer that this is an important point and it is one of the driving science questions of our paper. When we started the study, it was indeed our intention to understand the processes driving the observed albedo decline. Still, as we point out in our paper, we think the tools and datasets currently available (e.g., limited by spatial and spectral resolution) don’t allow us to properly separate the relative contribution of enhanced melting and impurities on the decline. This aspect is also complicated by the fact that melting and exposure of impurities are interlinked in a positive feedback. Because of the lack of knowledge of spatial and temporal distribution of surface impurities and how they vary during the season, it is difficult if not impossible, at this stage, to separate the two effects. One way to proceed is, as we suggest, to

1 start including impurities in our model and evaluate its outputs vs. observations. We also started
2 collecting hyperspectral data over Greenland (currently absent !) with the goal of, among other
3 things, addressing the issue raised by the reviewer.

4 After these revisions the paper should be publishable.

5 Specific comments

6 **Abstract:** In reading the abstract I note that the model projections of albedo decline are at a
7 smaller rate than you find in the 1996-2012 interval. You nicely expand this later in the
8 paper to suggest that the models are likely underestimating albedo decline. This seems an
9 important enough conclusion to try to work it into the abstract, lest the reader be left to
10 wonder why the large rate discrepancy exists

11 *R: Thanks. We modified the abstract accordingly.*

12 **Pg 5597 Line 13 -** Suggest continuing with ‘light absorbing impurities’ or LAI throughout
13 the manuscript. Simply ‘impurities’ is not sufficiently descriptive for a reader who jumps in
14 to a later section of the study without reading the introduction.

15 *R: We replaced ‘impurities’ with ‘LAI’, thanks.*

16 **Pg 5600 Line 16 –** Though not central to the paper, this discussion of densification is in-
17 accurate. A large fraction of this densification actually happens due to wind processes
18 which break and round grains forming windslab of density typically around 0.3-0.4. The
19 remaining densification happens by grain sliding. Additionally, and perhaps more
20 importantly, snow which has recaptured meltwater (held it until it refroze) frequently
21 exceeds densities of 0.55 in the percolation zone, at least in discrete layers.

22 *R: We modified the text to reflect reviewer’s suggestion.*

23 **Pg 5604 Lines 5-15** This discussion of potential MODIS degradation does not appear to be
24 up to date. A recent publication by Polashenski et al. 2015 suggests the degradation is
25 larger. Lyapustin et al., 2014 also suggest larger degradation. If the rate of 0.0059/decade
26 from Stroeve et al., 2013 remains accurate however, this still means that more than 25% of
27 the ice sheet wide albedo decline rate during the MODIS era (.02/decade 1996-2002) could
28 be attributed to MODIS degradation. This is significant and should be discussed as such. I
29 agree that the degradation is likely insignificant in the ‘dark band’

30 *R: We thank the reviewer for the note. The rate of 0.0059/decade refers to the TERRA sensor only
31 and we kindly remind the reviewer that the GLASS product uses a combination of both TERRA
32 and AQUA. Hence, the impact of sensor degradation is reduced on the final product. Moreover,
33 the TERRA sensor degradation is not linear and spectrally dependent, as pointed out in Wang et
34 al.. Therefore, we think that the suggestion that more than 25 % of the albedo decline might be
35 due to sensor degradation is an overestimation. We added this comment in the text. Concerning
36 the comment on the trend by Polashenski, we note that the Polashenski et al. analysis is different
37 than what we did. In the GLASS product, the 16-day MODIS albedo product (again TERRA and
38 AQUA combined and hence reducing the impact of sensor degradation) is used where
39 Polashenski is looking at the daily MODIS MOD10A1 TERRA product. The daily product*

1 provides biases at high solar zenith angles and it is more sensitive to latitudinal errors, as shown
2 by Alexander et al. (2015). We added this point in the revised version of our paper.

3 **If the reader mis-understands your conclusion (as I did first read through, when I skipped**
4 **to the conclusions) to be based on ice sheet wide discrepancies between MAR and GLASS,**
5 **the degradation appears to be a serious issue for your conclusion. Perhaps you can help the**
6 **clumsy reader a bit with more clarification in your conclusions.**

7 *R: Thanks for the comment. We added a sentence in the conclusions mentioning that degradation*
8 *can be an issue over the dry snow zone and that our hypothesis is likely more valid over the*
9 *ablation zone.*

10 **Pg5604 section 3.1, line 20... the trend stated here (-1702mmWE/decade) seems enormous**
11 **for a trend in snowfall. I don't think mean snowfall was 1702mm WE to begin with. Please**
12 **clarify/correct.**

13 *R: We checked again the numbers and the reported value appears to be correct. Note that the*
14 *mean cumulative SF value simulated by MAR over the whole ice sheet for the period 1996 – 2012*
15 *is ~ 150,000 mmWE.*

16 **Line 23 Low 2010-12 albedo is attributed to low snowfall. Why not melt? Melt extents were**
17 **greater than typical these years- the statement seems sort of offhand here when other**
18 **options remain available.**

19 *R: We, indeed, 'suggest' that reduced snowfall might have played a role. We modified the*
20 *sentence as follows: We suggest that for 2010 – 2012, beside surface melting, reduced summer*
21 *snowfall might have played a key role in the accelerated decline in albedo.*

22 **Pg 5605, sect. 3.2 Line 2 Fort → For**

23 *R: Done, thanks.*

24 **Pg 5606, sect 3.3 Line 17 This sentence seems to confuse your central thesis that exposure of**
25 **LAI deposited long ago is causing the albedo decline, by suggesting that local dust sourcing**
26 **is to blame, without also mentioning the theory you later focus on. The paper would be**
27 **strengthened by either dropping this sentence for later discussion or bringing both**
28 **processes into the discussion here.**

29 *R: Thanks. We removed this sentence.*

30 **Pg5607. Lines 19-22 This discussion seems to need strengthening. The conclusion that the**
31 **discrepancy arises from impurity deposition depends on the assumption that both MAR**
32 **and the observations are behaving as designed. But - is MAR accurately handling bare ice?**
33 **I think you need some in-situ evidence that it does or some more concrete support to the**
34 **statement that bare ice albedo doesn't typically drop below 0.45 (p5605 line28). The**
35 **conclusion you come to is likely correct, but in the absence of this evidence the reader is left**
36 **to question whether the discrepancy could be caused by something else.**

1 *R: We have revised the discussion to note the multiple possibilities for discrepancies between*
2 *MAR and GLASS, including the potential for errors in bare ice exposure from*
3 *MAR. Unfortunately we have no way of evaluating bare ice exposure as simulated by MAR,*
4 *although we believe this is something that could be done and are preparing for further research*
5 *in this area. In situ measurements of bare ice albedo have been conducted (e.g. Moustafa et al.,*
6 *2015). Measurements from Moustafa et al. (2015) suggest that “clean” ice surfaces have albedo*
7 *values that are generally higher than 0.5, while “dirty” ice surfaces have albedo values lower*
8 *than 0.3. The MAR value of 0.45 essentially attempts to account for the presence of both clean*
9 *and dirty surfaces, but as suggested by Alexander et al. (2014), generally overestimates albedo in*
10 *ablation areas. The analysis of Alexander et al. (2014) suggests that MAR exhibits a bimodal*
11 *distribution of bare ice albedo in the Greenland Ice Sheet ablation area, which is similar to the*
12 *distribution of bare ice values from MODIS. The bimodal distribution is attributed to the*
13 *presence of two surface types, ice and snow. These results indirectly suggest that MAR captures*
14 *at least the frequency of snow and ice in the ablation area fairly well (although the lower peak in*
15 *the distribution seems to be overestimated, suggesting that albedo for bare ice areas is*
16 *overestimated). The sensitivity experiment we have added to this paper shows that reducing the*
17 *bare ice albedo by 0.1 (roughly the difference found by Alexander et al., 2015) results in a*
18 *change in the albedo trend that is similar to the MAR – GLASS difference, and could explain a*
19 *portion of the trend. While these results suggest that a lack of impurities in MAR plays an*
20 *important role in the trend difference, we cannot conclude for certain or even provide error bars*
21 *regarding the magnitude of the impact of any individual factor on the trends, given the present*
22 *lack of available observations for evaluating MAR, and have attempted to make this clear in the*
23 *discussion section.*

24 **P 5608 Lines ~25 This discussion could be strengthened with a reference to core data. See**
25 **McConnell 2007.**

26 *R: Thanks. We added a reference and a sentence highlighting some of the results in McConnel*
27 *2007 that we think will strengthen the discussion.*

28 **P5609 This discussion, and conclusion at bottom of 5611 showing no evidence of an increase**
29 **in aerosol deposition could be supported by citation of the recent Polashenski et al paper in**
30 **GRL.**

31 *R: We added a reference to Polashenski et al. Thanks !*

32 **P 5613 line 5 and many other locations throughout. An albedo trend is stated without**
33 **discussing what months of the year this applies. I think it would be helpful to the reader to**
34 **clarify at each location what, exactly, the trend being discussed is – or is it possible to**
35 **categorically state you are referring to JJA albedo only throughout the paper ?**

36 *R: we added the term ‘summer’ when we thought it was necessary. We thank the reviewer for*
37 *this comment.*

38 **5614 line 9 – 10 . This statement is true if you are referring to large discrepancies in the**
39 **‘dark band’. It is not true if discussing ice sheet wide trends. There the discrepancy between**
40 **MAR and GLASS is too similar to the Terra degradation quoted to distinguish the two.**
41 **Here and throughout clarification is needed to focus on the dark band case (which supports**
42 **your case) vs. whole ice sheet treatment.**

1 *R: We modified the sentence to highlight the fact that Lines 9 -10 are correct for the ablation*
2 *zone, where the dark zone occurs and albedo decline is substantial.*

3 **5614 line14 oft he → of the**

4 *R: Done.*

5 **5616 line 22 “the value.. was estimated. . .” By who? Should there be a citation?**

6 *R: This section was removed.*

7 **5618 conclusions about grain growth with BC ‘doping.’ This section is accurately dis-**
8 **cussed as exploratory and fine to include if the authors choose, but it seems very weak to**
9 **me. These models likely don’t have the necessary physics to alter grain growth based on**
10 **absorption, and a gross change to albedo is a very crude way to explore this. I’m not sure**
11 **the conclusion made here “grain sizes are typically only about 1% larger for dirty snow” is**
12 **very defensible based only on this work, and an unformed reader might over extend this**
13 **very preliminary result. Mostly though, I think this exploration is a distraction in this work.**

14 *R: This section was removed.*

15 **5619 line 25. I think CESM actually does handle melt concentration based on obser- vations**
16 **by Doherty et al., Please verify this statement.**

17 *R: Thanks for pointing this out. We here refer to ‘regional’ climate models rather than Earth System*
18 *Models.*

19

The darkening of the Greenland ice sheet: trends, drivers and projections (1981 – 2100)

M. Tedesco^{1,2}, S. Doherty³, X. Fettweis⁴, P. Alexander^{2,5,6}, J. Jeyaratnam²,
and J. Stroeve⁷

[1] Lamont-Doherty Earth Observatory of the Columbia University, New York, NY

[2] The City College of New York – CUNY,

[3] Joint Institute for the Study of the Atmosphere and Ocean (JISAO), University of Washington, Seattle, WA USA

[4] University of Liege, Liege, Belgium

[5] NASA Goddard Institute for Space Studies, New York, NY USA

[6] The Graduate Center of the City University of New York

[7] University of Boulder, Colorado, USA

Abstract

The surface energy balance and meltwater production of the Greenland ice sheet (GrIS) are modulated by snow and ice albedo through the amount of absorbed solar radiation. Here we show, using spaceborne multispectral data collected during the three decades from 1981 to 2012, that summertime surface albedo over the GrIS decreased at a statistically significant (99 %) rate of 0.02 decade^{-1} between 1996 and 2012. Over the same period, albedo modeled by the Modèle Atmosphérique Régionale (MAR) also shows a decrease, though at a lower rate ($\sim -0.01 \text{ decade}^{-1}$) than that obtained from spaceborne data. We suggest that the discrepancy between modeled and measured albedo trends can be explained by the absence in the model of processes associated with the presence of light-absorbing impurities. The negative trend in observed albedo is confined to the regions of the GrIS that undergo melting in summer, with the dry-snow zone showing no trend. The period 1981 – 1996 also showed no statistically significant trend

over the whole GrIS. Analysis of MAR outputs indicates that the observed albedo decrease is attributable to the combined effects of increased near-surface air temperatures, which enhanced melt and promoted growth in snow grain size and the expansion of bare ice areas, and by trends in light-absorbing impurities (LAI) on the snow and ice surfaces. Neither aerosol models nor in-situ and remote sensing observations indicate increasing trends in LAI in the atmosphere over Greenland. Similarly, an analysis of the number of fires and BC emissions from fires points to the absence of trends for such quantities. This suggests that the apparent increase of LAI in snow and ice might be related to the exposure of a ‘dark band’ of dirty ice and to increased consolidation of LAI at the surface with melt, not to increased aerosol deposition. Albedo projections through the end of the century under different warming scenarios consistently point to continued darkening, with albedo anomalies averaged over the whole ice sheet lower by 0.08 in 2100 than in 2000, driven solely by a warming climate. Future darkening is likely underestimated because of known underestimates in modelled melting (as seen in hindcasts) and because the model albedo scheme does not currently include the effects of LAI, which have a positive feedback on albedo decline through increased melting, grain growth and darkening.

1 Introduction

The summer season over the Greenland ice sheet (GrIS) during the past two decades has been characterized by increased surface melting (Nghiem et al., 2012; Tedesco et al., 2011, 2014) and net mass loss (Shepherd et al., 2012). Notably, the summer of 2012 set new records for surface melt extent (Nghiem et al., 2012) and duration (Tedesco et al., 2013), and a record of 570 ± 100 Gt in total mass loss, doubling the average annual loss rate of 260 ± 100 Gt for the period 2003–2012 (Tedesco et al., 2014).

Net solar radiation is the most significant driver of summer surface melt over the GrIS, (van den Broeke et al., 2011; Tedesco et al., 2011), and is determined by the combination of the amount of incoming solar radiation and surface albedo. Variations in snow albedo are driven principally by changes in snow grain size and by the presence of light-absorbing impurities (LAI, Warren and Wiscombe, 1982). Generally, snow albedo

1 is highest immediately following new snowfall. In the normal course of *destructive*
2 *metamorphism* the snow grains become rounded, and large grains grow at the expense of
3 small grains, so the average grain radius r increases with time (LaChapelle, 1969).
4 Subsequently, warming and melt/freezing cycles catalyse grain growth, decreasing albedo
5 mostly in the near-infrared (NIR) region (Warren 1982). The absorbed solar radiation
6 associated with this albedo reduction promotes additional grain growth, further reducing
7 albedo, potentially accelerating melting. The presence of LAI such as soot (black carbon,
8 BC), dust, organic matter, algae and other biological material in snow or ice also reduces
9 the albedo, mostly in the visible and ultraviolet regions (Warren 1982). Such impurities
10 are deposited through dry and wet deposition, and their mixing ratios are enhanced
11 through snow water loss in sublimation and melting (Conway et al., 1996; Flanner et al.,
12 2007; Doherty et al., 2013). Besides grain growth and LAI, another cause of albedo
13 reduction over the GrIS is the exposure of bare ice: once layers of snow or firn are
14 removed through ablation, the exposure of the underlying bare ice will further reduce
15 surface albedo, as does the presence of melt pools on the ice surface (e.g., Tedesco et al.,
16 2011).

17 Most of the studies examining albedo over the whole GrIS have focused on data
18 collected by the Moderate Resolution Imaging Spectroradiometer (MODIS) starting in
19 2000 (e.g., Box et al., 2012; Tedesco et al., 2013). At the same time, regional climate
20 models (RCMs) have been employed to simulate the evolution and trends of surface
21 quantities over the GrIS back to the 1960s using reanalysis data for forcing (e.g., Fettweis
22 et al., 2012). Despite the increased complexity of models, and their inclusion of
23 increasingly sophisticated physics parameterizations, RCMs still suffer from incomplete
24 representation of processes that drive snow albedo changes, such as the spatial and
25 temporal distribution of LAI, and from the absence of in-situ grain size measurement to
26 validate modeled snow grain-size evolution. In this study, we first report the results from
27 an analysis of summer albedo over the whole GrIS from satellite for the period 1980 –
28 2012, hence expanding the temporal coverage with respect to previous studies. Then, we
29 combine the outputs of an RCM and in-situ observations with the satellite albedo
30 estimates to identify those processes responsible for the observed albedo trends. The
31 model, Modèle Atmosphérique Régionale (MAR), is used to simulate surface

1 temperature, grain size, exposed ice area, and surface albedo over Greenland at large
2 spatial scales. MAR-simulated surface albedo is tested against surface albedo retrieved
3 under the Global LAnd Surface Satellite (GLASS) project, and it is used to attribute
4 trends in GLASS albedo. Lastly, we project the evolution of mean summer albedo over
5 Greenland using the MAR model forced with the outputs of different Earth System
6 Models (ESMs) under different CO₂ scenarios. Discussion and conclusions follow the
7 presentation of the methods and results.

8 **2 Methods and data**

9 **2.1 The MAR regional climate model and its albedo scheme**

10 Simulations of surface energy balance quantities over the GrIS are performed using
11 the Modèle Atmosphérique Régionale (MAR; e.g., Fettweis et al., 2005, 2013). MAR is a
12 modular atmospheric model that uses the sigma-vertical coordinate to simulate airflow
13 over complex terrain and the Soil Ice Snow Vegetation Atmosphere Transfer scheme
14 (SISVAT, e.g., De Ridder and Gallée, 1998) as the surface model. MAR outputs have
15 been assessed over Greenland in several studies (e.g., Tedesco et al., 2011; Fettweis et
16 al., 2005; Vernon et al., 2013; Rae et al. 2012; Van Angelen et al., 2012), with recent
17 work specifically focusing on assessing simulated albedo over Greenland (Alexander et
18 al., 2014). A discussion of this evaluation is presented later in the manuscript. The snow
19 model in MAR is the CROCUS model of Brun et al., (1992), which calculates albedo for
20 snow and ice as a function of snow grain properties, which in turn are dependent on
21 energy and mass fluxes within the snowpack. The model configuration used here has 25
22 terrain-following sigma layers between the Earth's surface and the 5-hPa-model top. The
23 spatial configuration of the model uses the 25-km horizontal resolution computational
24 domain over Greenland described in Fettweis et al. (2005). The lateral and lower
25 boundary conditions are prescribed from meteorological fields modelled by the global
26 European Centre for Medium-Range Weather Forecasts (ECMWF) Interim Reanalysis
27 (ERA-Interim, <http://www.ecmwf.int/en/research/climate-reanalysis/era-interim>). Sea-
28 surface temperature and sea-ice cover are also prescribed in the model using the same
29 reanalysis data. The atmospheric model within MAR interacts with the CROCUS model,
30 which provides the state of the snowpack and associated quantities (e.g., albedo, grain

size). No nudging or interactive nesting was used in any of the experiments.

The MAR albedo scheme is summarized below. Surface albedo is expressed as a function of the optical properties of snow, the presence of bare ice, whether snow is overlying ice (and whether the surface is waterlogged), and the presence of clouds. In the version used here (MARv 3.5.1), the broadband albedo (α_s , 0.3 – 2.8 μm) of snow is a weighted average (Eq. 1) of the albedo in three spectral bands, α_1 , α_2 and α_3 , which are functions of the optical diameter of snow grains (d , in meters), as modified from equations by Brun et al. (1992; e.g., Lefebvre et al., 2003; Alexander et al., 2014):

$$\alpha_s = 0.58\alpha_1 + 0.32\alpha_2 + 0.10\alpha_3 \quad (1)$$

$$\alpha_1 = \max(0.94, 0.96 - 1.58 \sqrt{d}), (0.3 - 0.8 \mu\text{m}) \quad (2)$$

$$\alpha_2 = 0.95 - 15.4 \sqrt{d}, (0.8 - 1.5 \mu\text{m}) \quad (3)$$

$$\alpha_3 = 364 * \min(d, 0.0023) - 32.31 \sqrt{d} + 0.88, (1.5 - 2.8 \mu\text{m}) \quad (4)$$

The optical diameter d is, in turn, a function of snow grain properties and it evolves as described in Brun et al., (1992). In MAR, the albedo of snow is calculated by Eqs. 1-4, but it is not permitted to drop below 0.65.

For the transition from snow to ice, MAR makes the albedo an explicit function of density. On a polar ice sheet, densification of snow/firn/ice occurs in three stages, with a different physical process responsible for the densification in each stage (Herron and Langway, 1980; Arnaud et al., 2000). Newly-fallen snow can have density in the range 50-200 kg m^{-3} . After then, densification can occur due to wind processes, which break and round grains forming windslab of density typically around 300-400 kg m^{-3} . The remaining densification happens by *grain-boundary sliding*, attaining a maximum density of $\sim 550 \text{ kg m}^{-3}$ at the surface. Old melting snow at the surface in late summer typically has this density, but does not exceed it, because this is the maximum density that can be attained by grain-boundary sliding and corresponds to the density of random-packing of spheres (Benson, 1962, page 77). Further increases of density (the second stage) occur in *firn* under the weight of overlying snow, by *grain deformation* (pressure-sintering). In this case the density range is 550-830 kg m^{-3} . At a density of 830 kg m^{-3} the air becomes

closed off into bubbles and the material is called *ice*. In the third stage, the density of ice increases from 830 to 917 kg m⁻³ by shrinkage of air bubbles under pressure. Moving down the slope along the surface of the GrIS, at the transition between the accumulation area and the ablation area, the snow melts away, exposing firn. Continuing farther down, the firn melts away, exposing ice. The albedo of firn may be approximated as a function of its density, ρ , interpolating between the minimum albedo of snow and the maximum albedo of ice. In MAR these values of albedo are set to 0.65 and 0.55, respectively. We would then have for the density range of firn (550-830 kg m⁻³):

$$\alpha_{\text{firn}} = 0.55 + (0.65 - 0.55) (830 - \rho) / (830 - 550) \quad (5)$$

The MARv3.5.1 version used here maintains a minimum albedo of 0.65 for any density up to 830 kg m⁻³, and specifies the gradual transition from snow albedo to ice albedo across the density range 830-920 kg m⁻³. This means that the albedo of exposed firn is not allowed to drop below 0.65, with the result that the positive feedbacks of snow/firn/ice albedo will be muted in MAR. This aspect is being addressed in future versions of MAR (MAR v3.6) and a sensitivity analysis is being conducted to evaluate the impact of the changes on the albedo values when snow is transitioning from firn to ice. Such analysis is computationally expensive and preliminary outputs will be published once available.

In MAR, the albedo for bare ice is a function of the accumulated surface meltwater preceding runoff and specified minimum ($\alpha_{i,\text{min}}$) and maximum ($\alpha_{i,\text{max}}$) bare ice values:

$$\alpha_i = \alpha_{i,\text{min}} + (\alpha_{i,\text{max}} - \alpha_{i,\text{min}}) e^{(-M_{\text{SW}(t)} / K)} \quad (6)$$

Here $\alpha_{i,\text{min}}$ and $\alpha_{i,\text{max}}$ are set, respectively, to 0.4 and 0.55, K is a scale factor set to 200 kg m⁻², and $M_{\text{SW}(t)}$ is the time-dependent accumulated excess surface meltwater before runoff (in kg m⁻²).

When a snowpack with depth less than 10 cm is overlying a layer with a density exceeding 830 kg m⁻³ (i.e., ice), the albedo in MAR is a weighted, vertically-averaged

value of snow albedo (α_s) and ice albedo (α_i ; e.g., if snow depth is 3 cm then albedo is obtained by multiplying the snow albedo by 0.3 and adding the ice albedo multiplied by 0.7). When the snowpack depth exceeds 10 cm, the value is set to α_s . The presence of clouds can increase snow albedo because they absorb at the same NIR wavelengths where snow also absorbs, skewing the incident solar spectrum to wavelengths for which snow has higher albedo (Figure 5 of Grenfell et al., 1981; Figure 13 of Warren, 1982; Greuell and Konzelman, 1994), in which case the albedos of snow and ice are adjusted based on the cloud fraction modelled by MAR (Greuell and Konzelman, 1994).

2.2 The GLASS albedo product

The GLASS surface albedo product (<http://glcf.umd.edu/data/abd/>) is derived from a combination of data collected by the Advanced Very High Resolution Radiometer (AVHRR) and the MODerate resolution Imaging Spectroradiometer (MODIS, Liang et al., 2013). Shortwave broadband albedo ($0.3 - 3 \mu m$) is provided every 8 days at a spatial resolution of 0.05° (~ 56 km in latitude) for the period 1981 - 2012. GLASS albedo data with a resolution of 1 km is also available from 2000 to 2012 but it is not used here for consistency with the data available before 2000. There have been several efforts to make the AVHRR and MODIS albedo products consistent within the GLASS product, including the use of the same surface albedo spectra to train the regression and the use of a temporal filter and climatological background data to fill data gaps (Liang et al., 2013). Monthly averaged broadband albedos from GLASS-AVHRR and GLASS-MODIS were cross-compared over Greenland for those months when there was overlap (July 2000, 2003, and 2004), revealing consistency in GLASS retrieved albedo from the two sensors (He et al., 2013). More information on the GLASS data processing algorithm and product is available in Zhao et al. (2013) and Ying et al. (2014).

The GLASS product provides both black-sky albedo (i.e., albedo in the absence of a diffuse component of the incident radiation) and white-sky albedo (albedo in the absence of a direct component, with an isotropic diffuse component). The actual albedo is a value interpolated between these two according to the fraction of diffuse sunlight, which is a function of the aerosol optical depth (AOD) and cloud cover fraction. In the

1 absence of the full information needed to properly re-construct the actual albedo, here we
2 use in our analysis the black-sky albedo, because we focus mostly on albedo retrieved
3 under clear-sky conditions. Our analysis using the white-sky albedo (not shown here) is
4 fully consistent with the results obtained using the black-sky albedo and reported in the
5 following. A full description of the GLASS retrieval process and available products can
6 be found in Liang et al. (2013) and references therein. An assessment of the GLASS
7 product complementing existing studies is reported below.

8 Data collected by the MODIS TERRA and AQUA sensors are used in the GLASS
9 albedo retrieval for the period 2000 – 2012 (2000 – 2012 for TERRA and 2002 – 2012
10 for AQUA, respectively). Wang et al. (2012) have shown that the MODIS TERRA
11 sensor has been degrading at a pace that can be approximated by a second order
12 polynomial, with the coefficients being spectrally dependent. Over Greenland, the impact
13 of sensor degradation on albedo trends has been estimated at $-0.0059 \text{ decade}^{-1}$ (Stroeve et
14 al., 2013). Polashenski et al. (2015) found a much greater impact on retrieved broadband
15 albedo from TERRA sensor degradation ($-0.03 \text{ decade}^{-1}$). However, Polashenski et al.
16 (2015) use a daily product (MOD10A1) rather than a 16-day integrated product as in the
17 case of GLASS (e.g., Ying et al., 2014), which does account for BRDF at high solar
18 zenith angles. The performance of the MODIS daily product has been shown to
19 deteriorate with latitude (e.g., Alexander et al., 2015). On the other hand, the use of the
20 BRDF (as in the case of the GLASS product) improves the performance of the product at
21 high latitudes (Alexander et al., 2015). This, together with the good agreement between
22 the MCD43 albedo product and the surface station albedo data (Alexander et al., 2015)
23 gives us confidence in the GLASS trends.

24 We complement previous assessments of the MODIS and GLASS albedo,
25 evaluating the absolute accuracy of the GLASS retrievals by comparing monthly GLASS
26 albedo to in-situ measurements of albedo collected at automatic weather stations of the
27 Greenland climate network (GC-Net, Steffen and Box, 2001). GC-Net data are
28 distributed at hourly temporal resolution and were temporally averaged to match the
29 temporal window used in the GLASS product data. The root mean square error (RMSE),
30 percentage RMSE (pRMSE), and the slope of a linear fit between GLASS and in-situ
31 measured albedos for 12 stations are given in Table 1. The number of available years

used for the statistics is also reported for each station. We considered only stations for which at least 10 years were available for the analysis in at least one of the months. Our results are consistent with the findings reported by Alexander et al. (2014) and Stroeve et al., (2013, 2006) concerning the assessment of the MODIS albedo products over the GrIS. The mean value of the RMSE for all stations is 0.04-0.05 in all months, with individual station values as high as 0.15 for station JAR1 in August and as low as 0.01 for Summit and Saddle stations in June. The relatively large RMSE value for JAR1 (and other stations located within the ablation zone) is probably due to heterogeneity of albedo values within the pixel containing the location of the station and to the point-scale nature of the in-situ observations. At Summit, where spatial inhomogeneity on the surface is small, it is reasonable to assume that the effect of spatial scale and heterogeneity on the comparison is smaller.

3 Results

3.1 Albedo trends

The time series of the mean summer GLASS albedo values between 1981 and 2012 over Greenland can be separated into two distinct periods (Figure 1a): the period 1981 - 1996, when albedo shows no trend and a second period, 1996 – 2012, when a statistically significant trend (99 %) is detected. The year 1996 was identified as yielding the highest value of the coefficient of determination when fitting the albedo timeseries with two linear functions using a variable breaking point.

The GLASS albedo shows significant darkening ($p < 0.01$) of the surface of the GrIS for the 1996 – 2012 period, with the summer (JJA) albedo declining at a rate of 0.02 ± 0.004 decade⁻¹ (Figure 1a). About 25% of this decline might be attributed to sensor degradation, per the analysis of Stroeve et al. (2013). However, the TERRA sensor degradation is spectrally dependant and temporally non linear (Wang et al., 2012). This, together with the fact that the GLASS product uses a combination of both TERRA and AQUA data (which reduces the impact of the TERRA sensor degradation) indicates that impact of the sensor degradation on the observed decline is much smaller than 25 %. Over the same period, MAR-simulated summer near-surface temperature increased at a

rate of $0.74 \pm 0.5^\circ\text{C decade}^{-1}$ (Figure 1b, $p < 0.05$), consistent with observed enhanced surface melting (e.g., Fettweis et al., 2013). MAR simulations also point to positive trends between 1996 and 2012 in summer surface grain radius ($0.12 \pm 0.03 \text{ mm /decade}^{-1}$, $p < 0.01$, Figure 1c) and the extent of those regions where bare ice is exposed during summer ($380 \pm 190 \text{ km}^2 \text{ decade}^{-1}$, $p < 0.01$, Figure 1d). There is no statistically significant trend in GLASS summer albedo or MAR-simulated surface grain size and bare ice extent for the 1981-1996 period. Simulated summer snowfall (not plotted in the figure) does not show a statistically significant trend for the period 1996 – 2012 ($p < 0.1$, $-1702 \pm 790 \text{ mmWE /decade}^{-1}$). Notably, strong negative summer snowfall anomalies from 2010 to 2012 are simulated by MAR, down to -1.5 standard deviations below the 1981 – 2012 mean. We suggest that for 2010 - 2012, in addition to surface melting, reduced summer snowfall might have played a key role in the accelerated decline in summer albedo.

3.2 Drivers: surface grain size and bare ice

Inter-annual variability in the mean summer GLASS albedo is captured by the MAR albedo simulations (Figure 1a). For the period when the darkening has been identified, MAR albedo values explain $\sim 90 \%$ (de-trended) of the spaceborne-derived summer albedo interannual variability. A multi-linear regression analysis indicates that, over the same period, the interannual variability of summer values of surface grain size and bare ice extent simulated by MAR explain, respectively, 54% (grain size) and 65% (bare ice) of the inter-annual variability of GLASS albedo when considered separately. When linearly combined, grain size, bare ice extent and snowfall explain $\sim 85 \%$ of the GLASS inter-annual variability, with the influence of summer new snowfall alone explaining only 44% of the GLASS summer albedo variability.

The spatial distribution of observed summer albedo trends from space shows that the largest trends (in magnitude) occur over those regions where surface temperature, grain size, and bare ice exposure have also changed the most (Figure 2). In particular, darkening observed from space is most pronounced at lower elevations in southwest Greenland, with trends as large as $-0.20 \pm 0.07 \text{ decade}^{-1}$ (Figure 2a; note that the colour bar

only goes down to $-0.06 \text{ decade}^{-1}$ for graphical purposes), where trends in the number of days when simulated surface temperature exceeds 0°C (Figure 2b), grain size (Figure 2c) and the number of summer days when bare ice is exposed (Figure 2d) are the largest.

While MAR is able to capture a large component of the observed variability in albedo retrieved by GLASS, the simulated albedo trend is smaller in magnitude than that estimated using the GLASS product. The largest differences occur along the southwest margin of the ice sheet (Figure 3), where a “dark band” of outcropping layers of ice containing large concentrations of LAI is known to be present on the surface (Wientjes et al., 2011). In this region the number of days when surface temperature exceeds 0°C has increased, with trends of up to more than $20 \text{ days decade}^{-1}$ along the margins of the GrIS (Figure 1b). During this time-period GLASS albedo values are as low as 0.30, lower than that of bare ice (i.e., 0.45), consistent with in-situ measured values of dirty ice (Wientjes et al., 2010; Bøggild et al., 2010). Figure 4 shows the spatial distribution of MAR and GLASS mean JJA albedo for year 2010 over an area centred on the dark band in southwest Greenland, as well as the time series of GLASS albedo averaged over the same ice-covered area contained within the region identified by the black rectangle in Figure 4a. The black line in Figure 4c shows the GLASS spatially-averaged albedo within this region, with the top and the bottom margins of the grey area indicating, respectively, the maximum and minimum albedo values within that area. Note that we included only pixels that contained 100 % ice in all years (i.e. coloured areas in Figure 4a and b) in the calculation shown in Figure 4c, so trends are not driven by exposure of underlying land surface. Mean summer albedo from GLASS decreased over this area between 2005 and 2012 from ~ 0.6 to ~ 0.45 (vs. a decrease simulated by MAR of 0.075). Minimum summer albedo across all years averaged over the region is ~ 0.4 , but dips close to ~ 0.3 in 2010, a value consistent with dirty bare ice, as shown in previous studies (Wientjes et al., 2010; Wientjes et al., 2011; Bøggild, et. al., 2010). We hypothesise that the discrepancy along this dark band between MAR- and GLASS albedo values is likely due to trends in the concentrations of LAI in the snow and ice in this region, which are not currently captured by the model.

3.3 Drivers: light-absorbing impurities on the surface of the GrIS

MAR simulations of albedo in different spectral bands (see Eqs. 1-4) point to comparable trends in the visible ($0.3 - 0.8 \mu\text{m}$; $-0.009 \pm 0.005 \text{ decade}^{-1}$, $p < 0.05$) and near-infrared ($0.8 - 1.5 \mu\text{m}$; $-0.010 \pm 0.004 \text{ decade}^{-1}$, $p < 0.05$) bands (Figure 5a) and to a much smaller and not statistically significant trend in the shortwave infrared band ($1.5 - 2.8 \mu\text{m}$, $-0.003 \pm 0.004 \text{ decade}^{-1}$, $p > 0.1$). Because the GLASS product does not provide visible albedo (only broadband albedo), we extrapolated an estimate of the visible component of the GLASS albedo by subtracting the NIR and shortwave infrared albedo values computed with MAR from the GLASS broadband values, following the MAR albedo scheme (Eq. 1, Figure 5b). To evaluate the robustness of this approach, we compared anomalies (with respect to year 2000) in estimated GLASS visible albedo with those from the 16-day MODIS MCD43A3 product (Stroeve et al., 2013), which also has a visible albedo product (Figure 5b). The MODIS albedo product we used is distributed by Boston University (<https://lpdaac.usgs.gov/>) and makes use of all atmospherically-corrected MODIS reflectance measurements over 16-day periods, to provide an averaged albedo every 8 days. A semi-empirical bidirectional reflectance distribution function (BRDF) model is used to compute bi-hemispherical reflectance from these reflectance measurements (Schaaf et al., 2002). The comparison between the GLASS- and MODIS-retrieved visible albedo anomalies is shown in Figure 5b, indicating that the two visible albedo anomalies are highly consistent, with a mean absolute error of 0.01 and a standard deviation of 0.005. There are differences in the estimated summer albedo trends from MCD43A3 and GLASS over the 2002 – 2012 period, with the former being $-0.04 \pm 0.001 \text{ decade}^{-1}$ and the latter $-0.03 \pm 0.008 \text{ decade}^{-1}$. This difference could be due to the method we applied to estimate the visible component of the GLASS albedo, as well as other factors related to the data processing and algorithms used to extract albedo. Notably, however, the GLASS and MCD43 visible albedo trends are consistently about twice that estimated from the MAR model. The underestimated darkening by MAR relative to GLASS can be attributed to several factors, including the modeled spatial and temporal variability of the exposed bare ice area and the concentration of surface LAI on the ice surface, which is currently not included in the MAR albedo scheme. A lack of impurities in the MAR albedo scheme can affect simulated albedo trends in at least two ways: first,

1 the concentration of impurities over bare ice areas could be increasing, which would not
2 be captured by MAR; second, the lack of impurities in the MAR albedo scheme causes
3 bare ice areas to have an overestimated albedo. More frequent exposure of bare ice would
4 lead to a decline in annual average albedo over time, but if the underlying bare ice is
5 darker, such a trend would be larger. Thus, the difference in trends could result solely
6 from an overestimation of the bare ice albedo by MAR. We are not able to discern the
7 degree to which the difference is due to a) errors in the area and frequency of bare ice
8 exposure from MAR; b) increasing concentration of impurities not captured by MAR, or
9 c) overestimation of albedo of an unchanging impurity-covered bare ice surface. The
10 study by Alexander et al. (2015) suggests that bare ice albedo is, indeed, overestimated in
11 MAR. To test the impact of a fixed bare ice albedo on the simulated albedo trend, we
12 performed a sensitivity experiment in which daily albedo for those pixels showing bare
13 ice exposure is reduced by a fixed value of 0.1. The magnitude of the difference in trends
14 between the original MAR simulation (with no change on the bare ice albedo) and the
15 one with a modified albedo (Figure 6) is comparable to the difference between the MAR
16 and GLASS trends (Figure 3a), suggests that this factor alone could explain the
17 difference. To further investigate this aspect, we test the hypothesis of increased
18 concentration of LAI on the snow and ice surface. The concentrations of LAI in surface
19 snow and ice can increase either because of increased atmospheric deposition or because
20 of post-depositional processes, including (a) loss of snow water to sublimation and melt,
21 resulting in impurities accumulating at the surface as a lag-deposit (e.g., Doherty et al.,
22 2013), and (b) the outcropping of ‘dirty’ underlying ice associated with snow/firn
23 removal due to ablation. These processes are themselves driven by warming, and
24 therefore constitute positive feedbacks.

25 Quantifying the contribution of surface LAI to GLASS summer albedo trends is a
26 challenging task because of the relatively low impurity concentrations over most of the
27 GrIS (Doherty et al., 2010; Bond et al., 2013), and because of known limitations related
28 to remote sensing estimates of LAI from space (Warren, 2013). Moreover, quantifying
29 the causes of potential increased impurity concentrations on the surface (atmospheric
30 deposition vs. other factors) is also challenging, if not prohibitive, given the current state-
31 of-the-art of spaceborne measurements (e.g. accuracy of the satellite products) and the

1 scarcity of in-situ data. Therefore, in the next section, we look for trends in forest fires
2 and the emissions of BC from forest fires in the main source regions for aerosols over the
3 GrIS and assess whether atmospheric aerosol concentrations over the GrIS have
4 increased (as a proxy for whether the deposition of aerosol has increased).

5 **3.4 Attribution: Aerosol contributions to LAI in GrIS**

6 **3.4.1 Trends in GrIS LAI**

7 Ice core analyses of black carbon in the central regions of the GrIS have been used
8 to study long-term variability and trends in pollution deposition (McConnell et al., 2007;
9 Keegan et al., 2014). These records show that snow at these locations was significantly
10 more polluted in the first half of the 20th century than presently. Both these records and
11 in-situ measurements at Summit (Cachier and Pertuisot, 1994; Chylek et al., 1995; Hagler
12 et al., 2007; Doherty et al, 2010) also indicate that in recent decades, the snow in central
13 Greenland has been relatively clean, with concentrations smaller than 4 ng g⁻¹ for BC.
14 This amount of BC could lower snow albedo by only 0.002 for $r=100\ \mu\text{m}$, or 0.005 for
15 $r=500\ \mu\text{m}$ (Figure 5a of Dang et al., 2015). More recently, Polashenski et al. (2015)
16 analysed BC and dust concentrations in 2012-2014 snowfall along a transect in northwest
17 Greenland. They found similarly low concentrations of BC and concluded that albedo
18 decreases in their study region are unlikely to be attributable to increases in BC or dust.
19 Black carbon measurements from a high snowfall region of west central Greenland made
20 on an ice core collected in 2003 show that black carbon concentrations varied
21 significantly during the past 215 years, with an average annual concentration of 2.3 ng g⁻¹
22 during the period 1952 – 2002, characterized by high year-to-year variability in summer
23 and a gradual decline in winter BC concentrations through the end of the century
24 (McConnell et al., 2007). Snow sampled in 1983 at Dye-3 had a median of 2 ng g⁻¹
25 (Clarke and Noone, 1985). In 2008 and 2010, measurements 160 km away at Dye-2,
26 using the same method, had medians of 4 ng g⁻¹ in spring and 1 ng g⁻¹ in summer (Table 9
27 of Doherty et al, 2010).

28 In the absence of in-situ measurements of impurity concentration trends over
29 Greenland more broadly, or of trends in aerosol deposition rates (which are absent

entirely), we investigate trends in emissions from key sources of aerosols deposited to the GrIS and trends in Atmospheric Optical Depth (AOD) over GrIS.

3.4.2 Trends in fire count and BC emissions

Biomass burning in North America and Siberia is a significant source of combustion aerosol (BC and associated organics) to the GrIS (Hegg et al., 2009, 2010). Therefore, we investigated trends in the number of active fires in these two source regions, as well as BC emissions from fires in sub-regions within the northern hemisphere. For fire counts we used the MODIS monthly active fire products produced by the TERRA (MOD14CMH) and AQUA sensors (MYD14CMH) generated at 0.5° spatial resolution and distributed by the University of Maryland via anonymous ftp (http://www.fao.org/fileadmin/templates/gfims/docs/MODIS_Fire_Users_Guide_2.4.pdf, http://modis.gsfc.nasa.gov/data/dataproduct/dataproducts.php?MOD_NUMBER=14). The results of our analysis are summarised in Figure 7, showing the standardised (subtracting the mean and dividing by the standard deviation of the 2002 – 2012 baseline period) cumulative number of fires (April through August) detected over North America (NA) and Eurasia (EU) by the MOD14CMH and MYD14CMH GCM climatology products between 2002 and 2012. The figure shows large inter-annual variability but no significant trend (at 90 % level) in the number of fires over the two areas between 2002 and 2012. The period between 2004 and 2011, when enhanced melting occurred over the GrIS, shows a negative trend (though also in this case not statistically significant).

In addition to number of fires we looked for trends specifically in BC emissions from fires in potential source regions for GrIS, using estimates from the Global Fire Emissions Database (GFED version 4.1, <http://www.globalfiredata.org/>). There is a great deal of inter-annual variability in annual BC emissions from fires in all regions (Figure 8), with no statistically significant increase during the 1997-2012 or 1997-2014 periods from either of the Boreal source regions or from Central Asia or Europe. BC emissions from fires in Temperate North America increased by, on average, $0.35 \times 10^9 \text{ g yr}^{-1}$ during 1997-2014 and by $0.52 \times 10^9 \text{ g yr}^{-1}$ 1997-2012 ($p < 0.1$ in both cases), or an increase of 60% from 1997 to 2012. However, the total BC emissions from fires in this region constitute a small fraction of that from the Boreal regions. In addition, the only statistically

significant trend in regional BC emissions is a *decrease* in Central Asia (112.6×10^9 g yr⁻¹; $p=0.02$), when GrIS albedo has declined most precipitously, is a *decrease* in BC emissions (-12.6×10^9 g yr⁻¹; $p=0.02$) in Central Asia. Xing et al. (2013, 2015) point out that direct anthropogenic emissions have also been decreasing across almost all of the mid- to high-latitude northern hemisphere.

3.4.3 Trends in AOD over Greenland

To investigate trends in AOD over GrIS we look at AOD as simulated by models and as measured at ground-based stations at several locations around the GrIS. AOD is a measure of the total extinction (omni-directional scattering plus absorption) of sunlight as it passes through the atmosphere, and is related to atmospheric aerosol abundance. Thus, it is a metric for the mass of aerosol available to be potentially deposited onto the GrIS surface. In the aerosol models, we are able to examine trends in total AOD as well as in aerosol components: BC, dust and organic matter. In addition, we examined trends in modelled deposition fluxes of these species to the GrIS.

For our analysis, we used model results from the Aerosol Comparisons between Observations and Models (AeroCom) project, an open international initiative aimed at understanding the global aerosol and its impact on climate (Samset et al., 2014; Myhre et al., 2013; Jiao et al., 2014; Tsigaridis et al., 2014). The project combines a large number of observations and outputs from fourteen global models to test, document and compare state-of-the-art modelling of the global aerosol. We specifically show standardised (i.e., subtracting the mean and then dividing by the standard deviation) deposition fluxes of BC, dust and organic aerosols (OA) from the GISS modelE contribution to the AeroCom phase II series of model runs (<http://aerocom.met.no/aerocomhome.html>). The runs used here took as input the decadal emission data from the Coupled Model Intercomparison Project Phase 5 (CMIP5). In this case, we report the outputs of the NASA GISS ModelE obtained from the AeroCom. In particular, Figures 9 and 10 show modelled deposition fluxes at the two locations of Kangerlussuaq (Figure 9, 67°00'31"N, 50°41'21"W) and Summit (Figure 10, 72°34'47"N, 38°27'33"W) for the months of June, July and August and aerosol components (BC, dust and organic matter). These locations were selected as representative of the ablation zone (Kangerlussuaq) and the dry-snow zone (Summit).

1 The analysis of the NASA GISS ModelE AeroCom outputs shows no statistically
2 significant trend in the modelled fluxes for either location, consistent with the results
3 recently reported by Polashenski et al. (2015) for the dry snow zone. Results of the
4 analysis of fluxes over different areas point to similar conclusions. Similar results are
5 obtained when considering the months of January, February and March, when aerosol
6 concentration is expected to be higher. The results here presented complement other
7 studies (e.g. Stone et al., 2014) indicating that, since the 1980s, atmospheric
8 concentrations of BC measured at surface stations in the Arctic have decreased, with
9 variations attributed to changes in both anthropogenic and natural aerosol and aerosol
10 precursor emissions.

11 Mean summer values of AOD (550 nm) measured at three AERONET
12 (<http://aeronet.gsfc.nasa.gov>) Greenland sites based in Thule (northwest Greenland;
13 77°28'00"N, 69°13'50"W), Ittoqqortoormiit (east-central Greenland; 70°29'07"N,
14 21°58'00"W), and Kangerlussuaq during the period 2007 – 2013 (with the starting year
15 ranging between 2007 and 2009, depending on the site) are reported in Table 2, together
16 with their standard deviations. None of the stations show statistically significant trends in
17 AOD, consistent with the results of the analysis of the modelled deposition fluxes.

18 A recent study (Dumont et al., 2014) concluded that dust deposition has been increasing
19 over much of the GrIS and that this is driving lowered albedo across the ice sheet. That
20 conclusion was based on trends of an “impurity index”, which is the ratio of the
21 logarithm of albedo in the 545-565 nm MODIS band (where LAI affect albedo) to the
22 logarithm of albedo in the 841-876 nm band (where they do not). In the MODIS product
23 used in Dumont et al. (2014) study, albedo values rely on removal of the effects of
24 aerosols in the atmosphere. In the Dumont et al. (2014) study this correction was made
25 using simulations of atmospheric aerosols by the Monitoring Atmospheric Composition
26 and Climate (MACC) model. Their resulting “impurity index” shows positive trends, and
27 these are attributed in part (up to 30%) to increases in atmospheric aerosol not accounted
28 for by the model, and the remainder to increases in snow LAI. The latter is consistent
29 with our findings herein: that GrIS darkening is in part attributable to an increase in the
30 impurity content of surface snow. However, Dumont et al. (2014) assume that this

1 increase in surface snow LAI is a result of enhanced deposition from the atmosphere.
2 They do not account for the possibility that positive trends in impurity content may
3 instead be a result of a warming-driven in-snow processes. Indeed, their own table shows
4 variable AOD at AERONET stations in Greenland, but no trend over the period studied
5 (2007 – 2012).

6 The results of the analysis discussed above reinforce our argument that the decline in
7 the visible albedo over Greenland is probably not due to an increase in the rate of
8 deposition of LAI from the atmosphere, but instead are due to the consolidation of LAI at
9 the snow surface with warming-driven increases in melt and/or sublimation and with the
10 increased exposure of underlying dirty ice.

11 **4 Albedo projections through 2100**

12 We estimated future projections of summer albedo over the GrIS using MAR
13 forced with the outputs of three different Earth System Models (ESMs) from CMIP5
14 driven by two radiative forcing scenarios (Meinshausen et al., 2011) over the 120-year
15 period 1980 – 2100. The first scenario corresponds to an increase in the atmospheric
16 greenhouse gas concentration to a level of 850 ppm CO₂ equivalent (RCP45); the second
17 scenario increases CO₂ equivalent to > 1370 ppm in 2100 (RCP85) (Moss et al., 2010;
18 Meinshausen et al., 2011). The three ESMs used are the second generation of the
19 Canadian Earth System Model (CanESM2), the Norwegian Community Earth System
20 Model (NorESM1) and the Model for Interdisciplinary Research on Climate (MIROC5)
21 of the University of Tokyo, Japan. More information is available in Tedesco and Fettweis
22 (2012). The ESMs are used to generate MAR outputs for the historical period (1980 –
23 2005) and for future projections (2005 – 2100). The Canadian Earth System Model
24 (CanESM2, e.g. Arora and Boer, 2010, Chylek et al., 2011) combines the fourth
25 generation climate model (CanCM4) from the Canadian Center for Climate Modelling
26 and Analysis with the terrestrial carbon cycle based on the Canadian Terrestrial
27 Ecosystem Model (CTEM), which models the land-atmosphere carbon exchange. The
28 NorESM1 model is built under the structure of the Community Earth System Model
29 (CESM) of the National Center for Atmospheric Research (NCAR). The major difference
30 from the standard CESM configuration concerns a modification to the treatment of

atmospheric chemistry, aerosols, and clouds (Seland et al., 2008) and the ocean component. Lastly, MIROC5 is a coupled general circulation model developed at the Center for Climate System Research (CCSR) of the University of Tokyo, composed of the CCSR/NIES (National Institute of Environmental Studies) atmospheric general circulation model (AGCM 5.5) and the CCSR Ocean Component Model, including a dynamic-thermodynamic sea-ice model (e.g., Watanabe et al., 2010, 2011). We refer to Tedesco and Fettweis (2012) for the evaluation of the outputs of MAR when forced with the outputs of the ESMs during the historical period (1980 – 2005). All simulations consistently point to darkening accelerating through the end of the century (Figure 11), with summer albedo anomalies (relative to year 2000) as large as -0.08 by the end of the century over the whole ice sheet, and even greater (-0.1) over the western portion of the ice sheet (Figure 12). The magnitude of the projected albedo anomalies by 2100, however, is probably underestimated by our simulations, because (a) the model tends to underestimate melting when forced with the ESMs (Fettweis et al., 2013), and therefore underestimates grain size growth, and (b) the model currently does not account for the presence of LAI in the snow or on the ice surface, nor for the positive feedback between LAI and snow/ice melt..

5 Discussion

Our results show a darkening of the GrIS 1996-2012, and indicate that this darkening is associated with increased surface snow grain size, an expansion in the area and persistence of bare ice, and by an increase in surface snow light-absorbing impurity (LAI) concentrations. We find no evidence for general increases in the deposition of LAI across the GrIS, so we associate the higher surface snow impurity concentrations predominantly with the appearance of underlying dirty ice and the consolidation of LAI in surface snow resulting from snow melt. Inter-annual variability in the JJA GLASS albedo is captured by the MAR albedo simulations, with the latter explaining ~ 90 % of the spaceborne-derived albedo interannual variations for the period 1996 - 2012. The strong correlation between MAR and GLASS albedo time series for this period suggests that MAR is capturing the processes driving most of the albedo inter-annual variability (grain size metamorphism and bare ice exposure) and that these processes have more influence than those associated with the spatial and temporal variability of surface

1 impurity concentrations at seasonal timescales (currently not included in the MAR albedo
2 scheme). This is reinforced by the fact that the range of snow grain size found across the
3 GrIS produces larger changes in albedo than does the range of LAI concentrations
4 measured over the GrIS, at least in the cold-snow and percolation zones of the ice sheet.
5 As pointed out by Tedesco et al. (2015), for pure snow, grain growth from new snow
6 (with $r = 100 \mu\text{m}$) to old melting snow ($r = 1000 \mu\text{m}$) can reduce broadband albedo by \sim
7 10%. By comparison, adding 20 ng g^{-1} of BC, which has been found in the top layer of
8 melting GrIS snow, reduces albedo by only 1-2%, consistently with the results reported
9 by Polashenski et al. (2015).

10 Modeled (MAR) and retrieved (GLASS) albedo are compared, with the latter
11 showing stronger declines in GrIS albedo, particularly over the ablation zone. Based on
12 our analysis, we suggest that the difference between MAR and GLASS trends cannot be
13 driven solely by the MODIS sensor degradation on the TERRA satellite (also used in the
14 GLASS product), because the estimated impact of sensor degradation on the albedo trend
15 is much smaller than the difference between the MAR and GLASS trends, and because
16 the GLASS product is obtained by combining data from both TERRA and AQUA
17 satellites, hence likely reducing the impact of the TERRA sensor degradation on the
18 trends. This is especially true over the dark zone, where substantial melting occurs and
19 where the albedo decline is pronounced. As mentioned, a lack of impurities in the MAR
20 albedo scheme can affect simulated albedo trends in at least two ways: first, the
21 concentration of impurities over bare ice areas could be increasing or/and the lack of
22 impurities in the MAR albedo scheme causes bare ice areas to have an overestimated
23 albedo. Moreover, more frequent exposure of bare ice would lead to a decline in annual
24 average albedo over time, with such a trend being larger in the case of the presence of
25 impurity concentrations on the ice surface. Our sensitivity analysis of the simulated
26 trends on the bare ice albedo value indicates that the difference between MAR and
27 GLASS estimated trends is consistent with a relatively darker (e.g., containing LAI) bare
28 ice. Since MAR does not account for the presence of surface LAI, and because the impact
29 of LAI is mostly in the UV and visible portion of the spectrum, we suggest that another
30 mechanism explaining the difference of $-0.017 \text{ decade}^{-1}$ between the MAR and GLASS
31 visible albedo trends is associated with increasing mixing ratios of LAI in surface snow

1 and ice on some parts of the GrIS. As we pointed out, this could be due to a combination
2 of increased exposure of dirty ice with ablation (Wientjes and Oerlemans, 2010; Bøggild
3 et al., 2010), to enhanced melt consolidation with warming (e.g., Doherty et al., 2013), or
4 to increased deposition of LAI from the atmosphere. The absence of in-situ, spatially
5 distributed measurements to separate these processes means that we cannot quantify their
6 relative contributions to the darkening in the visible region. Based on our analysis of
7 trends in AOD over Greenland and the lack of a trend in forest-fire counts and BC in
8 North America and Eurasia, we argue that increased deposition of LAI is not a large
9 driver for the observed negative trends in Greenland surface albedo. An exception could
10 be an increase in the deposition of locally-transported dust near the glacial margins,
11 which would primarily affect the ablation zone. In particular, locally lofted dust may be
12 playing a substantial role in the southwest GrIS ablation zone. However, we note that
13 increased deposition is not needed in order to have an increase in the concentration of
14 LAI at the GrIS surface. As noted above, indeed, temperatures and melt rates have been
15 accelerating over the GrIS during the past decades (e.g., Tedesco et al., 2014). When
16 snow melts, snow water is removed from the surface more efficiently than particulate
17 impurities; the result is an increase in impurity concentrations in surface snow (e.g.
18 Flanner et al., 2007; Doherty et al., 2013). Large particles, such as dust, in particular, will
19 have poor mobility through the snowpack (Conway et al., 1996) so their concentration at
20 the surface is expected to increase with snowmelt. This effect may be especially
21 amplifying snow impurity content in the low-altitude ablation zone of the GrIS, where
22 enhanced melting has been occurring (e.g., Tedesco et al., 2014). Further, the albedo
23 reduction for a given concentration of an absorbing impurity in snow is greater in large-
24 grained snow than in small-grained snow (Figure 7 of Warren and Wiscombe, 1980;
25 Flanner et al., 2007), so climate warming itself will amplify the effect of LAI on surface
26 albedo. Warming may also lead to increased sublimation, removing snow water but not
27 particles from the snow surface, again increasing concentrations of LAI in surface snow.

28 Snow and ice warmed by increased temperatures and higher LAI concentrations
29 also promotes darkening via so-called 'bio-albedo', with biological growth on the surface
30 depressing the albedo. Green, pink, purple, brown and black pigmented algae, indeed,
31 occur in melting snow and ice. Microbes can bind to particulates, including BC, retaining

1 them at the surface in higher concentrations than in the parent snow and ice. The
2 magnitude of this source of darkening is currently unquantified, but as the climate warms
3 and melt seasons lengthen, biological habitats are expected to expand, with their
4 contribution to darkening likely increasing (Benning et al., 2014).

5 Quantifying the impact of aerosols on Greenland darkening is also made difficult by the
6 large disagreements among models in their predicted aerosol deposition rates over the
7 GrIS. We examine the contrast between AOD trends from the MACC model used by
8 Dumont et al., (2014) and the Goddard Chemistry Aerosol Radiation and Transport model
9 (GOCART). The GOCART model simulates major tropospheric aerosol components,
10 including sulphate, dust, BC, organic carbon (OC), and sea-salt aerosols using assimilated
11 meteorological fields of the Goddard Earth Observing System Data Assimilation System
12 (GEOS DAS), generated by the Goddard Global Modeling and Assimilation Office. Figure
13 13 compares results for AOD at 550 nm from MACC and GOCART for dust, organic
14 matter and black carbon for the domain bounded by 75 to 80°N and 30 to 50° W (the same
15 area considered by Dumont et al., 2014). The MACC model shows statistically significant
16 trends for dust ($p < 0.01$) and for total aerosols ($p < 0.05$). All remaining trends are not
17 statistically significant for both MACC and GOCART outputs (Figure 13).

18 Neither model represents the process of increased exposed silt/dust as Greenland
19 glaciers recede; therefore, we would not expect them to capture trends in dust from this
20 source. The inconsistency between the MACC and GOCART values and trends is
21 puzzling, and indicates that the simulation of aerosol deposition rates over Greenland
22 needs improvement.

23 **6 Summary and conclusions**

24 We studied the mean summer broadband albedo over the Greenland ice sheet
25 between 1981 and 2012 as estimated from spaceborne measurements and found that
26 summer albedo decreased at a rate of 0.02 decade^{-1} between 1996 and 2012. The analysis
27 of the outputs of the MAR regional climate model indicates that the observed darkening
28 is associated with increasing temperatures and enhanced melting occurring during the
29 same period, which in turn promote increased surface snow grain size as well as the
30 expansion and persistency of areas with exposed bare ice. The MAR model simulates

1 well the interannual variability in the retrieved GLASS albedo, but the albedo trend is
2 larger in the GLASS albedo product than in MAR, indicating that processes not
3 represented in the MAR physics account for some of the declining albedo. Specifically,
4 we suggest that the absence of the effects of light-absorbing impurities in MAR could
5 account for the difference. We also suggest that this hypothesis is supported by the trends
6 observed along the ablation zone, where the differences between observed and modeled
7 trends are more pronounced and the effect of the TERRA sensor degradation plays a
8 relatively small role. On the other hand, over the dry snow zone, our hypothesis requires
9 further testing, in view of the potentially higher impact of the sensor degradation on the
10 observed albedo trend. The analysis of modelled fields and in-situ data indicated an
11 absence of trends in aerosol optical depth over Greenland, as well as no significant trend
12 in particulate light-absorbing emissions (e.g. BC) from fires in likely source regions. This
13 is consistent with the absence of trends in surface aerosol concentrations measured
14 around the Arctic. Consequently, we suggest that the increased surface concentrations of
15 LAI associated with the darkening is not related to increased deposition of LAI, but
16 rather to post-depositional processes, including increased loss of snow water to
17 sublimation and melt and the outcropping of ‘dirty’ underlying ice associated with
18 snow/firn removal due to ablation.

19 Future projections of GrIS albedo obtained from MAR forced under different
20 warming scenarios point to continued darkening through the end of the century, with
21 regions along the edges of the ice sheet subject to the largest decrease, driven solely by
22 warming-driven changes in snow grain size, exposure of bare ice, and melt pool
23 formation. We hypothesise that projected darkening trends would be even greater in view
24 of the underestimated projected melting (and effect on albedo) and in view of the fact that
25 the current version of the MAR model does not account for the presence of surface LAI
26 and the associated positive direct and indirect impact on lowered albedo.

27 The drivers we identified to be responsible for the observed darkening are related to
28 endogenous processes rather than exogenous ones and are strongly driven by melting.
29 Because melting is projected to increase over the next decades, it is crucial to assess the
30 state of the art of studying, quantifying and projecting these processes as they will

1 inevitably impact, and be impacted by, future scenarios. Intrinsic limitations of current
2 observational tools and techniques, the scarcity of in-situ observations, and the albedo
3 schemes currently used in existing models of surface energy balance and mass balance
4 limit our ability to separate the contributions to darkening by the different processes,
5 especially with regard to the cause and evolution of surface impurity concentrations.
6 Moreover, as with all instruments, sensors undergo deterioration, and it can be difficult to
7 separate an albedo trend from sensor drift. This is especially true in the dry-snow zone,
8 where impurity concentrations are extremely low (only a few ppb in the case of BC). In
9 this regard, a recent study by Polashenski et al. (2015) suggests that the decline and
10 spectral shift in dry snow albedo over Greenland contains important contributions from
11 uncorrected Terra sensor degradation when using the MODIS data collection C5. The
12 new MODIS TERRA version (accounting for the sensor degradation) does not appear to
13 show any trend (Polashenski, *Pers. Comm.*), hence supporting the hypothesis of the
14 absence of trends of LAI deposition over the dry zone.

15 Remote sensing and in-situ observations should be complemented with models that
16 simulate the surface energy balance to account for the evolution of the snowpack, in
17 particular changes in surface grain size and exposure of bare ice. Simulations with
18 regional climate models can provide such quantities, but they do not currently account for
19 the transport and deposition of LAI to Greenland, the post-depositional evolution of
20 impurities in the snowpack, and the synergism between surface LAI and grain growth
21 (whereby a given impurity content causes more albedo reduction in coarse-grained snow
22 than in fine-grained snow). In this regard, the current parameterisation for snow albedo in
23 MAR is based on that of Brun et al. (1992), as part of an avalanche-forecasting model.
24 As a consequence of the results of this study, we began evaluating an alternative albedo
25 scheme using a parameterisation that can also account for the albedo reduction by
26 absorptive impurities (e.g. Dang et al., 2015). Moreover, we are also considering using
27 the firn/ice albedo parameterisation of Dadic et al (2013), based on measurements
28 covering the range of densities from 400 to 900 kg m⁻³.

29 Surface-based measurements are needed to test satellite-retrieved albedo and to
30 quantify the drivers behind albedo changes in different areas of Greenland. To date, most
31 surface-based observations have been made in the dry-snow zone or the percolation zone,

1 and they have generally focused on measuring the mixing ratios of BC (Hagler et al.,
2 2007; McConnell et al., 2007, 2011; Polashenski et al., 2015) or of the spectral light
3 absorption by all particulate components collectively (Doherty et al., 2010; Hegg et al.,
4 2009, 2010). The regions of Greenland that are darkening the most rapidly are within the
5 ablation zone. Here, there is no direct evidence that the rate of atmospheric deposition of
6 LAI has been increasing. In view of the cumulative effect of snowmelt leaving impurities
7 at the surface, the intra-seasonal variation of deposition may not be as important as the
8 exposure of LAI by melting. Changes in the abundances of light-absorbing algae and
9 other organic material with warmer temperatures may also be contributing to declining
10 albedo, particularly for the ice, but this is an essentially un-studied source of darkening.
11 Until measurements are made that quantify and distinguish the relative roles of each of
12 these factors in the darkening of the GrIS, it is not possible to reduce the uncertainty in
13 their contributions to the acceleration of surface melt. In addition to the need for targeted
14 ground observations, it is necessary for the models that simulate and project the evolution
15 of surface conditions over Greenland to start including the contribution of surface LAI,
16 their processes, and their impact on albedo, as well as aerosol models that account for
17 their deposition. Concurrently, spaceborne sensors or missions capable of separating the
18 contributions from the different processes (with increased spatial, spectral and
19 radiometric resolution) should be planned for remote sensing to become a more valuable
20 tool in this regard.

21 **Author contributions**

22 MT conceived the study, carried out the scientific analysis and wrote the main body
23 of the manuscript. SD co-wrote the manuscript and provided feedback on the analysis of
24 the impact of surface LAI on the albedo decrease. PA provided MODIS visible data for
25 the comparison with the GLASS-estimated visible albedo. JJ supported the reprojection
26 and analysis of GLASS and MAR data. XF contributed with the analysis of MAR
27 outputs. MT, SD, XF and JS edited the final version of the manuscript.

28 **Acknowledgments**

29 MT and PA were supported by NSF grants PLR1304807 and ANS 0909388, and NASA
30 grant NNX1498G. The authors are grateful to Kostas Tsirigadis (NASA GISS) for

1 providing the outputs of GISS modelE of the AeroCom phase II project and to Marie
2 Dumont, Eric Brun and Samuel Morin for the data used in Figure 13.

3 We thank Tao He at the University of Maryland, College Park, for the discussion
4 on the GLASS product. The authors thank Stephen Warren for providing suggestions and
5 guidance during the preparation of the manuscript, particularly for pointing out
6 limitations and providing suggestions on the albedo parameterisations.

7 **7 References**

- 8 Alexander, P. M., Tedesco, M., Fettweis, X., van de Wal, R. S. W., Smeets, C. J. P. P.
9 and van den Broeke, M. R.: Assessing spatio-temporal variability and trends (2000–
10 2013) of modelled and measured Greenland ice sheet albedo, *The Cryosphere*, 8(4),
11 2293–2312, 2014.
- 12 Arnaud, L., J.M. Barnola, and P. Duval, Physical modeling of the densification of
13 snow/firn and ice in the upper part of polar ice sheets. In *Physics of Ice Core Records*
14 (T. Hondoh, Ed.), Hokkaido University Press, Sapporo, Japan, 285–305, 2000
- 15 Arora V. K. and Boer G. J., Uncertainties in the 20th century carbon budget associated
16 with land use change *Glob. Change Biol.* **16**(12), 3327–3348, doi:10.1111/j.1365-
17 2486.2010.02202.x, 2010
- 18 Benning, L. G., Anesio, A. M., Lutz, S. and Tranter, M.: Biological impact on
19 Greenland's albedo, *Nature Geosci.* **7**(10), 691–691, doi:10.1038/ngeo2260, 2014.
- 20 Benson, C.S., 1962: *Stratigraphic Studies in the Snow and Firn of the Greenland Ice*
21 *Sheet*. Research Report 70, U.S. Army Snow, Ice, and Permafrost Research
22 Establishment (SIPRE), 93 pp.
- 23 Bøggild, C.E., R.E. Brandt, K.J. Brown, and S.G. Warren (2010), The ablation zone in
24 northeast Greenland: Ice types, albedos, and impurities. *J. Glaciol.*, **56**, 101–113.
- 25 Bond, T. C., S. J. Doherty, D. W. Fahey, P. M. Forster, T. Berntsen, B. J. DeAngelo, M.
26 G. Flanner, S. Ghan, B. Kärcher, D. Koch, S. Kinne, Y. Kondo, P. K. Quinn, M. C.
27 Sarofim, M. G. Schultz, M. Schulz, C. Venkataraman, H. Zhang, S. Zhang, N.
28 Bellouin, S. K. Guttikunda, P. K. Hopke, M. Z. Jacobon, J. W. Kaiser, Z. Klimont, U.
29 Lohmann, J. P. Schwarz, D. Shindell, T. Storelvmo, S. G. Warren and C. S. Zender,
30 Bounding the Role of Black Carbon in Climate: A scientific assessment, *J. Geophys.*
31 *Res.*, 118(11), 5380–5552, doi:10.1002/jgrd.50171, 2013.
- 32 Box, J. E., Fettweis, X., Stroeve, J. C., Tedesco, M., Hall, D. K., and Steffen, K.:
33 Greenland ice sheet albedo feedback: thermodynamics and atmospheric drivers, *The*
34 *Cryosphere*, 6, 821–839, doi:10.5194/tc-6-821-2012, 2012.
- 35 Brun, E., David, P., Sudul, M. and Brunot, G.: A numerical model to simulate snow-
36 cover stratigraphy for operational avalanche forecasting, *Journal of Glaciology*,
37 **38**(128), 13–22, 1992.

1 Cachier, H. and Pertuisot, M. H.: Particulate carbon in Arctic ice, *Analisis Magazine*, 22,
2 34–37, 1994

3 Ch'ylek, P., Johnson, B., Damiano, P. A., Taylor, K. C., and Clement, P.: Biomass
4 burning record and black carbon in the GISP2 ice core, *Geophys. Res. Lett.*, 22, 89–
5 92, 1995. –

6 Chylek ,P., Li ,J., Dubey ,M. K., Wang ,M. and Lesins G., Observed and model simulated
7 20th century Arctic temperature variability: Canadian Earth System Model
8 CanESM2 *Atmos. Chem. Phys. Discuss.* **11** 22893–22907, 2011

9 Clarke, A.D. and Noone, K.J.: Soot in the Arctic snowpack: A cause for perturbations in
10 radiative transfer, *Atmos. Environ.*, 19, 2045–2053, 1985.

11 Conway, H., A. Gades, and C. F. Raymond (1996), Albedo of dirty snow during
12 conditions of melt, *Water Resour. Res.*, **32**(6), 1713–1718.

13 Dadic, R., P.C. Mullen, M. Schneebeli, R.E. Brandt, and S.G. Warren, 2013: Effects of
14 bubbles, cracks, and volcanic tephra on the spectral albedo of bare ice near the Trans-
15 Antarctic Mountains: implications for sea-glaciers on Snowball Earth. *J. Geophys.*
16 *Res. (Earth Surfaces)*, 118, doi:10.1002/jgrf.20098.

17 Dang, C., R.E. Brandt, and S.G. Warren, 2015: Parameterizations for narrowband and
18 broadband albedo of pure snow, and snow containing mineral dust and black carbon.
19 *J. Geophys. Res.*, 120, doi:10.1002/2014JD022646.

20 De Ridder K., and Galle' H. Land surface-induced regional climate change in Southern
21 Israel,*Appl. Meteorol.*, 37, 1470-1485, 1998.

22 Doherty, S. J., Grenfell, T. C., Forsström, S., Hegg, D. L., Brandt, R. E. and Warren, S.
23 G.: Observed vertical redistribution of black carbon and other insoluble light-
24 absorbing particles in melting snow, *Journal of Geophysical Research: Atmospheres*,
25 118(11), 5553–5569, 2013.

26 Doherty, S. J., Warren, S. G., Grenfell, T. C., Clarke, A. D. and Brandt, R. E.: Light-
27 absorbing impurities in Arctic snow, *Atmos. Chem. Phys.*, 10(23), 11647–11680,
28 2010.

29 Dumont, M., Brun, E., Picard, G., Michou, M., Libois, Q., Petit, J.-R., Geyer, M.,
30 Morin, S. and Josse, B.: Contribution of light-absorbing impurities in snow to
31 Greenland's darkening since 2009, *Nature Geosci.*, 7(7), 509–512, 2014.

32 Fettweis, X., Franco, B., Tedesco, M., van Angelen, J. H., Lenaerts, J. T. M., van den
33 Broeke, M. R. and Gallée, H.: Estimating the Greenland ice sheet surface mass
34 balance contribution to future sea level rise using the regional atmospheric climate
35 model MAR, *The Cryosphere*, 7(2), 469–489, 2013.

36 Fettweis, X., Gallée, H., Lefebvre, F. and van Ypersele, J.-P.: Greenland surface mass
37 balance simulated by a regional climate model and comparison with satellite-derived
38 data in 1990–1991, *Climate Dynamics*, 24(6), 623–640, 2005.

- 1 Flanner, M. G., Zender, C. S., Randerson, J. T., and Rasch, P. J.: Present-day climate
2 forcing and response from black carbon in snow, *J. Geophys. Res.*, 112, D11202,
3 doi:10.1029/2006JD008003, 2007.
- 4 Grenfell, T.C., D.K. Perovich, and J.A. Ogren, 1981: Spectral albedos of an alpine
5 snowpack. *Cold Reg. Sci. Technol.*, 4, 121-127.
- 6 Greuell, W. and Konzelman, T.: Numerical modelling of the energy balance and the
7 englacial temperature of the Greenland Ice Sheet, Calculations for the ETH-Camp
8 location (West Greenland, 1155 m a.s.l.), *Global and Planetary Change*, 9, 91–114,
9 1994.
- 10 Hagler, G. S. W., Bergin, M. H., Smith, E. A., and Dibb, J. E.: A summer time series of
11 particulate carbon in the air and snow at Summit, Greenland, *J. Geophys. Res.*, 112,
12 D21309, doi:10.1029/2007JD008993, 2007.
- 13 He, T., Liang, S., Yu, Y., Wang, D., Gao, F. and Liu, Q.: Greenland surface albedo
14 changes in July 1981–2012 from satellite observations, *Environ. Res. Lett.*, 8(4),
15 044043, 2013.
- 16 Hegg, D. A., Warren, S. G., Grenfell, T. C., Doherty, S. J., Larson, T. V. and Clarke, A.
17 D.: Source Attribution of Black Carbon in Arctic Snow, *Environmental Science &*
18 *Technology*, 43(11), 4016–4021, 2009.
- 19 Hegg, D.A., S.G. Warren, T.C. Grenfell, S.J. Doherty, and A.D. Clarke, 2010: Sources
20 of light-absorbing aerosol in Arctic snow and their seasonal variation. *Atmos. Chem.*
21 *Phys.*, 10, 10923-10938 .
- 22 Herron, M.M., and C.C. Langway, Jr., 1980: Firn densification: An empirical model. *J.*
23 *Glaciol.*, 25, 373-385.
- 24 Ichoku, C. and Ellison, L.: Global top-down smoke-aerosol emissions estimation using
25 satellite fire radiative power measurements, *Atmos. Chem. Phys.*, 14(13), 6643–
26 6667, 2014.
- 27 Keegan, K. M., M. R. Albert, J. R. McConnell and I. Baker, climate change and forest
28 fires synergistically drive widespread melt events of the Greenland Ice Sheet, *PNAS*,
29 111, 7964-7967, doi: 10.1073/pnas.1405397111.
- 30 LaChapelle, E.R.: *Field Guide to Snow Crystals*, University of Washington Press, Seattle,
31 1969.
- 32 Jiao, C., et al.: An AeroCom assessment of black carbon in Arctic snow and sea ice,
33 *Atmos. Chem. Phys.*, 14(5), 2399–2417, 2014.
- 34 Lefebvre, F., Gallée, H, and van Ypersele, J.-P.: Modeling of snow and ice melt at ETH
35 Camp (West Greenland): a study of surface albedo,, 108, 4231,
36 doi:10.1029/2001JD001160, 2003
- 37 Liang, S., et al.: A long-term Global LAnd Surface Satellite (GLASS) data-set for
38 environmental studies, *International Journal of Digital Earth*, 6(sup1), 5–33, 2013.
- 39 Loeb, N.: In-flight calibration of NOAA AVHRR visible and near-IR bands over
40 Greenland and Antarctica, *International Journal of Remote Sensing*, 18, 477–490,
41 1997.

- 1 Masonis, S. J. and Warren, S. G.: Gain of the AVHRR visible channel as tracked using
2 bidirectional reflectance of Antarctic and Greenland snow, *International Journal of*
3 *Remote Sensing*, 22, 1495–1520, 2001.
- 4 McConnell, J. R., R. Edwards, G. L. Kok, M. G. Flanner, C. S. Zender, E. S. Saltzman,
5 J. R. Banta, D. R. Pasteris, M. M. Carter, and J. D. W. Kahl, 20th-century industrial
6 black carbon emissions altered Arctic climate forcing, *Science*, 317(5843), 1381–
7 1384, doi:10.1126/science.1144856, 2007.
- 8 McConnell, J. R., Edwards, R., Kok, G. L., Flanner, M. G., Zender, C. S. Saltzman, E.
9 S., Banta, J. R., Pasteris, D. R., Carter, M. M., and Kahl, J. D. W.: 20th century
10 industrial black carbon emissions altered Arctic climate forcing, *Science*, 317, 1381–
11 1384, doi:10.1126/science.1144856, 2007. Meinshausen, et al.: The RCP greenhouse
12 gas concentrations and their extensions from 1765 to 2300, *Climatic Change*, 109(1-
13 2), 213–241, 2011.
- 14 Moss, R. H., et al.: The next generation of scenarios for climate change research and
15 assessment, *Nature*, 463(7282), 747–756, 2010.
- 16 Myhre, et al.: Radiative forcing of the direct aerosol effect from AeroCom Phase II
17 simulations, *Atmos. Chem. Phys.*, 13(4), 1853–1877, 2013.
- 18 Nghiem, S. V., Hall, D. K., Mote, T. L., Tedesco, M., Albert, M. R., Keegan, K.,
19 Shuman, C. A., DiGirolamo, N. E. and Neumann, G.: The extreme melt across the
20 Greenland ice sheet in 2012, *Geophysical Research Letters*, 39(20), L20502, 2012.
- 21 Polashenski, C. M., J. E. Dibb, M. G. Flanner, J. Y. Chen, Z. R. Courville, A. M. Lai, J.
22 J. Schauer, M. M. Shafer, and M. Bergin: Neither dust nor black carbon causing
23 apparent albedo decline in Greenland's dry snow zone: Implications for MODIS C5
24 surface reflectance, *Geophys. Res. Lett.*, 42, 9319–9327,
25 doi:10.1002/2015GL065912, 2015.
- 26 Rae, J. G. L., Aðalgeirsdóttir, G., Edwards, T. L., Fettweis, X., Gregory, J. M., Hewitt,
27 H. T., Lowe, J. A., Lucas-Picher, P., Mottram, R. H., Payne, A. J., Ridley, J. K.,
28 Shannon, S. R., van de Berg, W. J., van de Wal, R. S. W. and van den Broeke, M.
29 R.: Greenland ice sheet surface mass balance: evaluating simulations and making
30 projections with regional climate models, *The Cryosphere*, 6(6), 1275–1294, 2012.
- 31 Rignot, E., Velicogna, I., van den Broeke, M. R., Monaghan, A. and Lenaerts, J. T. M.:
32 Acceleration of the contribution of the Greenland and Antarctic ice sheets to sea
33 level rise, *Geophysical Research Letters*, 38(5), L05503, 2011.
- 34 Samset, B. H., Myhre, G., Herber, A., Kondo, Y., Li, S. M., Moteki, N., Koike, M.,
35 Oshima, N., Schwarz, J. P., Balkanski, Y., Bauer, S. E., Bellouin, N., Bernsten, T.
36 K., Bian, H., Chin, M., Diehl, T., Easter, R. C., Ghan, S. J., Iversen, T., Kirkevåg,
37 A., Lamarque, J. F., Lin, G., Liu, X., Penner, J. E., Schulz, M., Seland, Ø., Skeie, R.
38 B., Stier, P., Takemura, T., Tsigaridis, K. and Zhang, K.: Modeled black carbon
39 radiative forcing and atmospheric lifetime in AeroCom Phase II constrained by
40 aircraft observations, *Atmospheric Chemistry and Physics Discussions*, 14(14),
41 20083–20115, 2014.

- 1 Schaaf, C. B., Gao, F., Strahler, A. H., Lucht, W., Li, X., Tsang, T., Strugnell, N. C.,
2 Zhang, X., Jin, Y., Muller, J. P., Lewis, P., Barnsley, M., Hobson, P., Disney, M.,
3 Roberts, G., Dunderdale, M., Doll, C., d'Entremont, R. P., Hu, B., Liang, S., Privette,
4 J. L. and Roy, D.: First operational BRDF, albedo nadir reflectance products from
5 MODIS, *Remote Sensing of Environment*, 115, 1296–1300, 2002.
- 6 Seland, O., T. Iversen, A. Kirkevåg and T. Storelvmo, Aerosol-climate interactions in the
7 CAM-Oslo atmospheric GCM and investigation of associated basic shortcomings
8 *Tellus A* **60** p 459–491. doi: 10.1111/j.1600-0870.2008.00318.x, 2008
- 9 Shepherd, A., et al.: A Reconciled Estimate of Ice-Sheet Mass Balance, *Science*,
10 338(6111), 1183–1189, 2012.
- 11 Steffen, K. and Box, J. E.: Surface climatology of the Greenland ice sheet: Greenland
12 Climate Network 1995–1999, *Journal of Geophysical Research*, 106(D24), 33951–
13 33964, 2001.
- 14 Stohl, A., et al.: Pan-Arctic enhancements of light absorbing aerosol concentrations due
15 to North American boreal forest fires during summer 2004, *J. Geophys. Res.*,
16 111(D22), D22214, 2006.
- 17 Stone, R. S., Sharma, S., Herber, A., Eleftheriadis, K. and Nelson, D. W.: A
18 characterization of Arctic aerosols on the basis of aerosol optical depth and black
19 carbon measurements, *Elementa: Science of the Anthropocene*, 2, 000027, 2014.
- 20 Stroeve, J., Box, J. E., Gao, F., Liang, S., Nolin, A. and Schaaf, C.: Accuracy assessment
21 of the MODIS 16-day albedo product for snow: comparisons with Greenland in situ
22 measurements, *Remote Sensing of Environment*, 94(1), 46–60, 2005.
- 23 Stroeve, J., Box, J. E., Wang, Z., Schaaf, C. and Barrett, A.: Re-evaluation of MODIS
24 MCD43 Greenland albedo accuracy and trends, *Remote Sensing of Environment*,
25 138, 199–214, 2013.
- 26 Tedesco, M. and Fettweis, X.: 21st century projections of surface mass balance changes
27 for major drainage systems of the Greenland ice sheet, *Environ. Res. Lett.*, 7(4),
28 045405, 2012.
- 29 Tedesco, M., Fettweis, X., Broeke, M. R. V. D., Wal, R. S. W. V. de, Smeets, C. J. P. P.,
30 Berg, W. J. V. de, Serreze, M. C. and Box, J. E.: The role of albedo and
31 accumulation in the 2010 melting record in Greenland, *Environ. Res. Lett.*, 6(1),
32 014005, 2011.
- 33 Tedesco, M., Fettweis, X., Mote, T., Wahr, J., Alexander, P., Box, J. E. and Wouters, B.:
34 Evidence and analysis of 2012 Greenland records from spaceborne observations, a
35 regional climate model and reanalysis data, *The Cryosphere*, 7(2), 615–630, 2013.
- 36 Tedesco, M., S. Doherty, S. Warren, J. Stroeve, P. Alexander, X. Fettweis, and M.
37 Tranter, 2015: What darkens the Greenland ice sheet? *EOS*, in press.
- 38 Tedesco, M., J. E. Box, J. Cappelen, X. Fettweis, T. Mote, A. K. Rennermalm, R. S. W.
39 van de Wal and J. Wahr, 2014: Greenland Ice Sheet in [2013 NOAA Arctic Report
40 Card]

1 Tsigaridis, K., et al.: The AeroCom evaluation and intercomparison of organic aerosol in
2 global models, *Atmospheric Chemistry and Physics Discussions*, 14(5), 6027–6161,
3 2014.

4 van Angelen, J. H., Lenaerts, J. T. M., Lhermitte, S., Fettweis, X., Kuipers Munneke, P.,
5 van den Broeke, M. R., van Meijgaard, E. and Smeets, C. J. P. P.: Sensitivity of
6 Greenland Ice Sheet surface mass balance to surface albedo parameterization: a
7 study with a regional climate model, *The Cryosphere*, 6(5), 1175–1186, 2012.

8 van den Broeke, M. R., C. J. P. P. Smeets, and R. S. W. van de Wal, The seasonal cycle
9 and interannual variability of surface energy balance and melt in the ablation zone of
10 the west Greenland ice sheet, *Cryosphere*, 5, 377–390, doi:10.5194/tc-5-377-2011.

11 Vernon, C. L., Bamber, J. L., Box, J. E., van den Broeke, M. R., Fettweis, X., Hanna, E.
12 and Huybrechts, P.: Surface mass balance model intercomparison for the Greenland
13 ice sheet, *The Cryosphere*, 7(2), 599–614, 2013.

14 Wang, D., Morton, D., Masek, J., Wu, A., Nagol, J., Xiong, X., Levy, R., Vermote, E.
15 and Wolfe, R.: Impact of sensor degradation on the MODIS NDVI time series,
16 *Remote Sensing of Environment*, 119, 55–61, 2012.

17 Warren, S. G.: Optical properties of snow, *Reviews of Geophysics and Space Physics*,
18 20(1), 67–89, 1982.

19 Warren, S. G.: Can black carbon in snow be detected by remote sensing? *Journal of*
20 *Geophysical Research: Atmospheres*, 118(2), 779–786, 2013.

21 Warren, S.G., and W.J. Wiscombe, 1980: A model for the spectral albedo of snow, II:
22 Snow containing atmospheric aerosols. *J. Atmos. Sci.*, **37**, 2734–2745.

23 Watanabe et al, Improved Climate Simulation by MIROC5: Mean States, Variability, and
24 Climate Sensitivity. *J. Climate*, **23**, 6312–6335, 2010

25 Watanabe S, Hajima T, Sudo K, Nagashima T, Takemura T, Okajima H, Nozawa T,
26 Kawase H, Abe M, Yokohata T, Ise T, Sato H, Kato E, Takata K, Emori S and
27 Kawamiya M 2011 MIROC-ESM: model description and basic results of CMIP5-
28 20c3m experiments, *Geosci. Model Dev. Discuss.*, **4**, 1063–1128, doi:10.5194/gmdd-
29 4-1063-2011

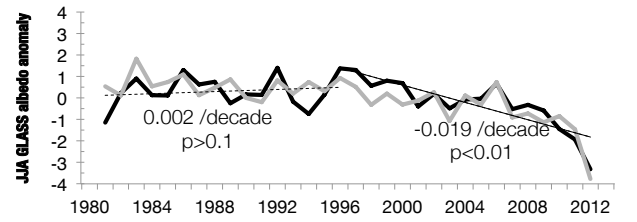
30 Wientjes, I. G. M. and Oerlemans, J.: An explanation for the dark region in the western
31 melt zone of the Greenland ice sheet, *The Cryosphere*, 4(3), 261–268, 2010.

32 Wientjes, I. G. M., van de Wal, R. S. W., Reichert, G. J., Sluijs, A. and Oerlemans, J.:
33 Dust from the dark region in the western ablation zone of the Greenland ice sheet,
34 *The Cryosphere*, 5, 589–601, 2011.

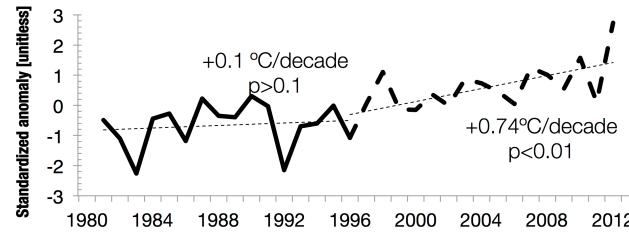
35 Xing, J., Mathur, R., Pleim, J., Hogrefe, C., Gan, C. M., Wong, D. C., Wei, C., Gilliam,
36 R. and Pouliot, G.: Observations and modeling of air quality trends over 1990–2010
37 across the Northern Hemisphere: China, the United States and Europe, *Atmos.*
38 *Chem. Phys.*, 15(5), 2723–2747, 2015.

- 1 Xing, J., Pleim, J., Mathur, R., Pouliot, G., Hogrefe, C., Gan, C. M. and Wei, C.:
2 Historical gaseous and primary aerosol emissions in the United States from 1990 to
3 2010, *Atmos. Chem. Phys.*, 13(15), 7531–7549, 2013.
- 4 Ying, Q., Qiang, L., Shunlin, L., Lizhao, W. Nanfeng, L. and Suhong L. : Direct-
5 Estimation Algorithm for Mapping Daily Land-Surface Broadband Albedo From
6 MODIS Data, *Geoscience and Remote Sensing, IEEE Transactions on* , vol.52, no.2,
7 pp.907-919, 2014, doi: 10.1109/TGRS.2013.2245670
- 8 Zhao, X.; Liang, S.; Liu, S.; Yuan, W.; Xiao, Z.; Liu, Q.; Cheng, J.; Zhang, X.; Tang,
9 H.; Zhang, X.; Liu, Q.; Zhou, G.; Xu, S.; Yu, K. The Global Land Surface Satellite
10 (GLASS) Remote Sensing Data Processing System and Products. *Remote Sens.*, 5,
11 2436-2450, 2013.
12

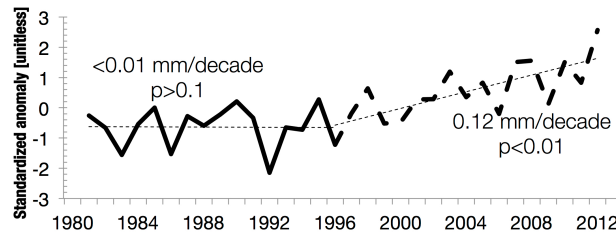
FIGURES



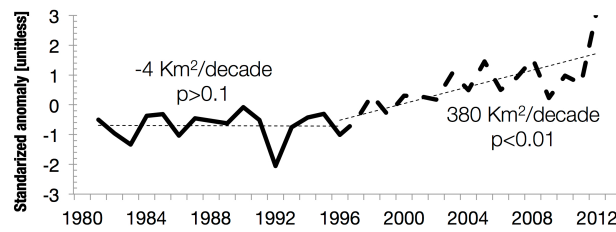
(a)



(b)



(c)



(d)

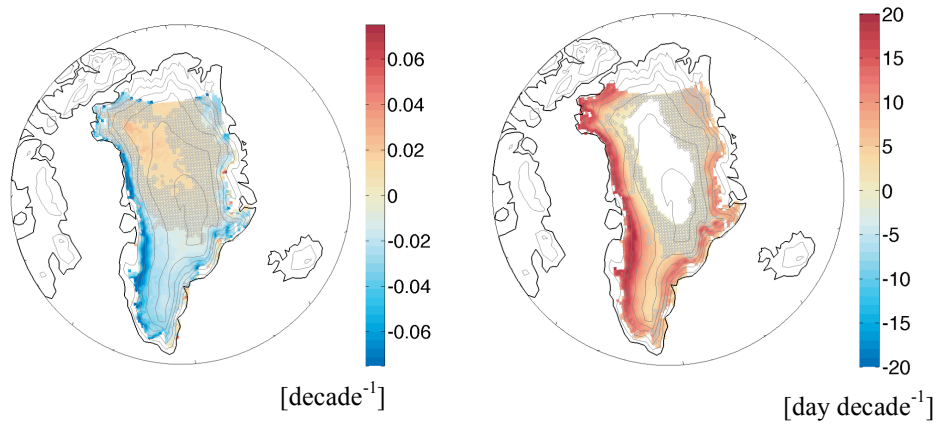
Figure 1 Mean summer standardized values plotted as time series for (a) albedo from GLASS (black) and MAR (grey), together with MAR-simulated values of (b) surface air temperature, (c) surface grain size (effective radius of optically “equivalent” sphere) and (d) bare ice exposed area. Trends for the periods 1981 – 1996 and 1996 – 2012 are reported in each plot. Trends in (a) refer to the GLASS albedo. The baseline 1981 – 2012 period is used to compute standardized anomalies, obtained by subtracting the mean and then dividing by the standard deviation of the values in the time series. All trends are computed from JJA averaged values over ice-covered areas only, not tundra.

1

2

3

4

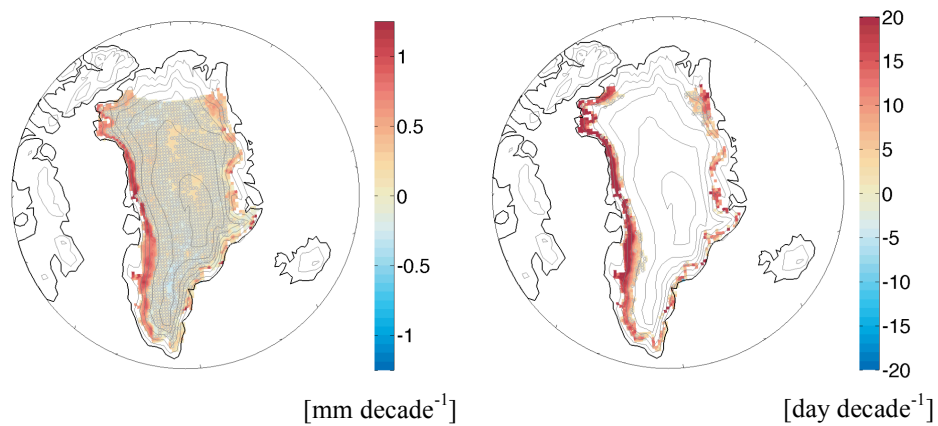


(a)

(b)

5

6



(c)

(d)

Figure 2 Maps of JJA trends (per decade) from 1996 to 2012, when darkening began to occur, for a) spaceborne estimated GLASS albedo, b) number of days when MAR-simulated surface air temperature exceeded 0°C , c) MAR-simulated surface grain size and d) number of days when bare ice is exposed as simulated by MAR. Regions where trends are not significant at a 95 % level are shown as grey-hatched areas. White regions over the north end of the ice sheet indicate areas or were not viewed by the satellite.

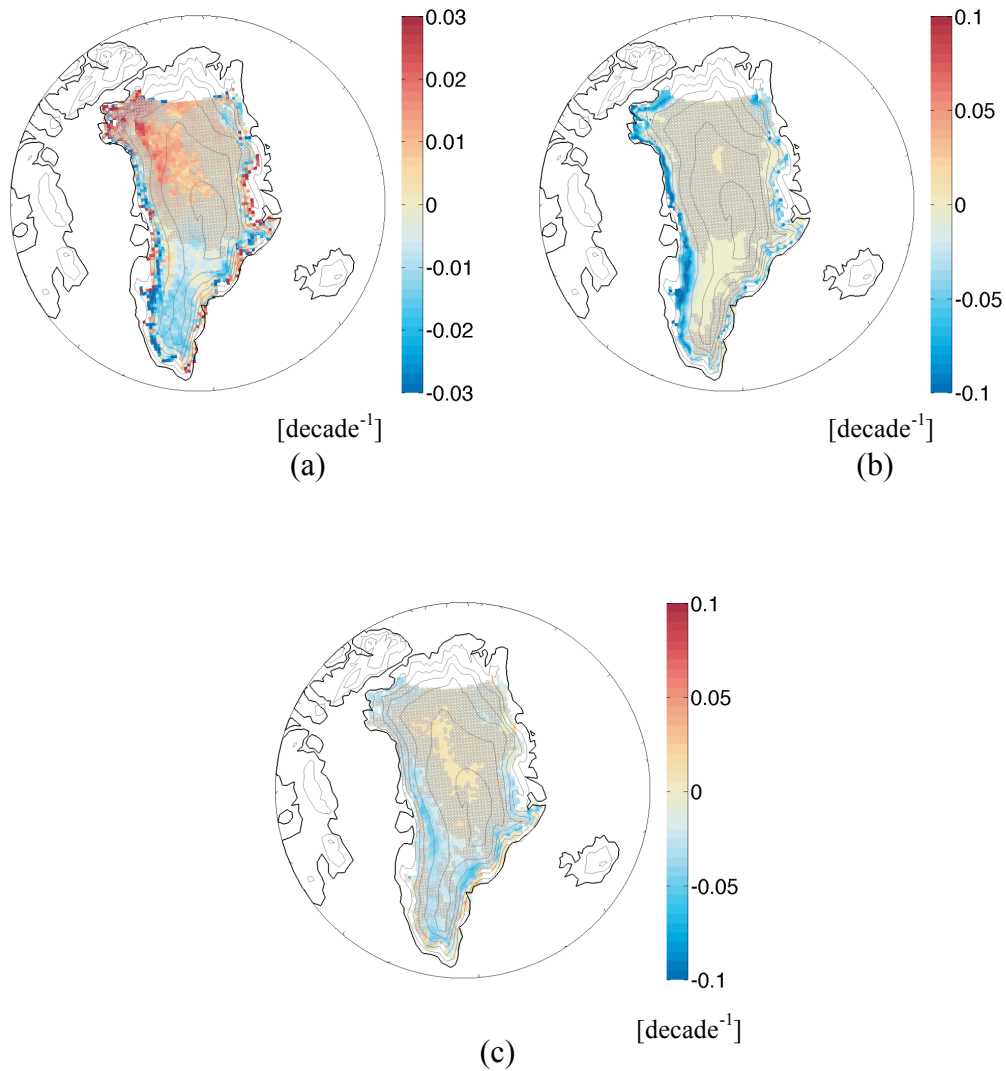
14

1

2

3

4



5

6

7

8

9

10

11

12

13

Figure 3 Differences between spaceborne measured and model-simulated albedo trends in different spectral regions. a) Difference between the GLASS and MAR trends (albedo change per decade), with positive values indicating those regions where MAR trend is smaller in magnitude than GLASS. Maps of JJA mean albedo trends (1996 – 2012) simulated by MAR for b) visible and c) near-infrared wavelengths.

1

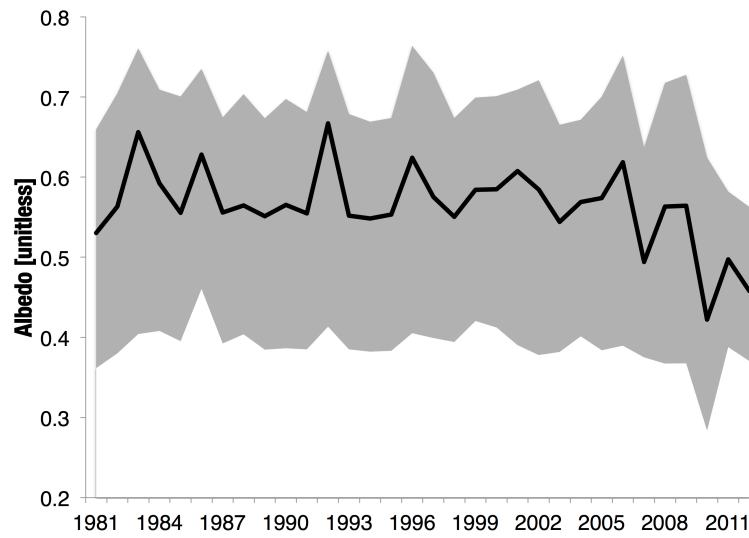
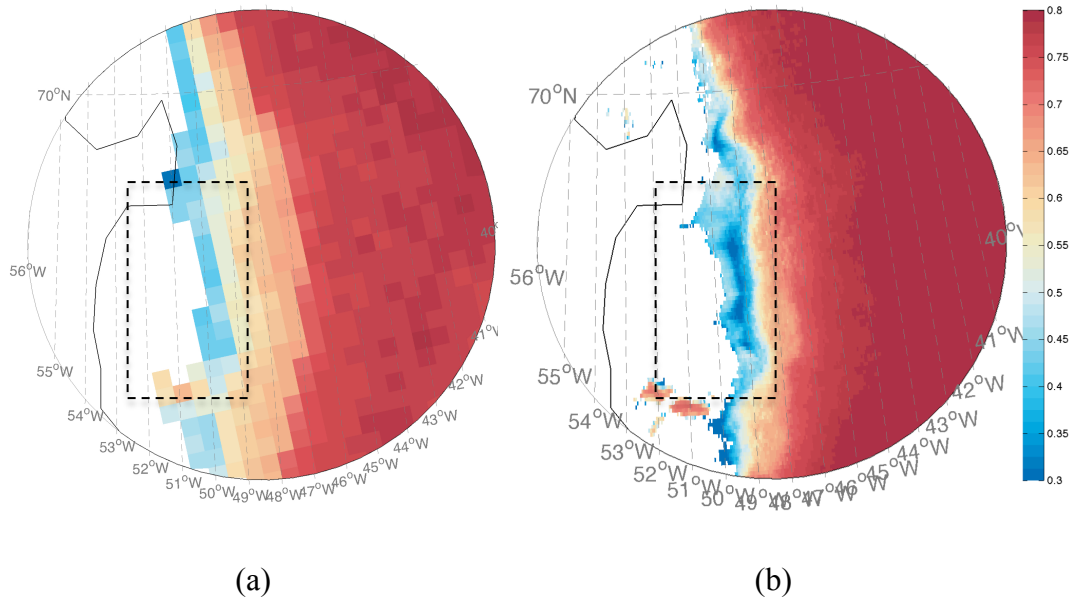
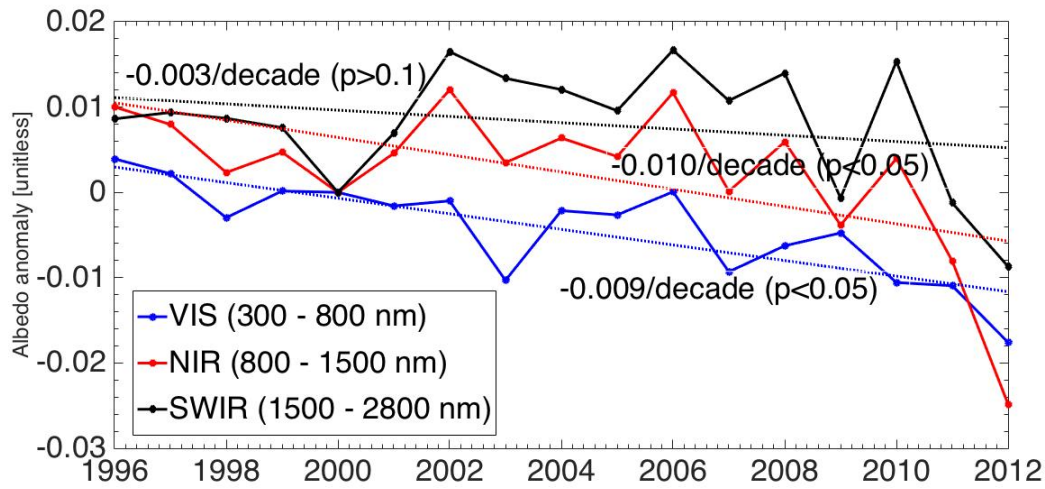
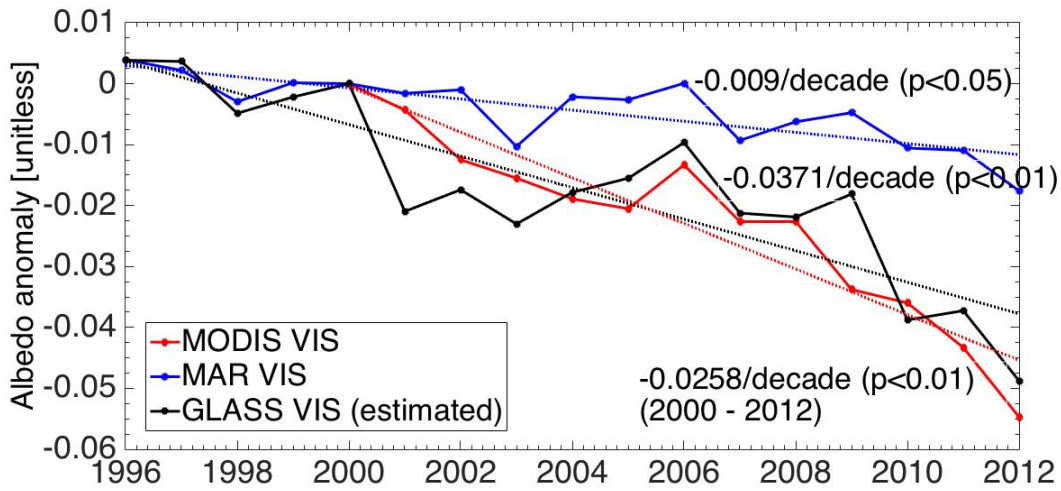


Figure 4 a) MAR and b) GLASS mean JJA albedo for year 2010 over an area including the dark band together with c) time series of mean JJA albedo for the ice-covered areas in the black rectangle. The black line in c) shows the GLASS spatially averaged albedo, where the top and the bottom of the grey area indicate, respectively, the maximum and minimum albedo within the black box in b).



(a)



(b)

Figure 5 Time series of modelled and measured mean summer (JJA) albedo anomalies (with respect to year 2000) in different spectral bands. a) Visible, near-infrared and shortwave-infrared albedo values simulated by MAR; b) as in a) but for the visible albedo only from MAR, MODIS (obtained from the product MCD43) and GLASS. Note that the vertical axis scale in (b) is different from that in (a).

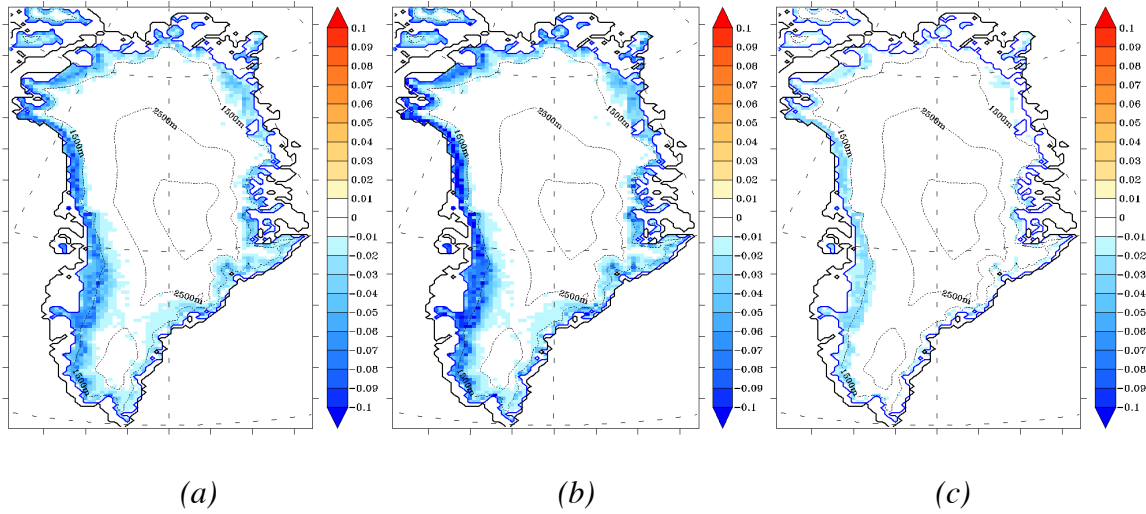
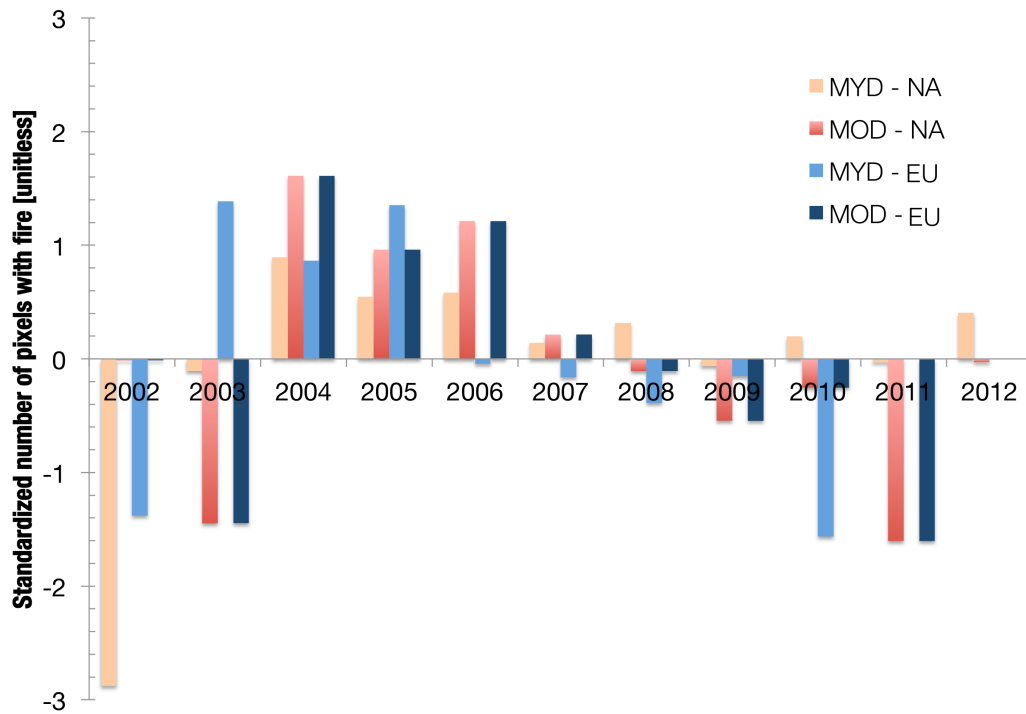


Figure 6 Maps of MAR-simulated albedo trends between 1996 and 2012 using a) the original MAR albedo scheme and b) the perturbed MAR outputs in which daily albedo is artificially decreased by 0.1 from the MAR-computed value for those regions where bare ice is exposed. c) Difference between the trends obtained with MAR original albedo scheme and the perturbed solution.

1

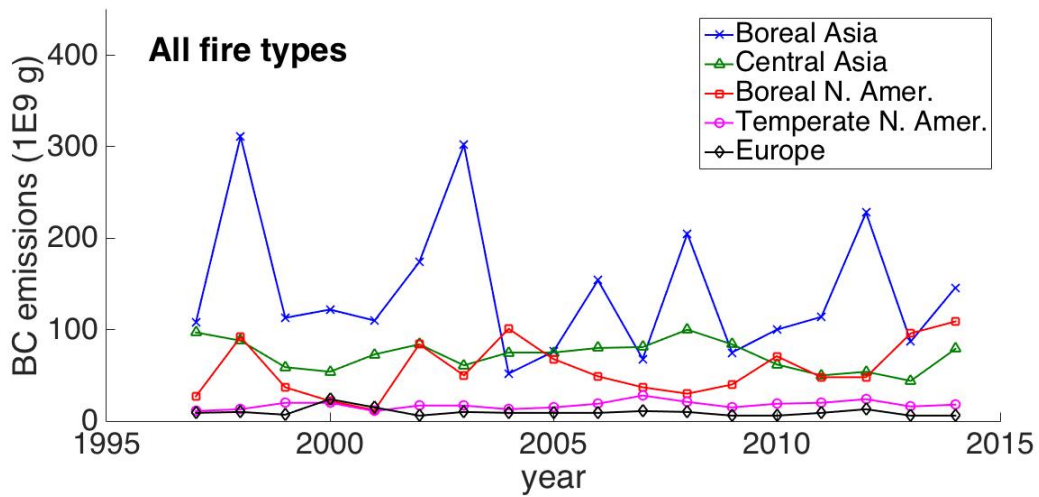


2

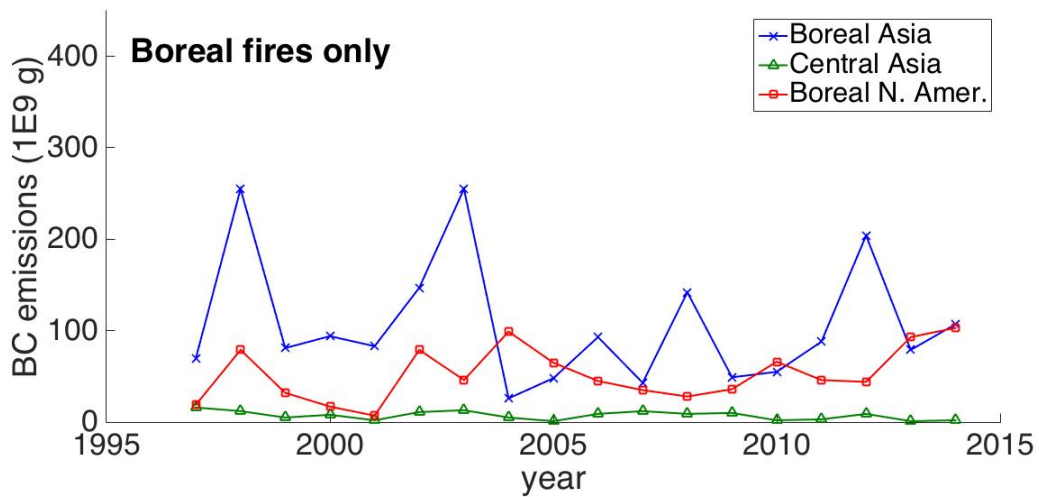
3 Figure 7 Standardised cumulative number of fires (April through August) detected over
 4 North America (NA) and Eurasia (EU) by the MOD14CMH and MYD14CMH GCM
 5 climatology products between 2002 and 2012.

6

7



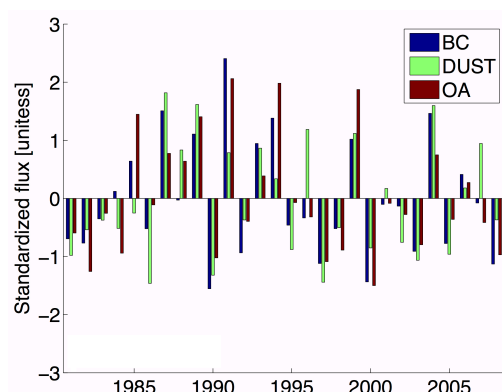
(a)



(b)

Figure 8 BC emissions [g] from fires in potential source regions for GrIS for a) all fire types and b) boreal fires only using estimates from the Global Fire Emissions Database (GFED version 4.1, <http://www.globalfiredata.org/>) between 1997 and 2014.

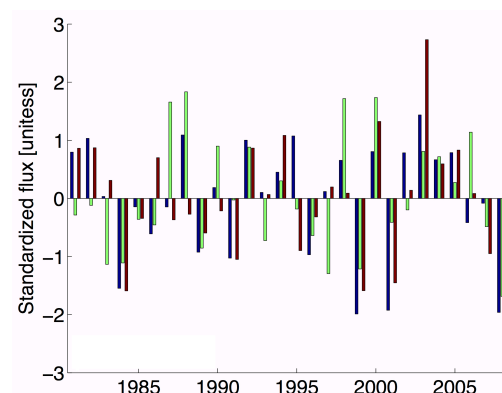
1



2

3

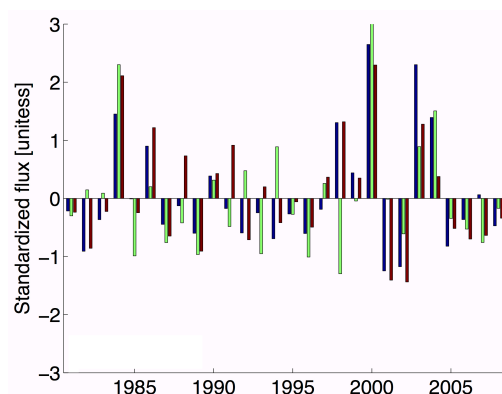
(a)



4

5

(b)



6

7

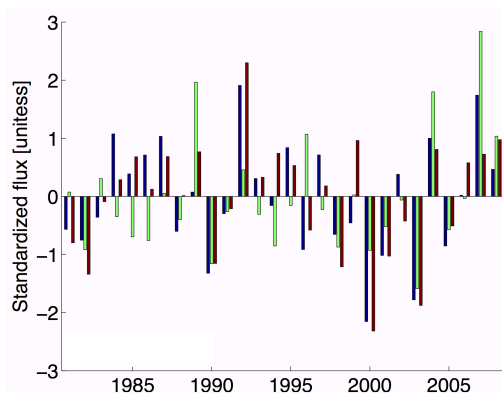
(c)

8 Figure 9 NASA GISS ModelE standardized deposition fluxes for BC, dust and organic
 9 aerosol at Kangerlussuaq for a) June, b) July and c) August (1981 – 2008) from the
 10 AEROCOM simulations.

11

12

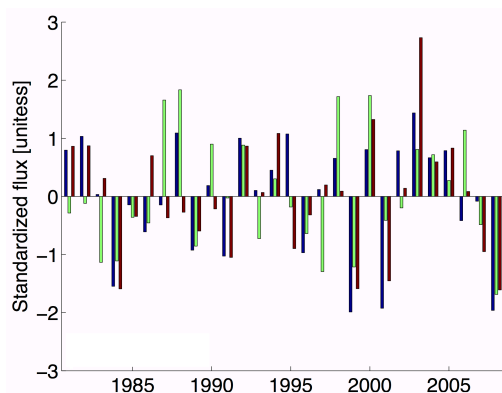
1



2

3

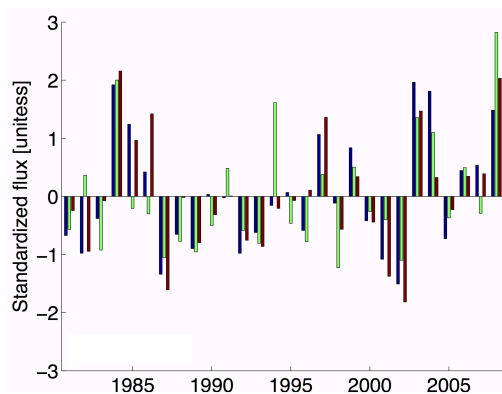
(a)



4

5

(b)



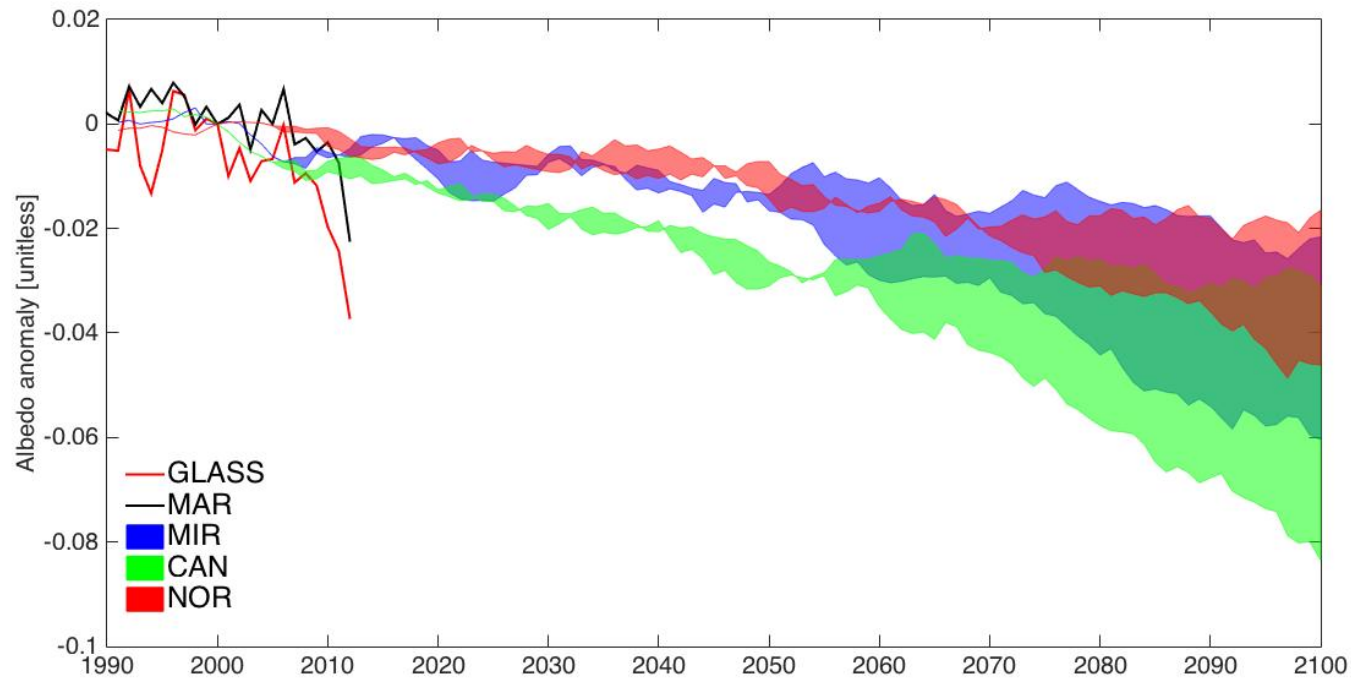
6

7

(c)

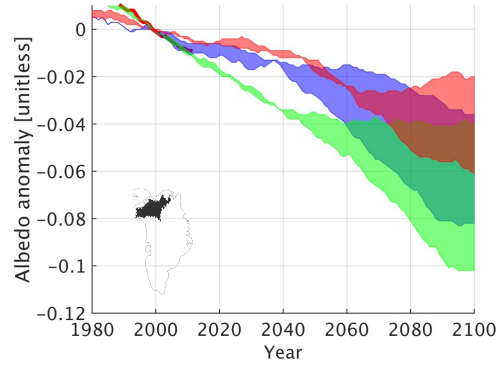
8

Figure 10 Same as Figure 9 but for Summit station.



1

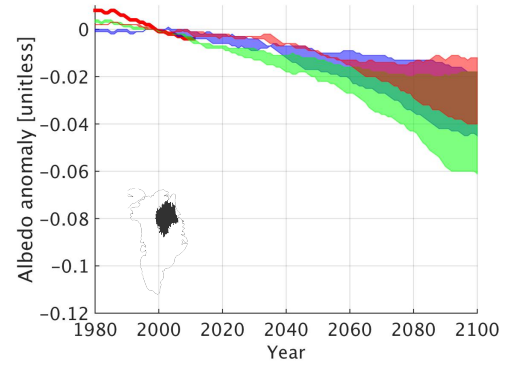
2 Figure 11 Projections of broadband albedo anomaly (with respect to year 2000) averaged over the whole GrIS for 1990-2012
 3 from MAR simulations and GLASS retrievals (black and red lines, respectively), and as projected by 2100. Future projections are
 4 simulated with MAR forced at its boundaries with the outputs of three ESMs under two warming scenarios, with the first scenario
 5 (RCP45) corresponding to an increase in the atmospheric greenhouse gas concentration to a level of 850 ppm CO₂ equivalent by
 6 2100 and the second (RCP85) to > 1370 pm CO₂ equivalent. The top and the bottom of the coloured area plots represent the
 7 results concerning the RCP45 (top) and RCP85 (bottom) scenarios. Semi-transparent colours are used to allow view of the
 8 overlapping data. Dark green corresponds to the case where MIROC5 and CANESM2 results overlap and brown to the case when
 9 the results from the three ESMs overlap.



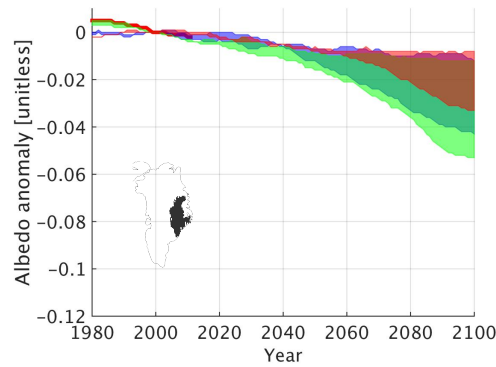
1

2

(a)



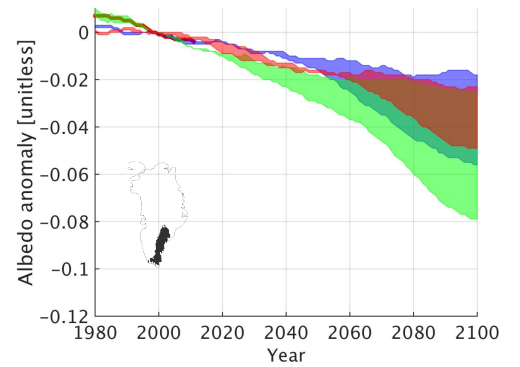
(b)



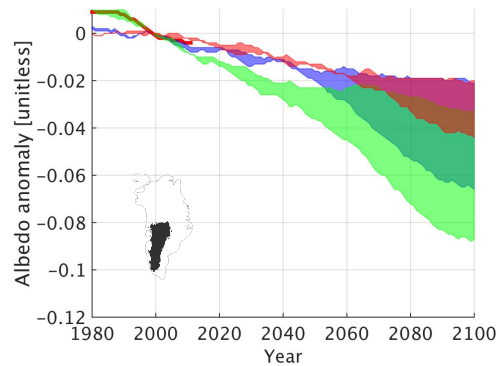
3

4

(c)



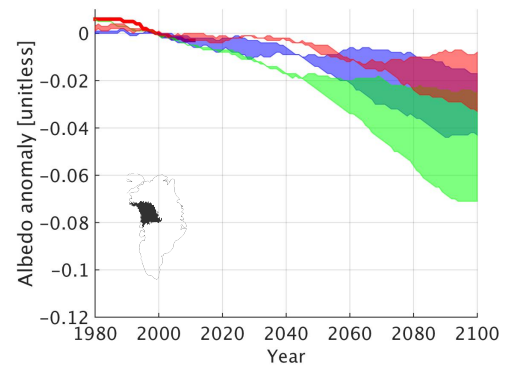
(d)



5

6

(e)



(f)

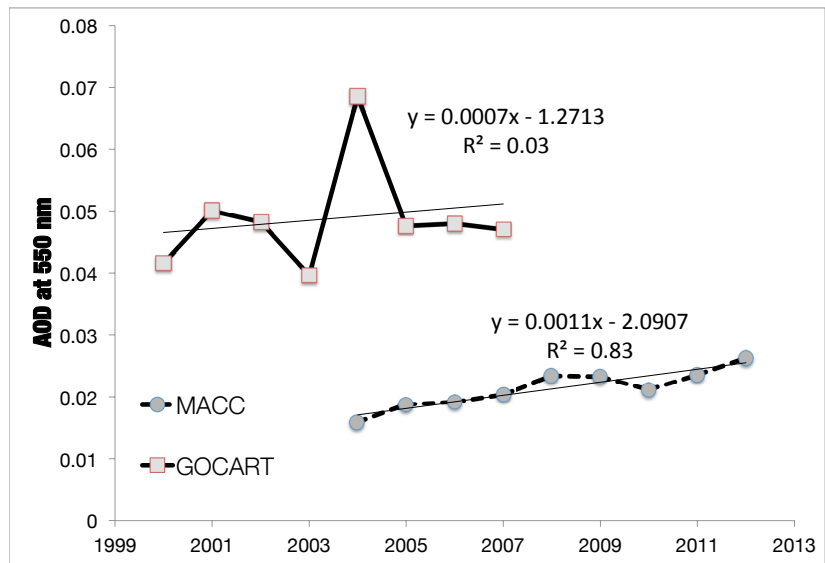
Figure 12 Same as Figure 11 but for different drainage regions of the GrIS, indicated by the small maps in each panel. Color scheme for the shaded regions is the same as Figure 10. The top and the bottom of each area plots represent the results concerning the RCP45 (bottom) and RCP85 (top) scenarios. Red lines represent the GLASS albedo averaged over the corresponding drainage region.

12

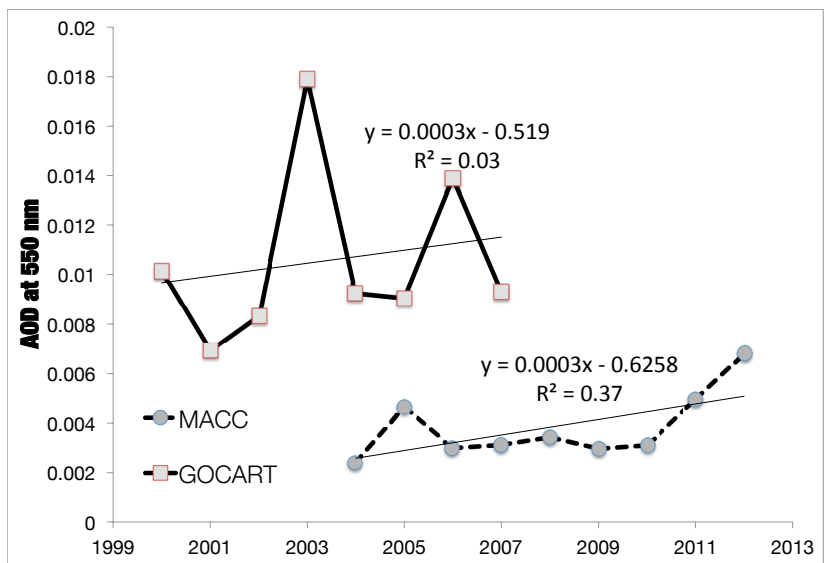
1

	June				July				August				JJA			
Station	rmse	Rmse [%]	slope	# of years	rmse	rmsep	slope	# of years	rmse	rmsep	slope	# of years	rmse	rmsep	slope	# of years
Swiss	0.12	19.60	-0.22	11	0.02	3.86	1.12	9	0.04	6.92	1.00	8	0.02	2.73	1.06	7
CP	0.07	8.72	0.12	12	0.06	7.40	0.14	14	0.06	7.21	0.11	13	0.07	8.20	-0.02	11
Humboldt	0.08	10.38	-0.16	8	0.07	9.31	0.35	9	0.08	9.98	0.39	10	0.07	9.42	0.27	8
Summit	0.01	1.45	0.85	15	0.02	2.25	-0.25	16	0.01	1.71	-0.68	16	0.01	1.22	0.12	15
TunuN	0.05	6.72	-0.66	15	0.06	7.89	0.79	15	0.07	8.84	0.69	15	0.06	7.53	0.37	15
Dye-2	0.02	2.58	0.57	14	0.02	2.15	0.75	14	0.01	1.73	0.68	15	0.01	1.54	0.82	12
Jar1	0.06	8.45	0.68	13	0.10	23.80	0.68	15	0.15	43.55	0.22	14	0.07	14.24	0.66	12
Saddle	0.01	1.28	0.94	14	0.02	1.95	0.61	14	0.01	1.75	0.46	14	0.01	1.31	0.71	14
NASAE	0.03	4.23	0.46	14	0.05	5.97	0.14	14	0.04	5.11	0.24	14	0.04	4.97	0.24	14
NASA SE	0.02	2.76	0.59	13	0.02	2.32	0.67	13	0.02	2.14	0.36	14	0.02	2.23	0.56	13
JAR2	0.06	12.27	0.20	11	0.05	10.00	-0.10	12	0.06	11.96	-0.06	11	0.04	8.51	0.16	10
Mean	0.048	7.13			0.0455	6.99			0.05	9.2			0.038	5.62		

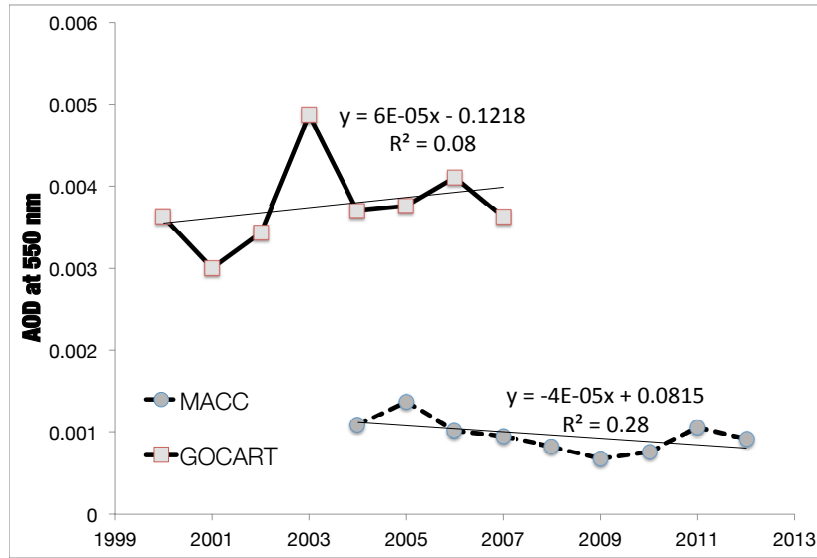
2 Table 1 Comparison between GLASS retrieved albedo and GC-NET in -situ albedo measurements, for monthly- and seasonally-
3 averaged albedos at twelve surface stations on the Greenland ice sheet.



(a)

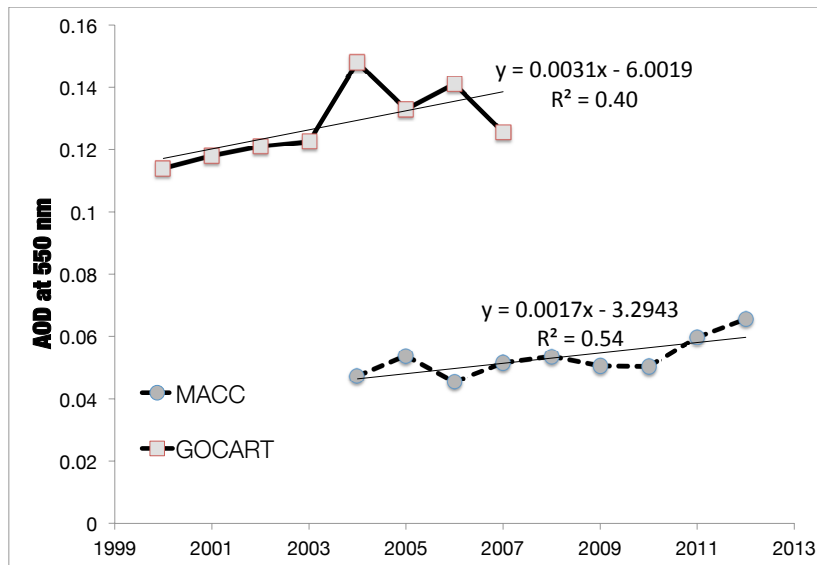


(b)



1

(c)



2

(d)

3 Figure 13 May – June averaged aerosol optical depth at 550 nm for a) dust, b) organic
 4 matter, c) black carbon and d) total obtained from the GOCART model and from the
 5 MACC model (as in Dumont et al., 2014) for the domain bounded by 75 to 80°N and 30
 6 to 50° W. All trends are not statistically significant with the exception of the MACC
 7 outputs for Dust ($p < 0.01$) and Total Aerosol ($p < 0.05$).

	STATION		
	Thule 77°28'00"N, 69°13'50"W	Ittoqqortoormiit 70°29'07"N, 21°58'00"W	Kangerlussuaq 67°00'31"N, 50°41'21"W
Year			
2007	0.042±0.010	N/A	N/A
2008	0.040±0.017	N/A	0.051±0.012
2009	0.093±0.020	N/A	0.088±0.017
2010	0.052±0.011	0.052±0.005	0.049±0.007
2011	0.060±0.017	0.072±0.041	0.053±0.012
2012	0.065±0.011	0.044±0.009	0.072±0.020
2013	0.050±0.007	0.053±0.009	0.066±0.010

1

2 Table 2 June-July-August mean and standard deviation of measured aerosol optical dep
3 (AOD) at 550 nm at the three sites of Thule, Ittoqqortoormiit and Kangerlussuaq of tl
4 AERONET network (AERONET web site, <http://aeronet.gsfc.nasa.gov>, 2013).

5

The darkening of the Greenland ice sheet: trends, drivers and projections (1981 – 2100)

M. Tedesco^{1,2}, S. Doherty³, X. Fettweis⁴, P. Alexander^{2,5,6}, J. Jeyaratnam²,
and J. Stroeve⁷

[1] [Lamont-Doherty Earth Observatory of the Columbia University, New York, NY](#)

[2] [The City College of New York – CUNY](#)

[3] [Joint Institute for the Study of the Atmosphere and Ocean \(JISAO\), University of Washington, Seattle, WA USA](#)

[4] [University of Liege, Liege, Belgium](#)

[5] [NASA Goddard Institute for Space Studies, New York, NY USA](#)

[6] [The Graduate Center of the City University of New York](#)

[7] [University of Boulder, Colorado, USA](#)

Abstract

The surface energy balance and meltwater production of the Greenland ice sheet (GrIS) are modulated by snow and ice albedo through the amount of absorbed solar radiation. Here we show, using spaceborne multispectral data collected during the three decades from 1981 to 2012, that summertime surface albedo over the GrIS decreased at a statistically significant (99 %) rate of 0.02 decade^{-1} between 1996 and 2012. Over the same period, albedo modeled by the Modèle Atmosphérique Régionale (MAR) also shows a decrease, though at a lower rate ($\sim -0.01 \text{ decade}^{-1}$) than that obtained from spaceborne data. We suggest that the discrepancy between modeled and measured albedo trends can be explained by the absence in the model of processes associated with the presence of light-absorbing impurities. The negative trend in observed albedo is confined to the regions of the GrIS that undergo melting in summer, with the dry-snow zone showing no trend. The period 1981 – 1996 also showed no statistically significant trend over the whole GrIS. Analysis of MAR outputs indicates that the observed albedo decrease is attributable to the combined effects of increased near-surface air temperatures, which enhanced melt and promoted growth in snow grain size and the expansion of bare ice areas, and by trends in light-absorbing impurities (LAI) on the snow and ice surfaces. Neither aerosol models nor in-situ and remote sensing observations indicate increasing trends in LAI in the atmosphere over Greenland. Similarly, an analysis of the number of fires and BC emissions from fires points to the absence of trends for such quantities. This suggests that the apparent increase of LAI in snow and ice might be related to the exposure of a ‘dark band’ of dirty ice and to increased consolidation of LAI at the surface with melt, not to increased aerosol deposition. Albedo projections through the end of the century under different warming scenarios consistently point to continued darkening, with albedo anomalies averaged over the whole ice sheet lower by 0.08 in 2100 than in 2000, driven solely by a warming climate. Future darkening is likely underestimated because of known underestimates in

Marco T 1/2/16 10:15

Deleted: ³

Marco T 1/2/16 10:15

Deleted: ⁴

Marco T 1/2/16 10:15

Deleted: ⁵

Marco T 1/2/16 10:15

Deleted: ¹

Marco T 1/2/16 10:15

Deleted: ⁶

Marco T 1/2/16 10:15

Deleted: ¹

Marco T 1/2/16 10:13

Deleted: E. Noble¹

Marco T 1/9/16 14:19

Deleted: email: cryocity@gmail.com

Marco T 1/2/16 10:14

Deleted: [2] The Graduate Center of the City University of New York [1]

Marco T 1/2/16 10:15

Deleted: 4

Marco T 1/2/16 10:15

Deleted: 5

Marco T 1/2/16 10:15

Deleted: 6

Marco T 1/4/16 07:57

Formatted: Superscript

Marco T 1/12/16 10:41

Deleted: trend

Marco T 1/12/16 10:42

Deleted: The analysis of the

Marco T 1/9/16 14:19

Deleted: of a regional climate model

Marco T 1/2/16 10:40

Deleted: impurities

Marco T 1/9/16 14:22

Deleted: ,

Marco T 1/9/16 14:22

Deleted: suggesting

Marco T 1/9/16 14:22

Deleted: their

Marco T 1/2/16 10:40

Deleted: impurities

modelled melting (as seen in hindcasts) and because the model albedo scheme does not currently include the effects of LAI, which have a positive feedback on albedo decline through increased melting, grain growth and darkening.

1 Introduction

The summer season over the Greenland ice sheet (GrIS) during the past two decades has been characterized by increased surface melting (Nghiem et al., 2012; Tedesco et al., 2011, 2014) and net mass loss (Shepherd et al., 2012). Notably, the summer of 2012 set new records for surface melt extent (Nghiem et al., 2012) and duration (Tedesco et al., 2013), and a record of 570 ± 100 Gt in total mass loss, doubling the average annual loss rate of 260 ± 100 Gt for the period 2003–2012 (Tedesco et al., 2014).

Net solar radiation is the most significant driver of summer surface melt over the GrIS, (van den Broeke et al., 2011; Tedesco et al., 2011), and is determined by the combination of the amount of incoming solar radiation and surface albedo. Variations in snow albedo are driven principally by changes in snow grain size and by the presence of light-absorbing impurities (LAI, Warren and Wiscombe, 1982). Generally, snow albedo is highest immediately following new snowfall. In the normal course of *destructive metamorphism* the snow grains become rounded, and large grains grow at the expense of small grains, so the average grain radius r increases with time (LaChapelle, 1969). Subsequently, warming and melt/freeze cycles catalyse grain growth, decreasing albedo mostly in the near-infrared (NIR) region (Warren 1982). The absorbed solar radiation associated with this albedo reduction promotes additional grain growth, further reducing albedo, potentially accelerating melting. The presence of LAI such as soot (black carbon, BC), dust, organic matter, algae and other biological material in snow or ice also reduces the albedo, mostly in the visible and ultraviolet regions (Warren 1982). Such impurities are deposited through dry and wet deposition, and their mixing ratios are enhanced through snow water loss in sublimation and melting (Conway et al., 1996; Flanner et al., 2007; Doherty et al., 2013). Besides grain growth and LAI, another cause of albedo reduction over the GrIS is the exposure of bare ice: once layers of snow or firn are removed through ablation, the exposure of the underlying bare ice will further reduce surface albedo, as does the presence of melt pools on the ice surface (e.g., Tedesco et al., 2011).

Most of the studies examining albedo over the whole GrIS have focused on data collected by the Moderate Resolution Imaging Spectroradiometer (MODIS) starting in 2000 (e.g., Box et al., 2012; Tedesco et al., 2013). At the same time, regional climate models (RCMs) have been employed to simulate the evolution and trends of surface quantities over the GrIS back to the 1960s using reanalysis data for forcing (e.g., Fettweis et al., 2012). Despite the increased complexity of models, and their inclusion of increasingly sophisticated physics parameterizations, RCMs still suffer from incomplete representation of processes that drive snow albedo changes, such as the spatial and temporal distribution of LAI, and from the absence of in-situ grain size measurement to validate modeled snow grain-size evolution. In this study, we first report the results from an analysis of summer albedo over the whole GrIS from satellite for the period 1980 – 2012, hence expanding the temporal coverage with respect to previous studies. Then, we combine the outputs of an RCM and in-situ observations with the satellite albedo

Marco T 1/2/16 08:49

Deleted: projected

Marco T 1/2/16 10:40

Deleted: light-absorbing impurities

Marco T 1/2/16 10:40

Deleted: light-absorbing impurities (hereafter, simply “impurities”, e.g.,

Marco T 1/2/16 10:41

Deleted: impurities

Marco T 1/2/16 10:41

Deleted: impurities

Marco T 1/2/16 10:41

Deleted: impurities

estimates to identify those processes responsible for the observed albedo trends. The model, Modèle Atmosphérique Régionale (MAR), is used to simulate surface temperature, [grain size](#), exposed ice area, and surface albedo over Greenland at large spatial scales. MAR-simulated surface albedo is tested against surface albedo retrieved under the Global LAnd Surface Satellite (GLASS) project, and it is used to attribute trends in GLASS albedo. Lastly, we project the evolution of mean summer albedo over Greenland using the MAR model forced with the outputs of different Earth System Models (ESMs) under different CO₂ scenarios. Discussion and conclusions follow the presentation of the methods and results.

2 Methods and data

2.1 The MAR regional climate model and its albedo scheme

Simulations of surface energy balance quantities over the GrIS are performed using the Modèle Atmosphérique Régionale (MAR; e.g., Fettweis et al., 2005, 2013). MAR is a modular atmospheric model that uses the sigma-vertical coordinate to simulate airflow over complex terrain and the Soil Ice Snow Vegetation Atmosphere Transfer scheme (SISVAT, e.g., De Ridder and Gallée, 1998) as the surface model. MAR outputs have been assessed over Greenland in several studies (e.g., Tedesco et al., 2011; Fettweis et al., 2005; Vernon et al., 2013; Rae et al. 2012; Van Angelen et al., 2012), with recent work specifically focusing on assessing simulated albedo over Greenland (Alexander et al., 2014). [A discussion of this evaluation is presented later in the manuscript.](#) The snow model in MAR is the CROCUS model of Brun et al., (1992), which calculates albedo for snow and ice as a function of snow grain properties, [which](#) in turn [are](#) dependent on energy and mass fluxes within the snowpack. The model configuration used here has 25 terrain-following sigma layers between the Earth's surface and the 5-hPa-model top. The spatial configuration of the model uses the 25-km horizontal resolution computational domain over Greenland described in Fettweis et al. (2005). The lateral and lower boundary conditions are prescribed from meteorological fields modelled by the global European Centre for Medium-Range Weather Forecasts (ECMWF) Interim Reanalysis (ERA-Interim, <http://www.ecmwf.int/en/research/climate-reanalysis/era-interim>). Sea-surface temperature and sea-ice cover are also prescribed in the model using the same reanalysis data. The atmospheric model within MAR interacts with the CROCUS model, which provides the state of the snowpack and associated quantities (e.g., albedo, grain size). No nudging or interactive nesting was used in any of the experiments.

The MAR albedo scheme is summarized below. Surface albedo is expressed as a function of the optical properties of snow, the presence of bare ice, whether snow is overlying ice (and whether the surface is waterlogged), and the presence of clouds. In the version used here (MARv 3.5.1), the broadband albedo (α_s , 0.3 – 2.8 μm) of snow is a weighted average (Eq. 1) of the albedo in three spectral bands, α_1 , α_2 and α_3 , which are functions of the optical diameter of snow grains (d , in meters), as modified from equations by Brun et al. (1992; e.g., Lefebvre et al., 2003; Alexander et al., 2014):

$$\alpha_s = 0.58\alpha_1 + 0.32\alpha_2 + 0.10\alpha_3 \quad (1)$$

$$\alpha_1 = \max(0.94, 0.96 - 1.58 \sqrt{d}), (0.3 - 0.8 \mu\text{m}) \quad (2)$$

Marco T 1/12/16 10:44

Deleted: by

Marco T 1/9/16 14:23

Deleted: s

Marco T 1/4/16 06:41

Formatted: Font:Times New Roman, 12 pt

Marco T 1/12/16 15:02

Deleted: +

$$\alpha_2 = 0.95 - 15.4 \sqrt{d}, (0.8 - 1.5 \mu\text{m}) \quad (3)$$

$$\alpha_3 = 364 * \min(d, 0.0023) - 32.31 \sqrt{d} + 0.88, (1.5 - 2.8 \mu\text{m}) \quad (4)$$

The optical diameter d is, in turn, a function of snow grain properties and it evolves as described in Brun et al., (1992). In MAR, the albedo of snow is calculated by Eqs. 1-4, but it is not permitted to drop below 0.65.

For the transition from snow to ice, MAR makes the albedo an explicit function of density. On a polar ice sheet, densification of snow/firn/ice occurs in three stages, with a different physical process responsible for the densification in each stage (Herron and Langway, 1980; Arnaud et al., 2000). Newly-fallen snow can have density in the range 50-200 kg m⁻³. After then, densification can occur due to wind processes, which break and round grains forming windslab of density typically around 300-400 kg m⁻³. The remaining densification happens by *grain-boundary sliding*, attaining a maximum density of ~550 kg m⁻³ at the surface. Old melting snow at the surface in late summer typically has this density, but does not exceed it, because this is the maximum density that can be attained by grain-boundary sliding and corresponds to the density of random-packing of spheres (Benson, 1962, page 77). Further increases of density (the second stage) occur in *firn* under the weight of overlying snow, by *grain deformation* (pressure-sintering). In this case the density range is 550-830 kg m⁻³. At a density of 830 kg m⁻³ the air becomes closed off into bubbles and the material is called *ice*. In the third stage, the density of ice increases from 830 to 917 kg m⁻³ by shrinkage of air bubbles under pressure. Moving down the slope along the surface of the GrIS, at the transition between the accumulation area and the ablation area, the snow melts away, exposing firn. Continuing farther down, the firn melts away, exposing ice. The albedo of firn may be approximated as a function of its density ρ , interpolating between the minimum albedo of snow and the maximum albedo of ice. In MAR these values of albedo are set to 0.65 and 0.55, respectively. We would then have for the density range of firn (550-830 kg m⁻³):

$$\alpha_{\text{firn}} = 0.55 + (0.65-0.55) (830-\rho)/(830-550) \quad (5)$$

The MARv3.5.1 version used here maintains a minimum albedo of 0.65 for any density up to 830 kg m⁻³, and specifies the gradual transition from snow albedo to ice albedo across the density range 830-920 kg m⁻³. This means that the albedo of exposed firn is not allowed to drop below 0.65, with the result that the positive feedbacks of snow/firn/ice albedo will be muted in MAR. This aspect is being addressed in future versions of MAR (MAR v3.6) and a sensitivity analysis is being conducted to evaluate the impact of the changes on the albedo values when snow is transitioning from firn to ice. Such analysis is computationally expensive and preliminary outputs will be published once available.

In MAR, the albedo for bare ice is a function of the accumulated surface meltwater preceding runoff and specified minimum ($\alpha_{i,\text{min}}$) and maximum ($\alpha_{i,\text{max}}$) bare ice values:

$$\alpha_i = \alpha_{i,\text{min}} + (\alpha_{i,\text{max}} - \alpha_{i,\text{min}}) e^{(-M_{\text{SW}(t)}/K)} \quad (6)$$

Marco T 1/12/16 10:45

Formatted: Not Highlight

Marco T 1/12/16 10:45

Formatted: Font:Times New Roman, 12 pt, Not Highlight

Marco T 1/12/16 10:45

Formatted: Not Highlight

Marco T 1/12/16 10:45

Formatted: Superscript, Not Highlight

Marco T 1/12/16 10:45

Formatted: Font:Times New Roman, 12 pt, Not Highlight

Marco T 1/6/16 07:06

Deleted: The snow densifies over time by

Marco T 1/2/16 08:53

Deleted:

Here $\alpha_{i,\min}$ and $\alpha_{i,\max}$ are set, respectively, to 0.4 and 0.55, K is a scale factor set to 200 kg m⁻², and $M_{SW(t)}$ is the time-dependent accumulated excess surface meltwater before runoff (in kg m⁻²).

When a snowpack with depth less than 10 cm is overlying a layer with a density exceeding 830 kg m⁻³ (i.e., ice), the albedo in MAR is a weighted, vertically-averaged value of snow albedo (α_s) and ice albedo (α_i ; e.g., if snow depth is 3 cm then albedo is obtained by multiplying the snow albedo by 0.3 and adding the ice albedo multiplied by 0.7). When the snowpack depth exceeds 10 cm, the value is set to α_s . The presence of clouds can increase snow albedo because they absorb at the same NIR wavelengths where snow also absorbs, skewing the incident solar spectrum to wavelengths for which snow has higher albedo (Figure 5 of Grenfell et al., 1981; Figure 13 of Warren, 1982; Greuell and Konzelman, 1994), in which case the albedos of snow and ice are adjusted based on the cloud fraction modelled by MAR (Greuell and Konzelman, 1994).

2.2 The GLASS albedo product

The GLASS surface albedo product (<http://glcf.umd.edu/data/abd/>) is derived from a combination of data collected by the Advanced Very High Resolution Radiometer (AVHRR) and the MODerate resolution Imaging Spectroradiometer (MODIS, Liang et al., 2013). Shortwave broadband albedo (0.3 – 3 μm) is provided every 8 days at a spatial resolution of 0.05° (~56 km in latitude) for the period 1981 - 2012. GLASS albedo data with a resolution of 1 km is also available from 2000 to 2012 but it is not used here for consistency with the data available before 2000. There have been several efforts to make the AVHRR and MODIS albedo products consistent within the GLASS product, including the use of the same surface albedo spectra to train the regression and the use of a temporal filter and climatological background data to fill data gaps (Liang et al., 2013). Monthly averaged broadband albedos from GLASS-AVHRR and GLASS-MODIS were cross-compared over Greenland for those months when there was overlap (July 2000, 2003, and 2004), revealing consistency in GLASS retrieved albedo from the two sensors (He et al., 2013). More information on the GLASS data processing algorithm and product is available in Zhao et al. (2013) and Ying et al. (2014).

The GLASS product provides both black-sky albedo (i.e., albedo in the absence of a diffuse component of the incident radiation) and white-sky albedo (albedo in the absence of a direct component, with an isotropic diffuse component). The actual albedo is a value interpolated between these two according to the fraction of diffuse sunlight, which is a function of the aerosol optical depth (AOD) and cloud cover fraction. In the absence of the full information needed to properly re-construct the actual albedo, here we use in our analysis the black-sky albedo, because we focus mostly on albedo retrieved under clear-sky conditions. Our analysis using the white-sky albedo (not shown here) is fully consistent with the results obtained using the black-sky albedo and reported in the following. A full description of the GLASS retrieval process and available products can be found in Liang et al. (2013) and references therein. An assessment of the GLASS product complementing existing studies is reported below.

Marco T 1/9/16 14:23

Formatted: Font:12 pt

Marco T 1/2/16 09:36

Deleted:)

Marco T 1/2/16 09:35

Deleted: .

Data collected by the MODIS TERRA and AQUA sensors are used in the GLASS albedo retrieval for the period 2000 – 2012 (2000 – 2012 for TERRA and 2002 – 2012 for AQUA, respectively). Wang et al. (2012) have shown that the MODIS TERRA sensor has been degrading at a pace that can be approximated by a second order polynomial, with the coefficients being spectrally dependent. Over Greenland, the impact of sensor degradation on albedo trends has been estimated at $-0.0059 \text{ decade}^{-1}$ (Stroeve et al., 2013). Polashenski et al. (2015) found a much greater impact on retrieved broadband albedo from TERRA sensor degradation ($-0.03 \text{ decade}^{-1}$). However, Polashenski et al. (2015) use a daily product (MOD10A1) rather than a 16-day integrated product as in the case of GLASS (e.g., Ying et al., 2014), which does account for BRDF at high solar zenith angles. The performance of the MODIS daily product has been shown to deteriorate with latitude (e.g., Alexander et al., 2015). On the other hand, the use of the BRDF (as in the case of the GLASS product) improves the performance of the product at high latitudes (Alexander et al., 2015). This, together with the good agreement between the MCD43 albedo product and the surface station albedo data (Alexander et al., 2015) gives us confidence in the GLASS trends.

We complement previous assessments of the MODIS and GLASS albedo, evaluating the absolute accuracy of the GLASS retrievals by comparing monthly GLASS albedo to in-situ measurements of albedo collected at automatic weather stations of the Greenland climate network (GC-Net, Steffen and Box, 2001). GC-Net data are distributed at hourly temporal resolution and were temporally averaged to match the temporal window used in the GLASS product data. The root mean square error (RMSE), percentage RMSE (pRMSE), and the slope of a linear fit between GLASS and in-situ measured albedos for 12 stations are given in Table 1. The number of available years used for the statistics is also reported for each station. We considered only stations for which at least 10 years were available for the analysis in at least one of the months. Our results are consistent with the findings reported by Alexander et al. (2014) and Stroeve et al., (2013, 2006) concerning the assessment of the MODIS albedo products over the GrIS. The mean value of the RMSE for all stations is 0.04-0.05 in all months, with individual station values as high as 0.15 for station JAR1 in August and as low as 0.01 for Summit and Saddle stations in June. The relatively large RMSE value for JAR1 (and other stations located within the ablation zone) is probably due to heterogeneity of albedo values within the pixel containing the location of the station and to the point-scale nature of the in-situ observations. At Summit, where spatial inhomogeneity on the surface is small, it is reasonable to assume that the effect of spatial scale and heterogeneity on the comparison is smaller.

3 Results

3.1 Albedo trends

The time series of the mean summer GLASS albedo values between 1981 and 2012 over Greenland can be separated into two distinct periods (Figure 1a): the period 1981 - 1996, when albedo shows no trend and a second period, 1996 – 2012, when a statistically significant trend (99 %) is detected. The year 1996 was identified as yielding the highest value of the coefficient of determination when fitting the albedo timeseries with two linear functions using a variable breaking point.

Marco T 1/9/16 10:51

Formatted: Font:(Default) Times New Roman, 12 pt, Not Superscript/ Subscript

Marco T 1/9/16 10:51

Formatted: Font:(Default) Times New Roman, 12 pt, Not Superscript/ Subscript

Marco T 1/9/16 10:51

Formatted: Font:(Default) Times New Roman, 12 pt, Not Superscript/ Subscript

Marco T 1/9/16 10:51

Formatted: Font:(Default) Times New Roman, 12 pt, Not Superscript/ Subscript

Marco T 1/9/16 10:51

Formatted: Font:(Default) Times New Roman, 12 pt, Not Superscript/ Subscript

Marco T 1/9/16 10:51

Formatted: Font:(Default) Times New Roman, 12 pt, Not Superscript/ Subscript

Marco T 1/9/16 10:51

Formatted: Font:(Default) Times New Roman, 12 pt, Not Superscript/ Subscript

Marco T 1/9/16 14:25

Deleted: Here w

Sarah Doherty 1/5/16 14:12

Comment [1]: per my email I think we need to enhance this discussion to respond to the Polashenski et al. analysis showing a much larger effect due to TERRA sensor degradation.

Marco T 1/4/16 08:07

Deleted:

The GLASS albedo shows significant darkening ($p < 0.01$) of the surface of the GrIS for the 1996 – 2012 period, with the summer (JJA) albedo declining at a rate of $0.02 \pm 0.004 \text{ decade}^{-1}$ (Figure 1a). About 25% of this decline might be attributed to sensor degradation, per the analysis of Stroeve et al. (2013). However, the TERRA sensor degradation is spectrally dependant and temporally non linear (Wang et al., 2012). This, together with the fact that the GLASS product uses a combination of both TERRA and AQUA data (which reduces the impact of the TERRA sensor degradation) indicates that impact of the sensor degradation on the observed decline is much smaller than 25 %. Over the same period, MAR-simulated summer near-surface temperature increased at a rate of $0.74 \pm 0.5^\circ\text{C decade}^{-1}$ (Figure 1b, $p < 0.05$), consistent with observed enhanced surface melting (e.g., Fettweis et al., 2013). MAR simulations also point to positive trends between 1996 and 2012 in summer surface grain radius ($0.12 \pm 0.03 \text{ mm /decade}^{-1}$, $p < 0.01$, Figure 1c) and the extent of those regions where bare ice is exposed during summer ($380 \pm 190 \text{ km}^2 \text{ decade}^{-1}$, $p < 0.01$, Figure 1d). There is no statistically significant trend in GLASS summer albedo or MAR-simulated surface grain size and bare ice extent for the 1981-1996 period. Simulated summer snowfall (not plotted in the figure) does not show a statistically significant trend for the period 1996 – 2012 ($p < 0.1$, $-1702 \pm 790 \text{ mmWE /decade}^{-1}$). Notably, strong negative summer snowfall anomalies from 2010 to 2012 are simulated by MAR, down to -1.5 standard deviations below the 1981 – 2012 mean. We suggest that for 2010 - 2012, in addition to surface melting, reduced summer snowfall might have played a key role in the accelerated decline in summer albedo.

3.2 Drivers: surface grain size and bare ice

Inter-annual variability in the mean summer GLASS albedo is captured by the MAR albedo simulations (Figure 1a). For the period when the darkening has been identified, MAR albedo values explain ~ 90 % (de-trended) of the spaceborne-derived summer albedo interannual variability. A multi-linear regression analysis indicates that, over the same period, the interannual variability of summer values of surface grain size and bare ice extent simulated by MAR explain, respectively, 54 % (grain size) and 65 % (bare ice) of the inter-annual variability of GLASS albedo when considered separately. When linearly combined, grain size, bare ice extent and snowfall explain ~ 85 % of the GLASS inter-annual variability, with the influence of summer new snowfall alone explaining only 44 % of the GLASS summer albedo variability.

The spatial distribution of observed summer albedo trends from space shows that the largest trends (in magnitude) occur over those regions where surface temperature, grain size, and bare ice exposure have also changed the most (Figure 2). In particular, darkening observed from space is most pronounced at lower elevations in southwest Greenland, with trends as large as $-0.20 \pm 0.07 \text{ decade}^{-1}$ (Figure 2a; note that the colour bar only goes down to $-0.06 \text{ decade}^{-1}$ for graphical purposes), where trends in the number of days when simulated surface temperature exceeds 0°C (Figure 2b), grain size (Figure 2c) and the number of summer days when bare ice is exposed (Figure 2d) are the largest.

While MAR is able to capture a large component of the observed variability in albedo retrieved by GLASS, the simulated albedo trend is smaller in magnitude than that

Marco T 1/9/16 14:26

Deleted: can

Marco T 1/9/16 14:26

Deleted:

Marco T 1/2/16 10:54

Deleted: t

Sarah Doherty 1/5/16 14:16

Comment [2]: If needed, we could note that this exceeds by far the trend even Polashenski et al. (2015) attribute to sensor degradation.

estimated using the GLASS product. The largest differences occur along the southwest margin of the ice sheet (Figure 3), where a “dark band” of outcropping layers of ice containing large concentrations of LAI is known to be present on the surface (Wientjes et al., 2011). In this region the number of days when surface temperature exceeds 0°C has increased, with trends of up to more than 20 days decade⁻¹ along the margins of the GrIS (Figure 1b). During this time-period GLASS albedo values are as low as 0.30, lower than that of bare ice (i.e., 0.45), consistent with in-situ measured values of dirty ice (Wientjes et al., 2010; Bøggild et al., 2010). Figure 4 shows the spatial distribution of MAR and GLASS mean JJA albedo for year 2010 over an area centred on the dark band in southwest Greenland, as well as the time series of GLASS albedo averaged over the same ice-covered area contained within the region identified by the black rectangle in Figure 4a. The black line in Figure 4c shows the GLASS spatially-averaged albedo within this region, with the top and the bottom margins of the grey area indicating, respectively, the maximum and minimum albedo values within that area. Note that we included only pixels that contained 100 % ice in all years (i.e. coloured areas in Figure 4a and b) in the calculation shown in Figure 4c, so trends are not driven by exposure of underlying land surface. Mean summer albedo from GLASS decreased over this area between 2005 and 2012 from ~ 0.6 to ~ 0.45 (vs. a decrease simulated by MAR of 0.075). Minimum summer albedo across all years averaged over the region is ~0.4, but dips close to ~0.3 in 2010, a value consistent with dirty bare ice, as shown in previous studies (Wientjes et al., 2010; Wientjes et al., 2011; Bøggild, et. al., 2010). We hypothesise that the discrepancy along this dark band between MAR- and GLASS albedo values is likely due to trends in the concentrations of LAI in the snow and ice in this region, which are not currently captured by the model.

3.3 Drivers: light-absorbing impurities on the surface of the GrIS

MAR simulations of albedo in different spectral bands (see Eqs. 1-4) point to comparable trends in the visible (0.3 – 0.8 µm; -0.009±0.005 decade⁻¹, p<0.05) and near-infrared (0.8 – 1.5 µm; -0.010±0.004 decade⁻¹, p<0.05) bands (Figure 5a) and to a much smaller and not statistically significant trend in the shortwave infrared band (1.5 – 2.8 µm, -0.003±0.004 decade⁻¹, p>0.1). Because the GLASS product does not provide visible albedo (only broadband albedo), we extrapolated an estimate of the visible component of the GLASS albedo by subtracting the NIR and shortwave infrared albedo values computed with MAR from the GLASS broadband values, following the MAR albedo scheme (Eq. 1, Figure 5b). To evaluate the robustness of this approach, we compared anomalies (with respect to year 2000) in estimated GLASS visible albedo with those from the 16-day MODIS MCD43A3 product (Stroeve et al., 2013), which also has a visible albedo product (Figure 5b). The MODIS albedo product we used is distributed by Boston University (<https://lpdaac.usgs.gov/>) and makes use of all atmospherically-corrected MODIS reflectance measurements over 16-day periods, to provide an averaged albedo every 8 days. A semi-empirical bidirectional reflectance distribution function (BRDF) model is used to compute bi-hemispherical reflectance from these reflectance measurements (Schaaf et al., 2002). The comparison between the GLASS- and MODIS-retrieved visible albedo anomalies is shown in Figure 5b, indicating that the two visible albedo anomalies are highly consistent, with a mean absolute error of 0.01 and a standard deviation of 0.005. There are differences in the estimated summer albedo trends from

Marco T 1/2/16 10:41

Deleted: impurities

Marco T 1/2/16 10:41

Deleted: impurities

Marco T 1/2/16 12:58

Deleted: This hypothesis is supported by previous studies such as the one by Wientjes et al. (2011), arguing that increased deposition of dust to this region of the ice sheet has significantly decreased the albedo.

Marco T 1/12/16 10:47

Deleted: but

Marco T 1/6/16 09:02

Deleted: -

MCD43A3 and GLASS over the 2002 – 2012 period, with the former being -0.04 ± 0.001 decade⁻¹ and the latter -0.03 ± 0.008 decade⁻¹. This difference could be due to the method we applied to estimate the visible component of the GLASS albedo, as well as other factors related to the data processing and algorithms used to extract albedo. Notably, however, the GLASS and MCD43 visible albedo trends are consistently about twice that estimated from the MAR model. The underestimated darkening by MAR relative to GLASS can be attributed to several factors, including the modeled spatial and temporal variability of the exposed bare ice area and the concentration of surface LAI on the ice surface, which is currently not included in the MAR albedo scheme. A lack of impurities in the MAR albedo scheme can affect simulated albedo trends in at least two ways: first, the concentration of impurities over bare ice areas could be increasing, which would not be captured by MAR; second, the lack of impurities in the MAR albedo scheme causes bare ice areas to have an overestimated albedo. More frequent exposure of bare ice would lead to a decline in annual average albedo over time, but if the underlying bare ice is darker, such a trend would be larger. Thus, the difference in trends could result solely from an overestimation of the bare ice albedo by MAR. We are not able to discern the degree to which the difference is due to a) errors in the area and frequency of bare ice exposure from MAR; b) increasing concentration of impurities not captured by MAR, or c) overestimation of albedo of an unchanging impurity-covered bare ice surface. The study by Alexander et al. (2015) suggests that bare ice albedo is, indeed, overestimated in MAR. To test the impact of a fixed bare ice albedo on the simulated albedo trend, we performed a sensitivity experiment in which daily albedo for those pixels showing bare ice exposure is reduced by a fixed value of 0.1. The magnitude of the difference in trends between the original MAR simulation (with no change on the bare ice albedo) and the one with a modified albedo (Figure 6) is comparable to the difference between the MAR and GLASS trends (Figure 3a), suggests that this factor alone could explain the difference. To further investigate this aspect, we test the hypothesis of increased concentration of LAI on the snow and ice surface. The concentrations of LAI in surface snow and ice can increase either because of increased atmospheric deposition or because of post-depositional processes, including (a) loss of snow water to sublimation and melt, resulting in impurities accumulating at the surface as a lag-deposit (e.g., Doherty et al., 2013), and (b) the outcropping of ‘dirty’ underlying ice associated with snow/firm removal due to ablation. These processes are themselves driven by warming, and therefore constitute positive feedbacks.

Quantifying the contribution of surface LAI to GLASS summer albedo trends is a challenging task because of the relatively low impurity concentrations over most of the GrIS (Doherty et al., 2010; Bond et al., 2013), and because of known limitations related to remote sensing estimates of LAI from space (Warren, 2013). Moreover, quantifying the causes of potential increased impurity concentrations on the surface (atmospheric deposition vs. other factors) is also challenging, if not prohibitive, given the current state-of-the-art of spaceborne measurements (e.g. accuracy of the satellite products) and the scarcity of in-situ data. Therefore, in the next section, we look for trends in forest fires and the emissions of BC from forest fires in the main source regions for aerosols over the GrIS and assess whether atmospheric aerosol concentrations over the GrIS have increased (as a proxy for whether the deposition of aerosol has increased).

Marco T 1/12/16 13:44

Deleted: . Because the MAR model does not account for the presence of surface impurities in the albedo scheme, we suggest that t

Marco T 1/12/16 14:34

Deleted: is consistent with an increase in the concentration of surface impurities.

Marco T 1/2/16 10:42

Deleted: impurities

Marco T 1/9/16 09:47

Formatted: Normal, Indent: First line: 0.3"

Marco T 1/2/16 10:42

Deleted: impurities

Marco T 1/2/16 10:42

Deleted: impurities

3.4 Attribution: Aerosol contributions to LAI in GrIS

3.4.1 Trends in GrIS LAI

Ice core analyses of black carbon in the central regions of the GrIS have been used to study long-term variability and trends in pollution deposition (McConnell et al., 2007; Keegan et al., 2014). These records show that snow at these locations was significantly more polluted in the first half of the 20th century than presently. Both these records and in-situ measurements at Summit (Cachier and Pertuisot, 1994; Chylek et al., 1995; Hagler et al., 2007; Doherty et al., 2010) also indicate that in recent decades, the snow in central Greenland has been relatively clean, with concentrations smaller than 4 ng g⁻¹ for BC. This amount of BC could lower snow albedo by only 0.002 for $r=100\text{ }\mu\text{m}$, or 0.005 for $r=500\text{ }\mu\text{m}$ (Figure 5a of Dang et al., 2015). More recently, Polashenski et al. (2015) analysed BC and dust concentrations in 2012-2014 snowfall along a transect in northwest Greenland. They found similarly low concentrations of BC and concluded that albedo decreases in their study region are unlikely to be attributable to increases in BC or dust. Black carbon measurements from a high snowfall region of west central Greenland made on an ice core collected in 2003 show that black carbon concentrations varied significantly during the past 215 years, with an average annual concentration of 2.3 ng g⁻¹ during the period 1952 – 2002, characterized by high year-to-year variability in summer and a gradual decline in winter BC concentrations through the end of the century (McConnell et al., 2007). Snow sampled in 1983 at Dye-3 had a median of 2 ng g⁻¹ (Clarke and Noone, 1985). In 2008 and 2010, measurements 160 km away at Dye-2, using the same method, had medians of 4 ng g⁻¹ in spring and 1 ng g⁻¹ in summer (Table 9 of Doherty et al., 2010).

In the absence of in-situ measurements of impurity concentration trends over Greenland more broadly, or of trends in aerosol deposition rates (which are absent entirely), we investigate trends in emissions from key sources of aerosols deposited to the GrIS and trends in Atmospheric Optical Depth (AOD) over GrIS.

3.4.2 Trends in fire count and BC emissions

Biomass burning in North America and Siberia is a significant source of combustion aerosol (BC and associated organics) to the GrIS (Hegg et al., 2009, 2010). Therefore, we investigated trends in the number of active fires in these two source regions, as well as BC emissions from fires in sub-regions within the northern hemisphere. For fire counts we used the MODIS monthly active fire products produced by the TERRA (MOD14CMH) and AQUA sensors (MYD14CMH) generated at 0.5° spatial resolution and distributed by the University of Maryland via anonymous ftp (http://www.fao.org/fileadmin/templates/gfims/docs/MODIS_Fire_Users_Guide_2.4.pdf, http://modis.gsfc.nasa.gov/data/dataproducts.php?MOD_NUMBER=14). The results of our analysis are summarised in Figure 7, showing the standardised (subtracting the mean and dividing by the standard deviation of the 2002 – 2012 baseline period) cumulative number of fires (April through August) detected over North America (NA) and Eurasia (EU) by the MOD14CMH and MYD14CMH GCM climatology products between 2002 and 2012. The figure shows large inter-annual variability but no significant trend (at 90 % level) in the number of fires over the two areas between 2002 and 2012.

The period between 2004 and 2011, when enhanced melting occurred over the GrIS, shows a negative trend (though also in this case not statistically significant).

In addition to number of fires we looked for trends specifically in BC emissions from fires in potential source regions for GrIS, using estimates from the Global Fire Emissions Database (GFED version 4.1, <http://www.globalfiredata.org/>). There is a great deal of inter-annual variability in annual BC emissions from fires in all regions (Figure 8), with no statistically significant increase during the 1997-2012 or 1997-2014 periods from either of the Boreal source regions or from Central Asia or Europe. BC emissions from fires in Temperate North America increased by, on average, $0.35 \times 10^9 \text{ g yr}^{-1}$ during 1997-2014 and by $0.52 \times 10^9 \text{ g yr}^{-1}$ 1997-2012 ($p < 0.1$ in both cases), or an increase of 60% from 1997 to 2012. However, the total BC emissions from fires in this region constitute a small fraction of that from the Boreal regions. In addition, the only statistically significant trend in regional BC emissions is a *decrease* in Central Asia ($112.6 \times 10^9 \text{ g yr}^{-1}$; $p = 0.02$), when GrIS albedo has declined most precipitously, is a *decrease* in BC emissions ($-12.6 \times 10^9 \text{ g yr}^{-1}$; $p = 0.02$) in Central Asia. Xing et al. (2013, 2015) point out that direct anthropogenic emissions have also been decreasing across almost all of the mid- to high-latitude northern hemisphere.

3.4.3 Trends in AOD over Greenland

To investigate trends in AOD over GrIS we look at AOD as simulated by models and as measured at ground-based stations at several locations around the GrIS. AOD is a measure of the total extinction (omni-directional scattering plus absorption) of sunlight as it passes through the atmosphere, and is related to atmospheric aerosol abundance. Thus, it is a metric for the mass of aerosol available to be potentially deposited onto the GrIS surface. In the aerosol models, we are able to examine trends in total AOD as well as in aerosol components: BC, dust and organic matter. In addition, we examined trends in modelled deposition fluxes of these species to the GrIS.

For our analysis, we used model results from the Aerosol Comparisons between Observations and Models (AeroCom) project, an open international initiative aimed at understanding the global aerosol and its impact on climate (Samset et al., 2014; Myhre et al., 2013; Jiao et al., 2014; Tsigaridis et al., 2014). The project combines a large number of observations and outputs from fourteen global models to test, document and compare state-of-the-art modelling of the global aerosol. We specifically show standardised (i.e., subtracting the mean and then dividing by the standard deviation) deposition fluxes of BC, dust and organic aerosols (OA) from the GISS modelE contribution to the AeroCom phase II series of model runs (<http://aerocom.met.no/aerocomhome.html>). The runs used here took as input the decadal emission data from the Coupled Model Intercomparison Project Phase 5 (CMIP5). In this case, we report the outputs of the NASA GISS ModelE obtained from the AeroCom. In particular, Figures 9 and 10 show modelled deposition fluxes at the two locations of Kangerlussuaq (Figure 9, $67^{\circ}00'31''\text{N}$, $50^{\circ}41'21''\text{W}$) and Summit (Figure 10, $72^{\circ}34'47''\text{N}$, $38^{\circ}27'33''\text{W}$) for the months of June, July and August and aerosol components (BC, dust and organic matter). These locations were selected as representative of the ablation zone (Kangerlussuaq) and the dry-snow zone (Summit). The analysis of the NASA GISS ModelE AeroCom outputs shows no statistically significant trend in the modelled fluxes for either location, consistent with the results

recently reported by Polashenski et al. (2015) for the dry snow zone. Results of the analysis of fluxes over different areas point to similar conclusions. Similar results are obtained when considering the months of January, February and March, when aerosol concentration is expected to be higher. The results here presented complement other studies (e.g. Stone et al., 2014) indicating that, since the 1980s, atmospheric concentrations of BC measured at surface stations in the Arctic have decreased, with variations attributed to changes in both anthropogenic and natural aerosol and aerosol precursor emissions.

Mean summer values of AOD (550 nm) measured at three AERONET (<http://aeronet.gsfc.nasa.gov>) Greenland sites based in Thule (northwest Greenland; 77°28'00"N, 69°13'50"W), Ittoqqortoormiit (east-central Greenland; 70°29'07"N, 21°58'00"W), and Kangerlussuaq during the period 2007 – 2013 (with the starting year ranging between 2007 and 2009, depending on the site) are reported in Table 2, together with their standard deviations. None of the stations show statistically significant trends in AOD, consistent with the results of the analysis of the modelled deposition fluxes.

A recent study (Dumont et al., 2014) concluded that dust deposition has been increasing over much of the GrIS and that this is driving lowered albedo across the ice sheet. That conclusion was based on trends of an “impurity index”, which is the ratio of the logarithm of albedo in the 545-565 nm MODIS band (where LAI affect albedo) to the logarithm of albedo in the 841-876 nm band (where they do not). In the MODIS product used in Dumont et al. (2014) study, albedo values rely on removal of the effects of aerosols in the atmosphere. In the Dumont et al. (2014) study this correction was made using simulations of atmospheric aerosols by the Monitoring Atmospheric Composition and Climate (MACC) model. Their resulting “impurity index” shows positive trends, and these are attributed in part (up to 30%) to increases in atmospheric aerosol not accounted for by the model, and the remainder to increases in snow LAI. The latter is consistent with our findings herein: that GrIS darkening is in part attributable to an increase in the impurity content of surface snow. However, Dumont et al. (2014) assume that this increase in surface snow LAI is a result of enhanced deposition from the atmosphere. They do not account for the possibility that positive trends in impurity content may instead be a result of a warming-driven in-snow processes. Indeed, their own table shows variable AOD at AERONET stations in Greenland, but no trend over the period studied (2007 – 2012).

The results of the analysis discussed above reinforce our argument that the decline in the visible albedo over Greenland is probably not due to an increase in the rate of deposition of LAI from the atmosphere, but instead are due to the consolidation of LAI at the snow surface with warming-driven increases in melt and/or sublimation and with the increased exposure of underlying dirty ice.

4 Albedo projections through 2100

We estimated future projections of summer albedo over the GrIS using MAR forced with the outputs of three different Earth System Models (ESMs) from CMIP5 driven by two radiative forcing scenarios (Meinshausen et al., 2011) over the 120-year period 1980 – 2100. The first scenario corresponds to an increase in the atmospheric

Marco T 1/9/16 09:47

Deleted: Therefore, in the next section, we focus on assessing whether atmospheric aerosol levels over the GrIS have increased (as a proxy for whether the deposition of aerosol has increased) and we look for trends in forest fires in the two of the main source regions for aerosols over the GrIS. ... [2]

Marco T 1/6/16 09:12

Deleted: s

Marco T 1/2/16 10:44

Deleted: impurities

Marco T 1/12/16 10:51

Deleted: .

Marco T 1/2/16 10:03

Deleted: fo

greenhouse gas concentration to a level of 850 ppm CO₂ equivalent (RCP45); the second scenario increases CO₂ equivalent to > 1370 ppm in 2100 (RCP85) (Moss et al., 2010; Meinshausen et al., 2011). The three ESMs used are the second generation of the Canadian Earth System Model (CanESM2), the Norwegian Community Earth System Model (NorESM1) and the Model for Interdisciplinary Research on Climate (MIROC5) of the University of Tokyo, Japan. More information is available in Tedesco and Fettweis (2012). The ESMs are used to generate MAR outputs for the historical period (1980 – 2005) and for future projections (2005 – 2100). The Canadian Earth System Model (CanESM2, e.g. Arora and Boer, 2010, Chylek et al., 2011) combines the fourth generation climate model (CanCM4) from the Canadian Center for Climate Modelling and Analysis with the terrestrial carbon cycle based on the Canadian Terrestrial Ecosystem Model (CTEM), which models the land-atmosphere carbon exchange. The NorESM1 model is built under the structure of the Community Earth System Model (CESM) of the National Center for Atmospheric Research (NCAR). The major difference from the standard CESM configuration concerns a modification to the treatment of atmospheric chemistry, aerosols, and clouds (Seland et al., 2008) and the ocean component. Lastly, MIROC5 is a coupled general circulation model developed at the Center for Climate System Research (CCSR) of the University of Tokyo, composed of the CCSR/NIES (National Institute of Environmental Studies) atmospheric general circulation model (AGCM 5.5) and the CCSR Ocean Component Model, including a dynamic-thermodynamic sea-ice model (e.g., Watanabe et al., 2010, 2011). We refer to Tedesco and Fettweis (2012) for the evaluation of the outputs of MAR when forced with the outputs of the ESMs during the historical period (1980 – 2005). All simulations consistently point to darkening accelerating through the end of the century (Figure 11), with summer albedo anomalies (relative to year 2000) as large as -0.08 by the end of the century over the whole ice sheet, and even greater (-0.1) over the western portion of the ice sheet (Figure 12). The magnitude of the projected albedo anomalies by 2100, however, is probably underestimated by our simulations, because (a) the model tends to underestimate melting when forced with the ESMs (Fettweis et al., 2013), and therefore underestimates grain size growth, and (b) the model currently does not account for the presence of LAI in the snow or on the ice surface, nor for the positive feedback between LAI and snow/ice melt.

5 Discussion

Our results show a darkening of the GrIS 1996-2012, and indicate that this darkening is associated with increased surface snow grain size, an expansion in the area and persistence of bare ice, and by an increase in surface snow light-absorbing impurity (LAI) concentrations. We find no evidence for general increases in the deposition of LAI across the GrIS, so we associate the higher surface snow impurity concentrations predominantly with the appearance of underlying dirty ice and the consolidation of LAI in surface snow resulting from snow melt. Inter-annual variability in the JJA GLASS albedo is captured by the MAR albedo simulations, with the latter explaining ~ 90 % of the spaceborne-derived albedo interannual variations for the period 1996 - 2012. The strong correlation between MAR and GLASS albedo time series for this period suggests that MAR is capturing the processes driving most of the albedo inter-annual variability (grain size metamorphism and bare ice exposure) and that these processes have more influence than those associated with the spatial and temporal variability of surface

Marco T 1/6/16 09:19

Deleted: Figure 9

Marco T 1/12/16 10:52

Deleted: more

Marco T 1/6/16 09:23

Deleted: Figure 10

Marco T 1/12/16 10:52

Deleted:

Marco T 1/12/16 10:52

Deleted: does not account for the presence of impurities on the ice surface and for the enhanced mixing ratios in the surface of melting snow

Marco T 1/12/16 10:54

Deleted: Our results indicate that a darkening of the GrIS associated with increasing temperatures and enhanced melting occurred between 1996 and 2012, promoted by increased surface snow grain size, by an expansion in the area and persistence of exposed bare ice, and by an increase in surface snow impurity concentrations. We

Marco T 1/2/16 10:44

Deleted: impurities

Marco T 1/2/16 10:44

Deleted: impurities

impurity concentrations at seasonal timescales (currently not included in the MAR albedo scheme). This is reinforced by the fact that the range of snow grain size found across the GrIS produces larger changes in albedo than does the range of LAI concentrations measured over the GrIS, at least in the cold-snow and percolation zones of the ice sheet. As pointed out by Tedesco et al. (2015), for pure snow, grain growth from new snow (with $r = 100 \mu\text{m}$) to old melting snow ($r = 1000 \mu\text{m}$) can reduce broadband albedo by $\sim 10\%$. By comparison, adding 20 ng g^{-1} of BC, which has been found in the top layer of melting GrIS snow, reduces albedo by only 1-2%, consistently with the results reported by Polashenski et al. (2015).

Modeled (MAR) and retrieved (GLASS) albedo are compared, with the latter showing stronger declines in GrIS albedo, particularly over the ablation zone. Based on our analysis, we suggest that the difference between MAR and GLASS trends cannot be driven solely by the MODIS sensor degradation on the TERRA satellite (also used in the GLASS product), because the estimated impact of sensor degradation on the albedo trend is much smaller than the difference between the MAR and GLASS trends, and because the GLASS product is obtained by combining data from both TERRA and AQUA satellites, hence likely reducing the impact of the TERRA sensor degradation on the trends. This is especially true over the dark zone, where substantial melting occurs and where the albedo decline is pronounced. As mentioned, a lack of impurities in the MAR albedo scheme can affect simulated albedo trends in at least two ways: first, the concentration of impurities over bare ice areas could be increasing or/and the lack of impurities in the MAR albedo scheme causes bare ice areas to have an overestimated albedo. Moreover, more frequent exposure of bare ice would lead to a decline in annual average albedo over time, with such a trend being larger in the case of the presence of impurity concentrations on the ice surface. Our sensitivity analysis of the simulated trends on the bare ice albedo value indicates that the difference between MAR and GLASS estimated trends is consistent with a relatively darker (e.g., containing LAI) bare ice. Since MAR does not account for the presence of surface LAI, and because the impact of LAI is mostly in the UV and visible portion of the spectrum, we suggest that another mechanism explaining the difference of $-0.017 \text{ decade}^{-1}$ between the MAR and GLASS visible albedo trends is associated with increasing mixing ratios of LAI in surface snow and ice on some parts of the GrIS. As we pointed out, this could be due to a combination of increased exposure of dirty ice with ablation (Wientjes and Oerlemans, 2010; Bøggild et al., 2010), to enhanced melt consolidation with warming (e.g., Doherty et al., 2013), or to increased deposition of LAI from the atmosphere. The absence of in-situ, spatially distributed measurements to separate these processes means that we cannot quantify their relative contributions to the darkening in the visible region. Based on our analysis of trends in AOD over Greenland and the lack of a trend in forest-fire counts and BC in North America and Eurasia, we argue that increased deposition of LAI is not a large driver for the observed negative trends in Greenland surface albedo. An exception could be an increase in the deposition of locally-transported dust near the glacial margins, which would primarily affect the ablation zone. In particular, locally lofted dust may be playing a substantial role in the southwest GrIS ablation zone. However, we note that increased deposition is not needed in order to have an increase in the concentration of LAI at the GrIS surface. As noted above, indeed, temperatures and melt rates have been accelerating over the GrIS during the past decades (e.g., Tedesco et al., 2014). When

Marco T 1/12/16 10:56

Deleted:

Marco T 1/12/16 10:56

Deleted: This is plausible also in view of the relatively large impact on albedo due to grain size metamorphism by comparison to the expected albedo decrease associated with the impurity concentrations measured over the GrIS

Marco T 1/6/16 08:30

Deleted: %.

Marco T 1/9/16 14:32

Deleted: T

Marco T 1/9/16 14:32

Deleted: was

Marco T 1/2/16 10:03

Deleted:

Marco T 1/12/16 14:44

Deleted: Instead, s

Marco T 1/2/16 10:44

Deleted: impurities

Marco T 1/2/16 10:44

Deleted: impurities

Marco T 1/12/16 14:47

Deleted: can be attributed to

Marco T 1/2/16 10:44

Deleted: impurities

Marco T 1/2/16 10:44

Deleted: impurities

Marco T 1/2/16 10:44

Deleted: light-absorbing impurities

Marco T 1/2/16 10:45

Deleted: impurities

snow melts, snow water is removed from the surface more efficiently than particulate impurities; the result is an increase in impurity concentrations in surface snow (e.g. Flanner et al., 2007; Doherty et al., 2013). Large particles, such as dust, in particular, will have poor mobility through the snowpack (Conway et al., 1996) so their concentration at the surface is expected to increase with snowmelt. This effect may be especially amplifying snow impurity content in the low-altitude ablation zone of the GrIS, where enhanced melting has been occurring (e.g., Tedesco et al., 2014). Further, the albedo reduction for a given concentration of an absorbing impurity in snow is greater in large-grained snow than in small-grained snow (Figure 7 of Warren and Wiscombe, 1980; Flanner et al., 2007), so climate warming itself will amplify the effect of LAI on surface albedo. Warming may also lead to increased sublimation, removing snow water but not particles from the snow surface, again increasing concentrations of LAI in surface snow.

Snow and ice warmed by increased temperatures and higher LAI concentrations also promotes darkening via so-called 'bio-albedo', with biological growth on the surface depressing the albedo. Green, pink, purple, brown and black pigmented algae, indeed, occur in melting snow and ice. Microbes can bind to particulates, including BC, retaining them at the surface in higher concentrations than in the parent snow and ice. The magnitude of this source of darkening is currently unquantified, but as the climate warms and melt seasons lengthen, biological habitats are expected to expand, with their contribution to darkening likely increasing (Benning et al., 2014).

Quantifying the impact of aerosols on Greenland darkening is also made difficult by the large disagreements among models in their predicted aerosol deposition rates over the GrIS. We examine the contrast between AOD trends from the MACC model used by Dumont et al., (2014) and the Goddard Chemistry Aerosol Radiation and Transport model (GOCART). The GOCART model simulates major tropospheric aerosol components, including sulphate, dust, BC, organic carbon (OC), and sea-salt aerosols using assimilated meteorological fields of the Goddard Earth Observing System Data Assimilation System (GEOS DAS), generated by the Goddard Global Modeling and Assimilation Office. Figure 13 compares results for AOD at 550 nm from MACC and GOCART for dust, organic matter and black carbon for the domain bounded by 75 to 80°N and 30 to 50° W (the same area considered by Dumont et al., 2014). The MACC model shows statistically significant trends for dust ($p < 0.01$) and for total aerosols ($p < 0.05$). All remaining trends are not statistically significant for both MACC and GOCART outputs (Figure 13).

Neither model represents the process of increased exposed silt/dust as Greenland glaciers recede; therefore, we would not expect them to capture trends in dust from this source. The inconsistency between the MACC and GOCART values and trends is puzzling, and indicates that the simulation of aerosol deposition rates over Greenland needs improvement.

6 Summary and conclusions

We studied the mean summer broadband albedo over the Greenland ice sheet between 1981 and 2012 as estimated from spaceborne measurements and found that summer albedo decreased at a rate of 0.02 decade^{-1} between 1996 and 2012. The analysis of the outputs of the MAR regional climate model indicates that the observed darkening is associated with increasing temperatures and enhanced melting occurring during the

Marco T 1/2/16 10:45

Deleted: impurities

Marco T 1/2/16 10:45

Deleted: impurities

Marco T 1/12/16 11:00

Deleted: The presence of surface impurities also promotes the evolution of the so-called 'bioalbedo'

Marco T 1/12/16 11:00

Deleted: For example, in Figure 11

Marco T 1/12/16 11:00

Deleted: w

Marco T 1/6/16 09:26

Deleted: Figure 11

Marco T 1/4/16 07:41

Deleted: no significant trend in deposited aerosols, and MACC shows a trend only for dust

Marco T 1/6/16 09:26

Deleted: Figure 11

Marco T 1/2/16 10:07

Deleted: captures trends in

Marco T 1/2/16 10:22

Deleted: Light-absorbing impurities in snow affect albedo not only directly, but also indirectly by absorbing sunlight, warming the snowpack, and accelerating snow grain size growth. We started studying the magnitude of this "indirect effect" of impurities on snow grain size, and therefore albedo, by modifying the albedo scheme within MAR. Specifically, we reduced the visible component of the albedo, α_v in Eq. 2, by between 0.01 and 0.05 to simulate the effects of impurities. This was, in turn, used in Eq. 1 to compute the broadband albedo. The value of 0.05 was estimated as the maximum estimated albedo decrease for BC concentrations measured in the cold snow and percolation zones of the GIS. The value of -0.05 used in our simulations for each iteration of MAR likely overestimates the effect of impurities on grain size at the beginning of the melting season, but underestimates the effect during the melting season when impurities tend to concentrate at the snow surface (Doherty et al., 2013). Higher concentrations of impurities are present along the margins of the ice sheet because of their proximity to local sources of dust and the proliferation of algae and microorganisms on the ice surface, so the effect of impurities on grain size is likely larger there. Still the results of this synthetic experiment can provide an initial indication of the indirect effect of impurities on the evolution of the snowpack and its albedo. We specifically focused for our experiment on an area of $100 \times 100 \text{ km}^2$... [3]

1 same period, which in turn promote increased surface snow grain size as well as the
 2 expansion and persistency of areas with exposed bare ice. The MAR model simulates
 3 well the interannual variability in the retrieved GLASS albedo, but the albedo trend is
 4 larger in the GLASS albedo product than in MAR, indicating that processes not
 5 represented in the MAR physics account for some of the declining albedo. Specifically,
 6 we suggest that the absence of the effects of light-absorbing impurities in MAR could
 7 account for the difference. We also suggest that this hypothesis is supported by the trends
 8 observed along the ablation zone, where the differences between observed and modeled
 9 trends are more pronounced and the effect of the TERRA sensor degradation plays a
 10 relatively small role. On the other hand, over the dry snow zone, our hypothesis requires
 11 further testing, in view of the potentially higher impact of the sensor degradation on the
 12 observed albedo trend. The analysis of modelled fields and in-situ data indicated an
 13 absence of trends in aerosol optical depth over Greenland, as well as no significant trend
 14 in particulate light-absorbing emissions (e.g. BC) from fires in likely source regions. This
 15 is consistent with the absence of trends in surface aerosol concentrations measured
 16 around the Arctic. Consequently, we suggest that the increased surface concentrations of
 17 LAI associated with the darkening is not related to increased deposition of LAI, but
 18 rather to post-depositional processes, including increased loss of snow water to
 19 sublimation and melt and the outcropping of ‘dirty’ underlying ice associated with
 20 snow/firm removal due to ablation.

21 Future projections of GrIS albedo obtained from MAR forced under different
 22 warming scenarios point to continued darkening through the end of the century, with
 23 regions along the edges of the ice sheet subject to the largest decrease, driven solely by
 24 warming-driven changes in snow grain size, exposure of bare ice, and melt pool
 25 formation. We hypothesise that projected darkening trends would be even greater in view
 26 of the underestimated projected melting (and effect on albedo) and in view of the fact that
 27 the current version of the MAR model does not account for the presence of surface LAI
 28 and the associated positive direct and indirect impact on lowered albedo.

29 The drivers we identified to be responsible for the observed darkening are related to
 30 endogenous processes rather than exogenous ones and are strongly driven by melting.
 31 Because melting is projected to increase over the next decades, it is crucial to assess the
 32 state of the art of studying, quantifying and projecting these processes as they will
 33 inevitably impact, and be impacted by, future scenarios. Intrinsic limitations of current
 34 observational tools and techniques, the scarcity of in-situ observations, and the albedo
 35 schemes currently used in existing models of surface energy balance and mass balance
 36 limit our ability to separate the contributions to darkening by the different processes,
 37 especially with regard to the cause and evolution of surface impurity concentrations.
 38 Moreover, as with all instruments, sensors undergo deterioration, and it can be difficult to
 39 separate an albedo trend from sensor drift. This is especially true in the dry-snow zone,
 40 where impurity concentrations are extremely low (only a few ppb in the case of BC). In
 41 this regard, a recent study by Polashenski et al. (2015) suggests that the decline and
 42 spectral shift in dry snow albedo over Greenland contains important contributions from
 43 uncorrected Terra sensor degradation when using the MODIS data collection C5. The
 44 new MODIS TERRA version (accounting for the sensor degradation) does not appear to

Marco T 1/10/16 15:08

Deleted: conclude

Marco T 1/2/16 10:45

Deleted: impurities

Marco T 1/2/16 10:45

Deleted: impurities

Marco T 1/2/16 10:45

Deleted: impurities

Marco T 1/2/16 08:32

Formatted: Font:12 pt

show any trend (Polashenski, *Pers. Comm.*), hence supporting the hypothesis of the absence of trends of LAI deposition over the dry zone.

Remote sensing and in-situ observations should be complemented with models that simulate the surface energy balance to account for the evolution of the snowpack, in particular changes in surface grain size and exposure of bare ice. Simulations with regional climate models can provide such quantities, but they do not currently account for the transport and deposition of LAI to Greenland, the post-depositional evolution of impurities in the snowpack, and the synergism between surface LAI and grain growth (whereby a given impurity content causes more albedo reduction in coarse-grained snow than in fine-grained snow). In this regard, the current parameterisation for snow albedo in MAR is based on that of Brun et al. (1992), as part of an avalanche-forecasting model. As a consequence of the results of this study, we began evaluating an alternative albedo scheme using a parameterisation that can also account for the albedo reduction by absorptive impurities (e.g. Dang et al., 2015). Moreover, we are also considering using the firn/ice albedo parameterisation of Dadic et al (2013), based on measurements covering the range of densities from 400 to 900 kg m⁻³.

Surface-based measurements are needed to test satellite-retrieved albedo and to quantify the drivers behind albedo changes in different areas of Greenland. To date, most surface-based observations have been made in the dry-snow zone or the percolation zone, and they have generally focused on measuring the mixing ratios of BC (Hagler et al., 2007; McConnell et al., 2007, 2011; Polashenski et al., 2015) or of the spectral light absorption by all particulate components collectively (Doherty et al., 2010; Hegg et al., 2009, 2010). The regions of Greenland that are darkening the most rapidly are within the ablation zone. Here, there is no direct evidence that the rate of atmospheric deposition of LAI has been increasing. In view of the cumulative effect of snowmelt leaving impurities at the surface, the intra-seasonal variation of deposition may not be as important as the exposure of LAI by melting. Changes in the abundances of light-absorbing algae and other organic material with warmer temperatures may also be contributing to declining albedo, particularly for the ice, but this is an essentially un-studied source of darkening. Until measurements are made that quantify and distinguish the relative roles of each of these factors in the darkening of the GrIS, it is not possible to reduce the uncertainty in their contributions to the acceleration of surface melt. In addition to the need for targeted ground observations, it is necessary for the models that simulate and project the evolution of surface conditions over Greenland to start including the contribution of surface LAI, their processes, and their impact on albedo, as well as aerosol models that account for their deposition. Concurrently, spaceborne sensors or missions capable of separating the contributions from the different processes (with increased spatial, spectral and radiometric resolution) should be planned for remote sensing to become a more valuable tool in this regard.

Author contributions

MT conceived the study, carried out the scientific analysis and wrote the main body of the manuscript. SD co-wrote the manuscript and provided feedback on the analysis of the impact of surface LAI on the albedo decrease. PA provided MODIS visible data for the comparison with the GLASS-estimated visible albedo. JJ supported the reprojection

Marco T 1/2/16 08:32

Formatted: Font:12 pt, Not Italic

Marco T 1/2/16 08:32

Formatted: Font:12 pt

Marco T 1/2/16 08:32

Formatted: Font:12 pt

Marco T 1/12/16 11:02

Deleted:

Marco T 1/2/16 10:45

Deleted: impurities

Marco T 1/2/16 10:45

Deleted: impurities

Marco T 1/2/16 10:46

Deleted: impurities

Marco T 1/2/16 10:46

Deleted: impurities

Marco T 1/2/16 10:46

Deleted: impurities

Marco T 1/2/16 10:46

Deleted: impurities

Marco T 1/2/16 10:16

Deleted: EN provided the MAR simulations for the sensitivity of grain-size evolution to changes in the visible albedo.

1 and analysis of GLASS and MAR data. XF contributed with the analysis of MAR
2 outputs. MT, SD, XF and JS edited the final version of the manuscript.

3 Acknowledgments

4 MT and PA were supported by NSF grants PLR1304807 and ANS 0909388, and NASA
5 grant NNX1498G. The authors are grateful to Kostas Tsirigadis (NASA GISS) for
6 providing the outputs of GISS modelE of the AeroCom phase II project and to Marie
7 Dumont, Eric Brun and Samuel Morin for the data used in [Figure 13](#).

8 We thank Tao He at the University of Maryland, College Park, for the discussion
9 on the GLASS product. The authors thank Stephen Warren for providing suggestions and
10 guidance during the preparation of the manuscript, particularly for pointing out
11 limitations and providing suggestions on the albedo parameterisations.

12 7 References

- 13 Alexander, P. M., Tedesco, M., Fettweis, X., van de Wal, R. S. W., Smeets, C. J. P. P.
14 and van den Broeke, M. R.: Assessing spatio-temporal variability and trends (2000–
15 2013) of modelled and measured Greenland ice sheet albedo, *The Cryosphere*, 8(4),
16 2293–2312, 2014.
- 17 Arnaud, L., J.M. Barnola, and P. Duval, Physical modeling of the densification of
18 snow/firn and ice in the upper part of polar ice sheets. In *Physics of Ice Core Records*
19 (T. Hondoh, Ed.), Hokkaido University Press, Sapporo, Japan, 285–305, 2000
- 20 Arora V. K. and Boer G. J., Uncertainties in the 20th century carbon budget associated
21 with land use change *Glob. Change Biol.* **16**(12), 3327–3348, doi:10.1111/j.1365-
22 2486.2010.02202.x, 2010
- 23 Benning, L. G., Anesio, A. M., Lutz, S. and Tranter, M.: Biological impact on
24 Greenland's albedo, *Nature Geosci.* 7(10), 691–691, doi:10.1038/ngeo2260, 2014.
- 25 Benson, C.S., 1962: *Stratigraphic Studies in the Snow and Firn of the Greenland Ice*
26 *Sheet*. Research Report 70, U.S. Army Snow, Ice, and Permafrost Research
27 Establishment (SIPRE), 93 pp.
- 28 Bøggild, C.E., R.E. Brandt, K.J. Brown, and S.G. Warren (2010), The ablation zone in
29 northeast Greenland: Ice types, albedos, and impurities. *J. Glaciol.*, **56**, 101–113.
- 30 Bond, T. C., S. J. Doherty, D. W. Fahey, P. M. Forster, T. Berntsen, B. J. DeAngelo, M.
31 G. Flanner, S. Ghan, B. Kärcher, D. Koch, S. Kinne, Y. Kondo, P. K. Quinn, M. C.
32 Sarofim, M. G. Schultz, M. Schulz, C. Venkataraman, H. Zhang, S. Zhang, N.
33 Bellouin, S. K. Guttikunda, P. K. Hopke, M. Z. Jacobon, J. W. Kaiser, Z. Klimont, U.
34 Lohmann, J. P. Schwarz, D. Shindell, T. Storelvmo, S. G. Warren and C. S. Zender,
35 Bounding the Role of Black Carbon in Climate: A scientific assessment, *J. Geophys.*
36 *Res.*, 118(11), 5380–5552, doi:10.1002/jgrd.50171, 2013.
- 37 Box, J. E., Fettweis, X., Stroeve, J. C., Tedesco, M., Hall, D. K., and Steffen, K.:
38 Greenland ice sheet albedo feedback: thermodynamics and atmospheric drivers, *The*
39 *Cryosphere*, 6, 821–839, doi:10.5194/tc-6-821-2012, 2012.

Marco T 1/6/16 09:26

Deleted:

Marco T 1/6/16 09:26

Deleted: Figure 11

Marco T 1/2/16 12:23

Deleted: -

- 1 Brun, E., David, P., Sudul, M. and Brunot, G.: A numerical model to simulate snow-
2 cover stratigraphy for operational avalanche forecasting, *Journal of Glaciology*,
3 38(128), 13–22, 1992.
- 4 Cachier, H. and Pertuisot, M. H.: Particulate carbon in Arctic ice, *Analisis Magazine*, 22,
5 34–37, 1994
- 6 Ch'ylek, P., Johnson, B., Damiano, P. A., Taylor, K. C., and Clement, P.: Biomass
7 burning record and black carbon in the GISP2 ice core, *Geophys. Res. Lett.*, 22, 89–
8 92, 1995. –
- 9 Chylek ,P., Li ,J., Dubey ,M. K., Wang ,M. and Lesins G., Observed and model simulated
10 20th century Arctic temperature variability: Canadian Earth System Model
11 CanESM2 *Atmos. Chem. Phys. Discuss.* **11** 22893–22907, 2011
- 12 Clarke, A.D. and Noone, K.J.: Soot in the Arctic snowpack: A cause for perturbations in
13 radiative transfer, *Atmos. Environ.*, 19, 2045–2053, 1985.
- 14 Conway, H., A. Gades, and C. F. Raymond (1996), Albedo of dirty snow during
15 conditions of melt, *Water Resour. Res.*, **32**(6), 1713–1718.
- 16 Dadic, R., P.C. Mullen, M. Schneebeli, R.E. Brandt, and S.G. Warren, 2013: Effects of
17 bubbles, cracks, and volcanic tephra on the spectral albedo of bare ice near the Trans-
18 Antarctic Mountains: implications for sea-glaciers on Snowball Earth. *J. Geophys.*
19 *Res. (Earth Surfaces)*, 118, doi:10.1002/jgrf.20098.
- 20 Dang, C., R.E. Brandt, and S.G. Warren, 2015: Parameterizations for narrowband and
21 broadband albedo of pure snow, and snow containing mineral dust and black carbon.
22 *J. Geophys. Res.*, 120, doi:10.1002/2014JD022646.
- 23 De Ridder K., and Galle' H. Land surface-induced regional climate change in Southern
24 Israel, *Appl. Meteorol.*, 37, 1470–1485, 1998.
- 25 Doherty, S. J., Grenfell, T. C., Forsström, S., Hegg, D. L., Brandt, R. E. and Warren, S.
26 G.: Observed vertical redistribution of black carbon and other insoluble light-
27 absorbing particles in melting snow, *Journal of Geophysical Research: Atmospheres*,
28 118(11), 5553–5569, 2013.
- 29 Doherty, S. J., Warren, S. G., Grenfell, T. C., Clarke, A. D. and Brandt, R. E.: Light-
30 absorbing impurities in Arctic snow, *Atmos. Chem. Phys.*, 10(23), 11647–11680,
31 2010.
- 32 Dumont, M., Brun, E., Picard, G., Michou, M., Libois, Q., Petit, J.-R., Geyer, M.,
33 Morin, S. and Josse, B.: Contribution of light-absorbing impurities in snow to
34 Greenland's darkening since 2009, *Nature Geosci.*, 7(7), 509–512, 2014.
- 35 Fettweis, X., Franco, B., Tedesco, M., van Angelen, J. H., Lenaerts, J. T. M., van den
36 Broeke, M. R. and Gallée, H.: Estimating the Greenland ice sheet surface mass
37 balance contribution to future sea level rise using the regional atmospheric climate
38 model MAR, *The Cryosphere*, 7(2), 469–489, 2013.

- 1 Fettweis, X., Gallée, H., Lefebvre, F. and van Ypersele, J.-P.: Greenland surface mass
2 balance simulated by a regional climate model and comparison with satellite-derived
3 data in 1990–1991, *Climate Dynamics*, 24(6), 623–640, 2005.
- 4 Flanner, M. G., Zender, C. S., Randerson, J. T., and Rasch, P. J.: Present-day climate
5 forcing and response from black carbon in snow, *J. Geophys. Res.*, 112, D11202,
6 doi:10.1029/2006JD008003, 2007.
- 7 Grenfell, T.C., D.K. Perovich, and J.A. Ogren, 1981: Spectral albedos of an alpine
8 snowpack. *Cold Reg. Sci. Technol.*, 4, 121-127.
- 9 Greuell, W. and Konzelman, T.: Numerical modelling of the energy balance and the
10 englacial temperature of the Greenland Ice Sheet, Calculations for the ETH-Camp
11 location (West Greenland, 1155 m a.s.l.), *Global and Planetary Change*, 9, 91–114,
12 1994.
- 13 Hagler, G. S. W., Bergin, M. H., Smith, E. A., and Dibb, J. E.: A summer time series of
14 particulate carbon in the air and snow at Summit, Greenland, *J. Geophys. Res.*, 112,
15 D21309, doi:10.1029/2007JD008993, 2007.
- 16 He, T., Liang, S., Yu, Y., Wang, D., Gao, F. and Liu, Q.: Greenland surface albedo
17 changes in July 1981–2012 from satellite observations, *Environ. Res. Lett.*, 8(4),
18 044043, 2013.
- 19 Hegg, D. A., Warren, S. G., Grenfell, T. C., Doherty, S. J., Larson, T. V. and Clarke, A.
20 D.: Source Attribution of Black Carbon in Arctic Snow, *Environmental Science &*
21 *Technology*, 43(11), 4016–4021, 2009.
- 22 Hegg, D.A., S.G. Warren, T.C. Grenfell, S.J. Doherty, and A.D. Clarke, 2010: Sources
23 of light-absorbing aerosol in Arctic snow and their seasonal variation. *Atmos. Chem.*
24 *Phys.*, 10, 10923-10938 .
- 25 Herron, M.M., and C.C. Langway, Jr., 1980: Firn densification: An empirical model. *J.*
26 *Glaciol.*, 25, 373-385.
- 27 Ichoku, C. and Ellison, L.: Global top-down smoke-aerosol emissions estimation using
28 satellite fire radiative power measurements, *Atmos. Chem. Phys.*, 14(13), 6643–
29 6667, 2014.
- 30 Keegan, K. M., M. R. Albert, J. R. McConnell and I. Baker, climate change and forest
31 fires synergistically drive widespread met events of the Greenland Ice Sheet, *PNAS*,
32 111, 7964-7967, doi: 10.1073/pnas.1405397111.
- 33 LaChapelle, E.R.: *Field Guide to Snow Crystals*, University of Washington Press, Seattle,
34 1969.
- 35 Jiao, C., et al.: An AeroCom assessment of black carbon in Arctic snow and sea ice,
36 *Atmos. Chem. Phys.*, 14(5), 2399–2417, 2014.
- 37 Lefebvre, F., Gallée, H., and van Ypersele, J.-P.: Modeling of snow and ice melt at ETH
38 Camp (West Greenland): a study of surface albedo,, 108, 4231,
39 doi:10.1029/2001JD001160, 2003
- 40 Liang, S., et al.: A long-term Global LAnd Surface Satellite (GLASS) data-set for
41 environmental studies, *International Journal of Digital Earth*, 6(sup1), 5–33, 2013.
- 42 Loeb, N.: In-flight calibration of NOAA AVHRR visible and near-IR bands over
43 Greenland and Antarctica, *International Journal of Remote Sensing*, 18, 477–490,
44 1997.

- 1 Masonis, S. J. and Warren, S. G.: Gain of the AVHRR visible channel as tracked using
2 bidirectional reflectance of Antarctic and Greenland snow, *International Journal of*
3 *Remote Sensing*, 22, 1495–1520, 2001.
- 4 [McConnell, J. R., R. Edwards, G. L. Kok, M. G. Flanner, C. S. Zender, E. S. Saltzman,](#)
5 [J. R. Banta, D. R. Pasteris, M. M. Carter, and J. D. W. Kahl, 20th-century industrial](#)
6 [black carbon emissions altered Arctic climate forcing, *Science*, 317\(5843\), 1381–](#)
7 [1384, doi:10.1126/science.1144856, 2007.](#)
- 8 McConnell, J. R., Edwards, R., Kok, G. L., Flanner, M. G., Zender, C. S. Saltzman, E.
9 S., Banta, J. R., Pasteris, D. R., Carter, M. M., and Kahl, J. D. W.: 20th century
10 industrial black carbon emissions altered Arctic climate forcing, *Science*, 317, 1381–
11 1384, doi:10.1126/science.1144856, 2007. Meinshausen, et al.: The RCP greenhouse
12 gas concentrations and their extensions from 1765 to 2300, *Climatic Change*, 109(1-
13 2), 213–241, 2011.
- 14 Moss, R. H., et al.: The next generation of scenarios for climate change research and
15 assessment, *Nature*, 463(7282), 747–756, 2010.
- 16 Myhre, et al.: Radiative forcing of the direct aerosol effect from AeroCom Phase II
17 simulations, *Atmos. Chem. Phys.*, 13(4), 1853–1877, 2013.
- 18 Nghiem, S. V., Hall, D. K., Mote, T. L., Tedesco, M., Albert, M. R., Keegan, K.,
19 Shuman, C. A., DiGirolamo, N. E. and Neumann, G.: The extreme melt across the
20 Greenland ice sheet in 2012, *Geophysical Research Letters*, 39(20), L20502, 2012.
- 21 Polashenski, C. M., J. E. Dibb, M. G. Flanner, J. Y. Chen, Z. R. Courville, A. M. Lai, J.
22 J. Schauer, M. M. Shafer, and M. Bergin: Neither dust nor black carbon causing
23 apparent albedo decline in Greenland's dry snow zone: Implications for MODIS C5
24 surface reflectance, *Geophys. Res. Lett.*, 42, 9319–9327,
25 doi:10.1002/2015GL065912, 2015.
- 26 Rae, J. G. L., Aðalgeirsdóttir, G., Edwards, T. L., Fettweis, X., Gregory, J. M., Hewitt,
27 H. T., Lowe, J. A., Lucas-Picher, P., Mottram, R. H., Payne, A. J., Ridley, J. K.,
28 Shannon, S. R., van de Berg, W. J., van de Wal, R. S. W. and van den Broeke, M.
29 R.: Greenland ice sheet surface mass balance: evaluating simulations and making
30 projections with regional climate models, *The Cryosphere*, 6(6), 1275–1294, 2012.
- 31 Rignot, E., Velicogna, I., van den Broeke, M. R., Monaghan, A. and Lenaerts, J. T. M.:
32 Acceleration of the contribution of the Greenland and Antarctic ice sheets to sea
33 level rise, *Geophysical Research Letters*, 38(5), L05503, 2011.
- 34 Samset, B. H., Myhre, G., Herber, A., Kondo, Y., Li, S. M., Moteki, N., Koike, M.,
35 Oshima, N., Schwarz, J. P., Balkanski, Y., Bauer, S. E., Bellouin, N., Bernsten, T.
36 K., Bian, H., Chin, M., Diehl, T., Easter, R. C., Ghan, S. J., Iversen, T., Kirkevåg,
37 A., Lamarque, J. F., Lin, G., Liu, X., Penner, J. E., Schulz, M., Seland, Ø., Skeie, R.
38 B., Stier, P., Takemura, T., Tsigaridis, K. and Zhang, K.: Modeled black carbon
39 radiative forcing and atmospheric lifetime in AeroCom Phase II constrained by
40 aircraft observations, *Atmospheric Chemistry and Physics Discussions*, 14(14),
41 20083–20115, 2014.

- 1 Schaaf, C. B., Gao, F., Strahler, A. H., Lucht, W., Li, X., Tsang, T., Strugnell, N. C.,
2 Zhang, X., Jin, Y., Muller, J. P., Lewis, P., Barnsley, M., Hobson, P., Disney, M.,
3 Roberts, G., Dunderdale, M., Doll, C., d'Entremont, R. P., Hu, B., Liang, S., Privette,
4 J. L. and Roy, D.: First operational BRDF, albedo nadir reflectance products from
5 MODIS, *Remote Sensing of Environment*, 115, 1296–1300, 2002.
- 6 Seland, O., T. Iversen, A. Kirkevåg and T. Storelvmo, Aerosol-climate interactions in the
7 CAM-Oslo atmospheric GCM and investigation of associated basic shortcomings
8 *Tellus A* **60** p 459–491. doi: 10.1111/j.1600-0870.2008.00318.x, 2008
- 9 Shepherd, A., et al.: A Reconciled Estimate of Ice-Sheet Mass Balance, *Science*,
10 338(6111), 1183–1189, 2012.
- 11 Steffen, K. and Box, J. E.: Surface climatology of the Greenland ice sheet: Greenland
12 Climate Network 1995-1999, *Journal of Geophysical Research*, 106(D24), 33951–
13 33964, 2001.
- 14 Stohl, A., et al.: Pan-Arctic enhancements of light absorbing aerosol concentrations due
15 to North American boreal forest fires during summer 2004, *J. Geophys. Res.*,
16 111(D22), D22214, 2006.
- 17 Stone, R. S., Sharma, S., Herber, A., Eleftheriadis, K. and Nelson, D. W.: A
18 characterization of Arctic aerosols on the basis of aerosol optical depth and black
19 carbon measurements, *Elementa: Science of the Anthropocene*, 2, 000027, 2014.
- 20 Stroeve, J., Box, J. E., Gao, F., Liang, S., Nolin, A. and Schaaf, C.: Accuracy assessment
21 of the MODIS 16-day albedo product for snow: comparisons with Greenland in situ
22 measurements, *Remote Sensing of Environment*, 94(1), 46–60, 2005.
- 23 Stroeve, J., Box, J. E., Wang, Z., Schaaf, C. and Barrett, A.: Re-evaluation of MODIS
24 MCD43 Greenland albedo accuracy and trends, *Remote Sensing of Environment*,
25 138, 199–214, 2013.
- 26 Tedesco, M. and Fettweis, X.: 21st century projections of surface mass balance changes
27 for major drainage systems of the Greenland ice sheet, *Environ. Res. Lett.*, 7(4),
28 045405, 2012.
- 29 Tedesco, M., Fettweis, X., Broeke, M. R. V. D., Wal, R. S. W. V. de, Smeets, C. J. P. P.,
30 Berg, W. J. V. de, Serreze, M. C. and Box, J. E.: The role of albedo and
31 accumulation in the 2010 melting record in Greenland, *Environ. Res. Lett.*, 6(1),
32 014005, 2011.
- 33 Tedesco, M., Fettweis, X., Mote, T., Wahr, J., Alexander, P., Box, J. E. and Wouters, B.:
34 Evidence and analysis of 2012 Greenland records from spaceborne observations, a
35 regional climate model and reanalysis data, *The Cryosphere*, 7(2), 615–630, 2013.
- 36 Tedesco, M., S. Doherty, S. Warren, J. Stroeve, P. Alexander, X. Fettweis, and M.
37 Tranter, 2015: What darkens the Greenland ice sheet? *EOS*, in press.
- 38 Tedesco, M., J. E. Box, J. Cappelen, X. Fettweis, T. Mote, A. K. Rennermalm, R. S. W.
39 van de Wal and J. Wahr, 2014: Greenland Ice Sheet in [2013 *NOAA Arctic Report*
40 *Card*]

- 1 Tsigaridis, K., et al.: The AeroCom evaluation and intercomparison of organic aerosol in
2 global models, *Atmospheric Chemistry and Physics Discussions*, 14(5), 6027–6161,
3 2014.
- 4 van Angelen, J. H., Lenaerts, J. T. M., Lhermitte, S., Fettweis, X., Kuipers Munneke, P.,
5 van den Broeke, M. R., van Meijgaard, E. and Smeets, C. J. P. P.: Sensitivity of
6 Greenland Ice Sheet surface mass balance to surface albedo parameterization: a
7 study with a regional climate model, *The Cryosphere*, 6(5), 1175–1186, 2012.
- 8 van den Broeke, M. R., C. J. P. P. Smeets, and R. S. W. van de Wal, The seasonal cycle
9 and interannual variability of surface energy balance and melt in the ablation zone of
10 the west Greenland ice sheet, *Cryosphere*, 5, 377-390, doi:10.5194/tc-5-377-2011.
- 11 Vernon, C. L., Bamber, J. L., Box, J. E., van den Broeke, M. R., Fettweis, X., Hanna, E.
12 and Huybrechts, P.: Surface mass balance model intercomparison for the Greenland
13 ice sheet, *The Cryosphere*, 7(2), 599–614, 2013.
- 14 Wang, D., Morton, D., Masek, J., Wu, A., Nagol, J., Xiong, X., Levy, R., Vermote, E.
15 and Wolfe, R.: Impact of sensor degradation on the MODIS NDVI time series,
16 *Remote Sensing of Environment*, 119, 55–61, 2012.
- 17 Warren, S. G.: Optical properties of snow, *Reviews of Geophysics and Space Physics*,
18 20(1), 67–89, 1982.
- 19 Warren, S. G.: Can black carbon in snow be detected by remote sensing? *Journal of*
20 *Geophysical Research: Atmospheres*, 118(2), 779–786, 2013.
- 21 Warren, S.G., and W.J. Wiscombe, 1980: A model for the spectral albedo of snow, II:
22 Snow containing atmospheric aerosols. *J. Atmos. Sci.*, **37**, 2734-2745.
- 23 Watanabe et al, Improved Climate Simulation by MIROC5: Mean States, Variability, and
24 Climate Sensitivity. *J. Climate*, **23**, 6312–6335, 2010
- 25 Watanabe S, Hajima T, Sudo K, Nagashima T, Takemura T, Okajima H, Nozawa T,
26 Kawase H, Abe M, Yokohata T, Ise T, Sato H, Kato E, Takata K, Emori S and
27 Kawamiya M 2011 MIROC-ESM: model description and basic results of CMIP5-
28 20c3m experiments, *Geosci. Model Dev. Discuss.*, **4**, 1063-1128, doi:10.5194/gmdd-
29 4-1063-2011
- 30 Wientjes, I. G. M. and Oerlemans, J.: An explanation for the dark region in the western
31 melt zone of the Greenland ice sheet, *The Cryosphere*, 4(3), 261–268, 2010.
- 32 Wientjes, I. G. M., van de Wal, R. S. W., Reichert, G. J., Sluijs, A. and Oerlemans, J.:
33 Dust from the dark region in the western ablation zone of the Greenland ice sheet,
34 *The Cryosphere*, 5, 589–601, 2011.
- 35 Xing, J., Mathur, R., Pleim, J., Hogrefe, C., Gan, C. M., Wong, D. C., Wei, C., Gilliam,
36 R. and Pouliot, G.: Observations and modeling of air quality trends over 1990–2010
37 across the Northern Hemisphere: China, the United States and Europe, *Atmos.*
38 *Chem. Phys.*, 15(5), 2723–2747, 2015.

Xing, J., Pleim, J., Mathur, R., Pouliot, G., Hogrefe, C., Gan, C. M. and Wei, C.:
Historical gaseous and primary aerosol emissions in the United States from 1990 to
2010, *Atmos. Chem. Phys.*, 13(15), 7531–7549, 2013.

Ying, Q., Qiang, L., Shunlin, L., Lizhao, W. Nanfeng, L. and Suhong L. : Direct-
Estimation Algorithm for Mapping Daily Land-Surface Broadband Albedo From
MODIS Data, *Geoscience and Remote Sensing, IEEE Transactions on* , vol.52, no.2,
pp.907-919, 2014, doi: 10.1109/TGRS.2013.2245670

Zhao, X.; Liang, S.; Liu, S.; Yuan, W.; Xiao, Z.; Liu, Q.; Cheng, J.; Zhang, X.; Tang,
H.; Zhang, X.; Liu, Q.; Zhou, G.; Xu, S.; Yu, K. The Global Land Surface Satellite
(GLASS) Remote Sensing Data Processing System and Products. *Remote Sens.*, 5,
2436-2450, 2013.

Marco T 1/9/16 10:57

Formatted: Font:12 pt

Marco T 1/9/16 10:57

Formatted: Font:12 pt

Marco T 1/9/16 10:57

Formatted: Font:12 pt

Marco T 1/9/16 10:57

Formatted: Font:12 pt

Marco T 1/9/16 10:57

Formatted: Font:12 pt

Marco T 1/9/16 10:57

Formatted: Font:12 pt

Marco T 1/9/16 10:57

Formatted: Font:12 pt

Marco T 1/9/16 10:57

Formatted: Font:12 pt

Marco T 1/9/16 10:57

Formatted: Font:12 pt

Marco T 1/9/16 10:57

Formatted: Font:12 pt

Marco T 1/9/16 10:57

Formatted: Font:12 pt

Marco T 1/9/16 10:57

Formatted: Font:12 pt

Marco T 1/2/16 09:58

Formatted: Font:(Default) Times New
Roman, 12 pt

FIGURES

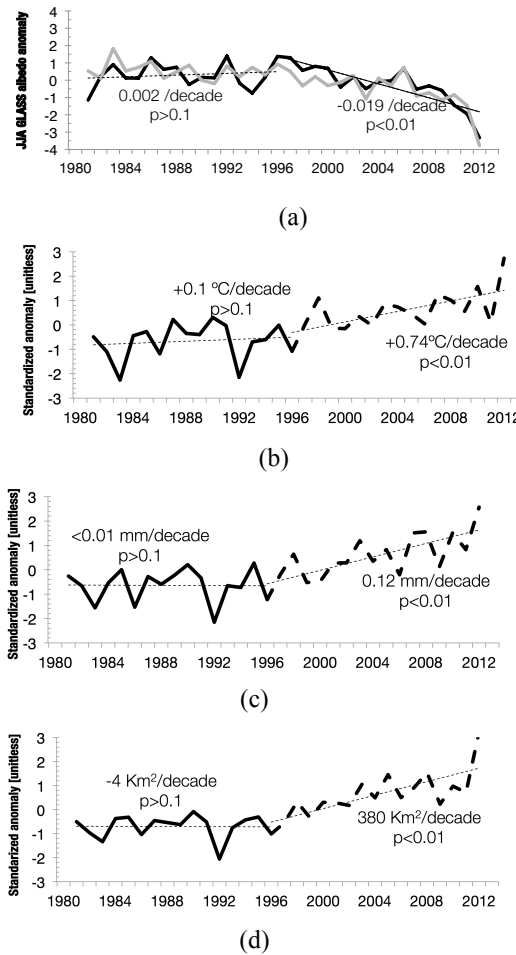


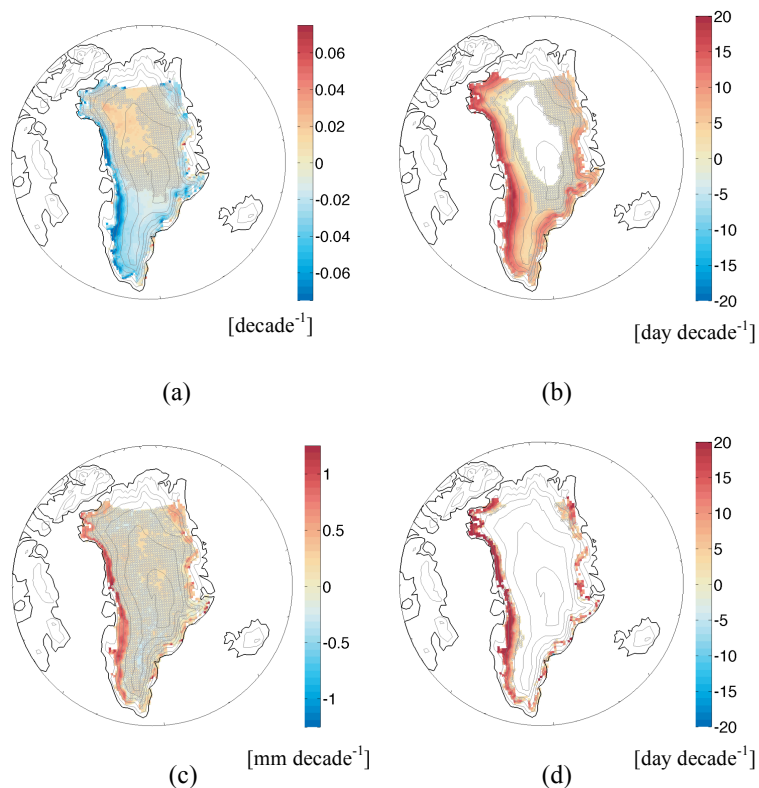
Figure 1 Mean summer standardized values plotted as time series for (a) albedo from GLASS (black) and MAR (grey), together with MAR-simulated values of (b) surface air temperature, (c) surface grain size (effective radius of optically “equivalent” sphere) and (d) bare ice exposed area. Trends for the periods 1981 – 1996 and 1996 – 2012 are reported in each plot. Trends in (a) refer to the GLASS albedo. The baseline 1981 – 2012 period is used to compute standardized anomalies, obtained by subtracting the mean and then dividing by the standard deviation of the values in the time series. All trends are computed from JJA averaged values over ice-covered areas only, not tundra.

1

2

3

4



5

6

7

8

9

10

11

12

13

14

Figure 2 Maps of JJA trends (per decade) from 1996 to 2012, when darkening began to occur, for a) [spaceborne estimated](#) GLASS albedo, b) number of days when [MAR-simulated](#) surface air temperature exceeded 0°C , c) [MAR-simulated](#) surface grain size and d) number of days when bare ice is exposed [as simulated by MAR](#). Regions where trends are not significant at a 95 % level are shown as grey-hatched areas. White regions over the north end of the ice sheet indicate areas or were not viewed by the satellite.

1

2

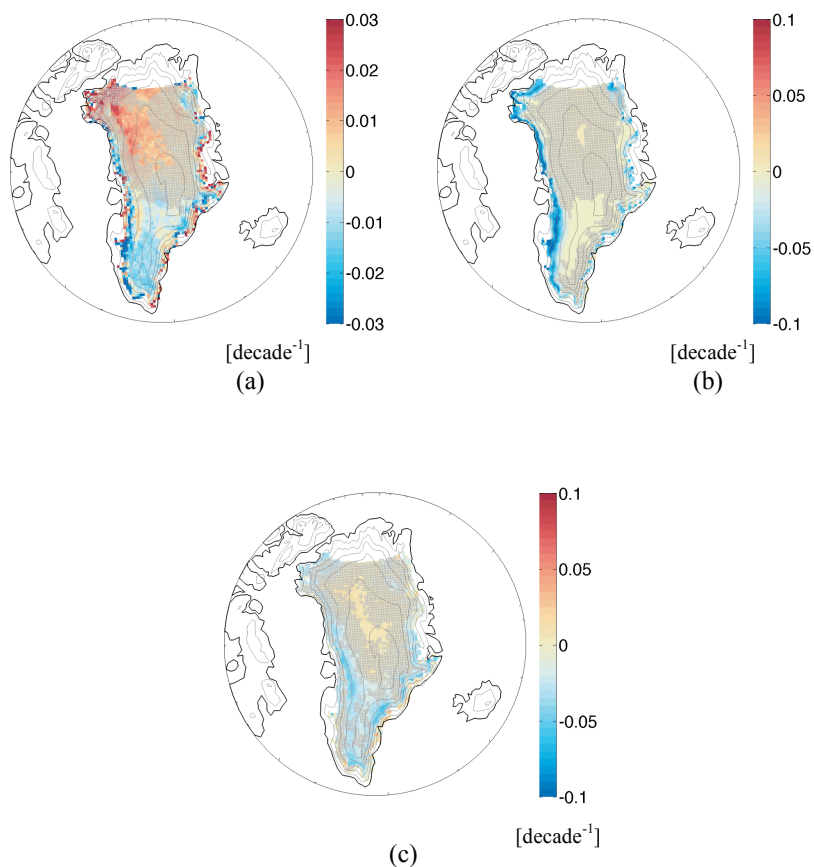
3

4

5

6

7 Figure 3 Differences between spaceborne measured and model-simulated albedo
 8 trends in different spectral regions. a) Difference between the [GLASS](#) and [MAR](#)
 9 trends (albedo change per decade), with positive values indicating those regions
 10 where MAR trend is smaller in magnitude than GLASS. Maps of JJA mean albedo
 11 trends (1996 – 2012) simulated by MAR for b) visible and c) near-infrared
 12 wavelengths.
 13



Marco T 1/2/16 12:23

Deleted: MAR

Marco T 1/2/16 12:23

Deleted: GLASS

1

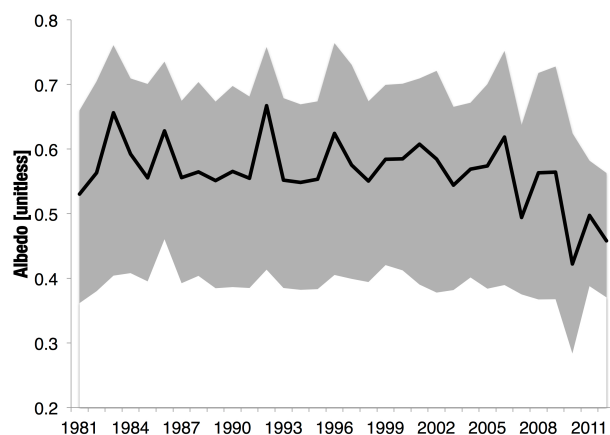
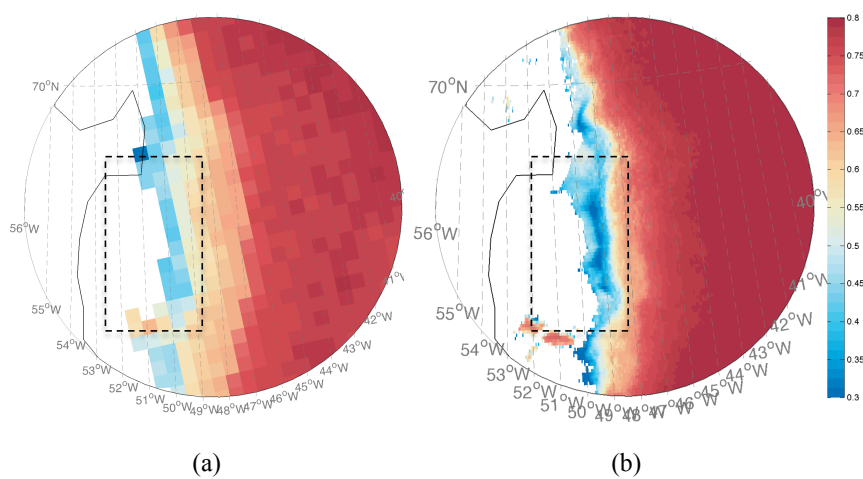
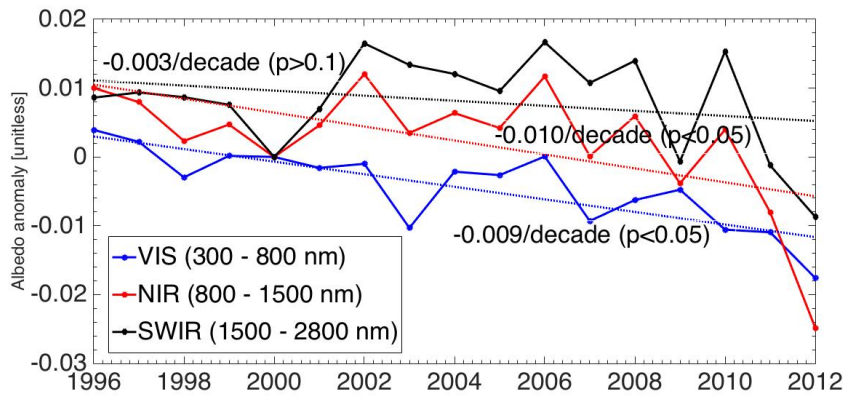
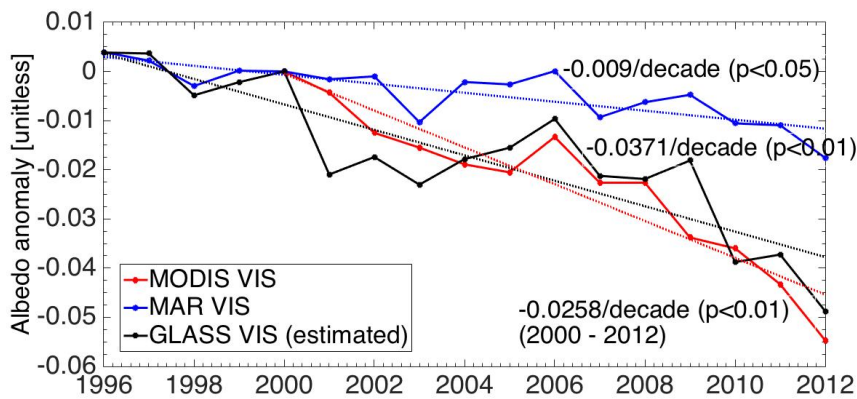


Figure 4 a) MAR and b) GLASS mean JJA albedo for year 2010 over an area including the dark band together with c) time series of mean JJA albedo for the ice-covered areas in the black rectangle. The black line in c) shows the GLASS spatially averaged albedo, where the top and the bottom of the grey area indicate, respectively, the maximum and minimum albedo within the black box in b).



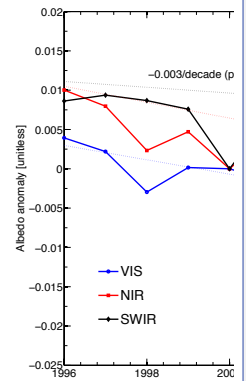
(a)



(b)

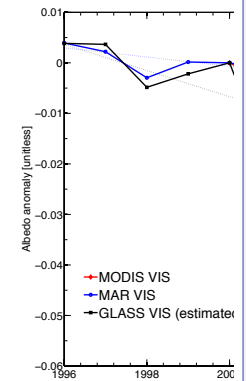
Figure 5 Time series of modelled and measured mean summer (JJA) albedo anomalies (with respect to year 2000) in different spectral bands. a) Visible, near-infrared and shortwave-infrared albedo values simulated by MAR; b) as in a) but for the visible albedo only from MAR, MODIS (obtained from the product MCD43) and GLASS. Note that the vertical axis scale in (b) is different from that in (a).

Marco T 1/6/16 09:05

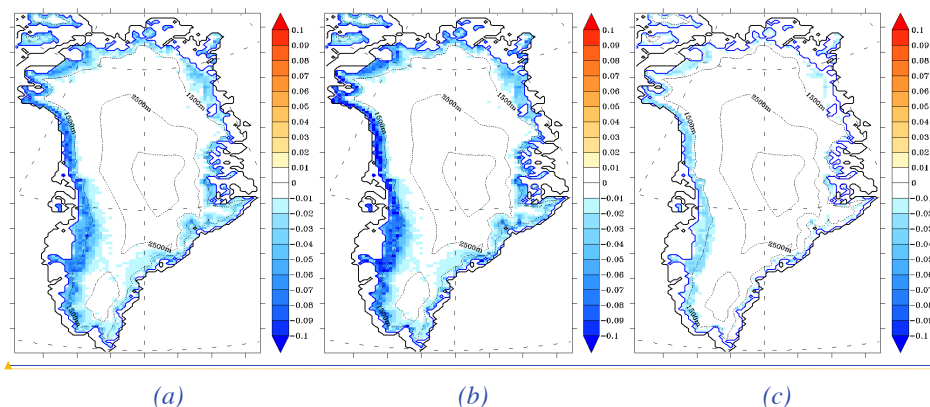


Deleted:

Marco T 1/6/16 09:05



Deleted:



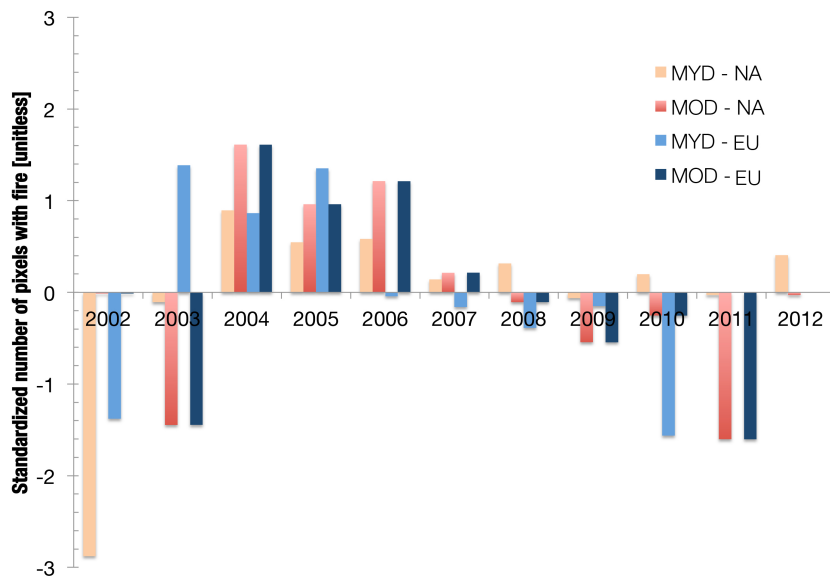
(a) (b) (c)
 Figure 6 Maps of MAR-simulated albedo trends between 1996 and 2012 using a) the original MAR albedo scheme and b) the perturbed MAR outputs in which daily albedo is artificially decreased by 0.1 from the MAR-computed value for those regions where bare ice is exposed. c) Difference between the trends obtained with MAR original albedo scheme and the perturbed solution.

Unknown
 Formatted: Font:(Default) Times, Italic

Marco T 1/12/16 14:12
 Formatted: Font:Not Italic

Marco T 1/12/16 14:12
 Formatted: Font:Not Italic

1

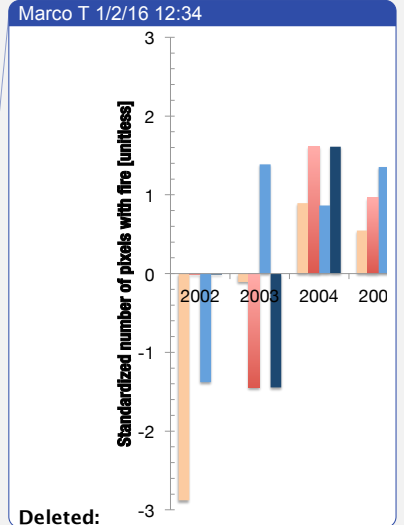


2

3 Figure 7 Standardised cumulative number of fires (April through August) detected over
4 North America (NA) and Eurasia (EU) by the MOD14CMH and MYD14CMH GCM
5 climatology products between 2002 and 2012.

6

7

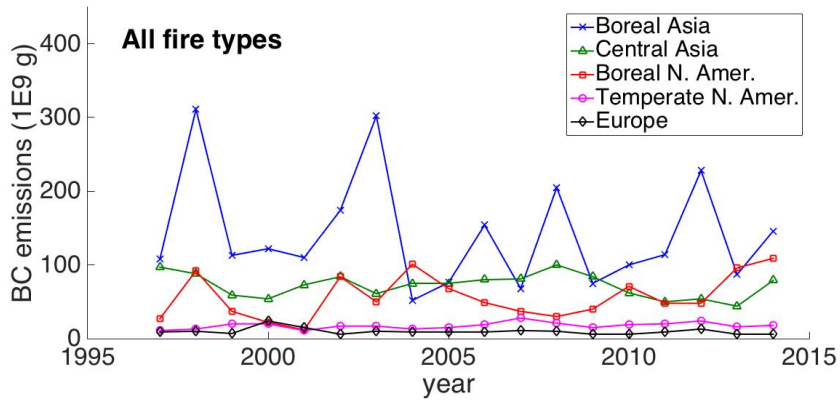


Deleted: Unknown
Formatted: Font:(Default) Times

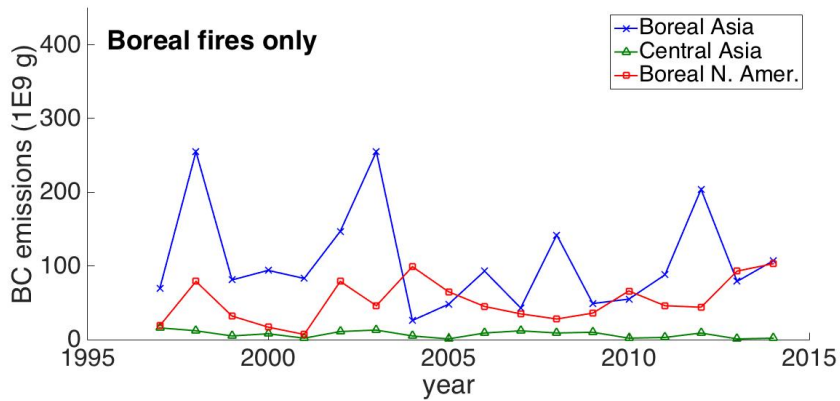
Marco T 1/12/16 14:16
Deleted: z

Marco T 1/2/16 12:36
Deleted: . .

Marco T 1/2/16 12:36
Formatted: Justified, Line spacing: single



(a)



(b)

Figure 8 BC emissions [g] from fires in potential source regions for GrIS for a) all fire types and b) boreal fires only using estimates from the Global Fire Emissions Database (GFED version 4.1, <http://www.globalfiredata.org/>) between 1997 and 2014.

Marco T 1/6/16 11:24

Formatted: Centered, Line spacing: single

Marco T 1/2/16 12:36

Formatted: Justified, Line spacing: single

Marco T 1/6/16 11:27

Formatted: Centered, Line spacing: single

Marco T 1/6/16 09:17

Formatted: Caption, Justified, Line spacing: single

1

2

3

4

5

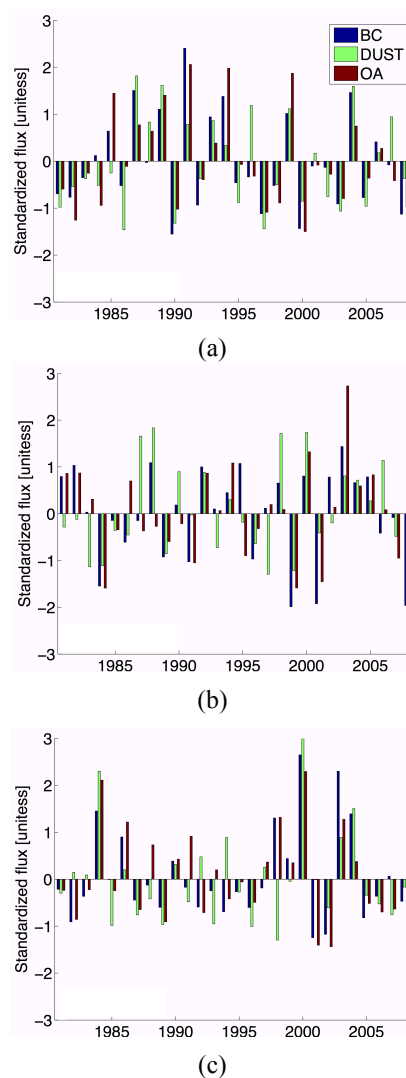
6

7

8 | Figure 9 [NASA GISS ModelE standardized deposition fluxes for BC, dust and organic](#)
9 [aerosol at Kangerlussuaq for a\) June, b\) July and c\) August \(1981 – 2008\) from the](#)
10 [AEROCOM simulations.](#)

11

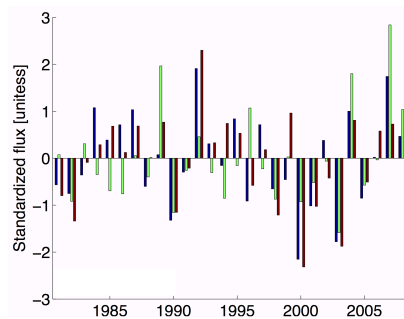
12



Marco T 1/2/16 08:40

Deleted: standardized deposition fluxes for BC, dust and organic aerosol at Kangerlussuaq for a) June, b) July and c) August (1981 – 2008)

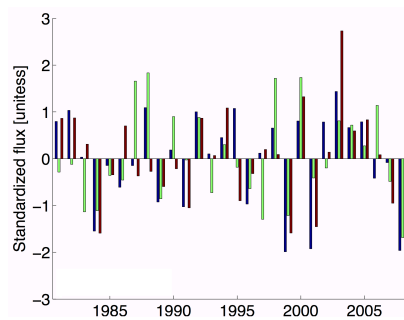
1



(a)

2

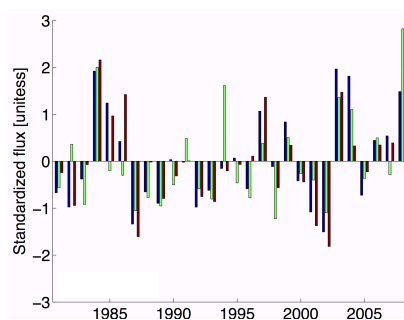
3



(b)

4

5



(c)

6

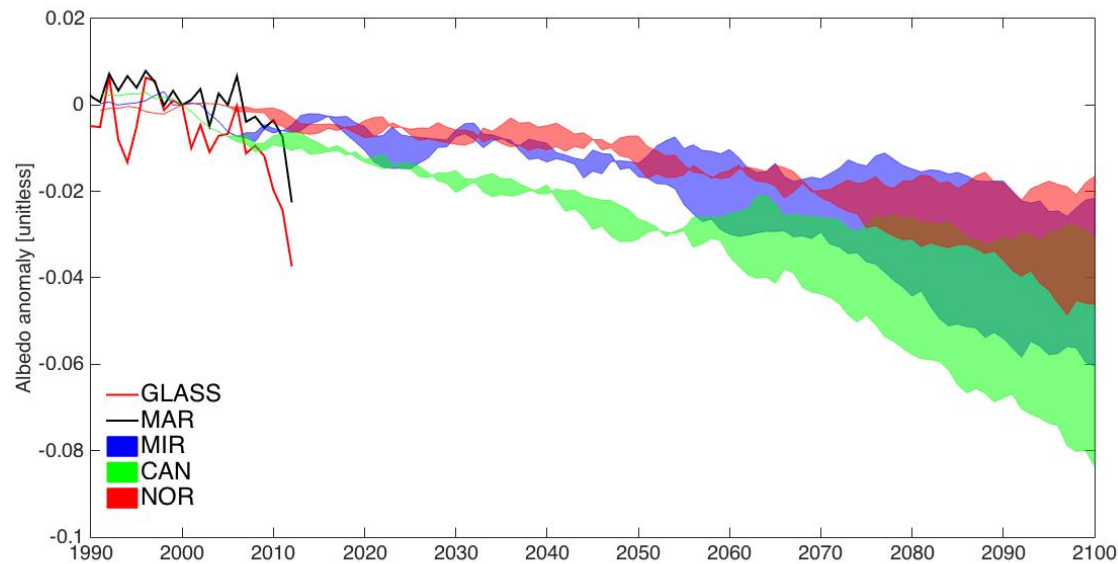
7

8

Figure 10 Same as [Figure 9](#) but for Summit station.

Marco T 1/12/16 14:13

Deleted: Figure 8Figure 8



Marco T 9/1/15 17:36
Formatted: Justified, Line spacing: single

Marco T 1/2/16 10:33
Deleted: bottom
Marco T 1/2/16 10:33
Deleted: top

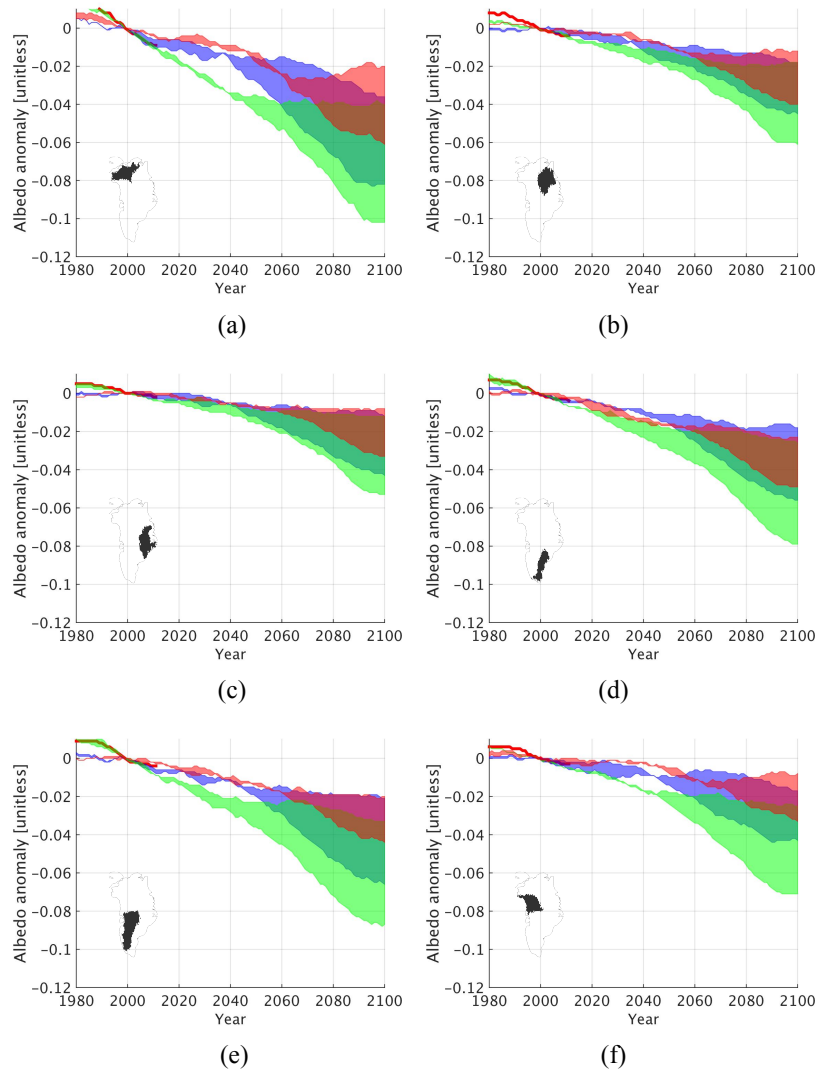


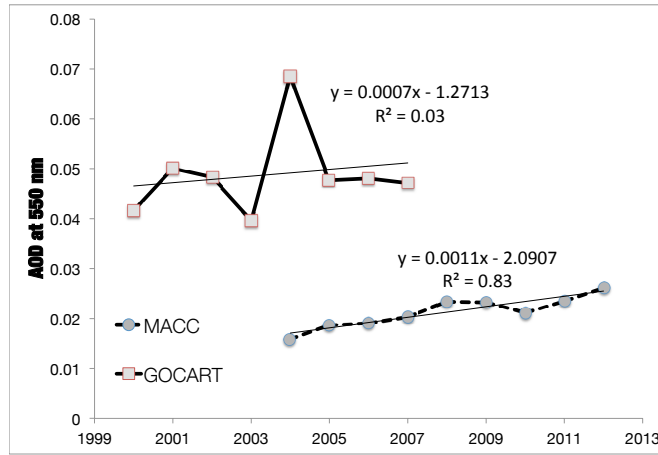
Figure 12 Same as Figure 11 but for different drainage regions of the GrIS, indicated by the small maps in each panel. Color scheme for the shaded regions is the same as Figure 10. The top and the bottom of each area plots represent the results concerning the RCP45 (bottom) and RCP85 (top) scenarios. Red lines represent the GLASS albedo averaged over the corresponding drainage region.

Marco T 1/6/16 09:

Deleted: Figure 9F

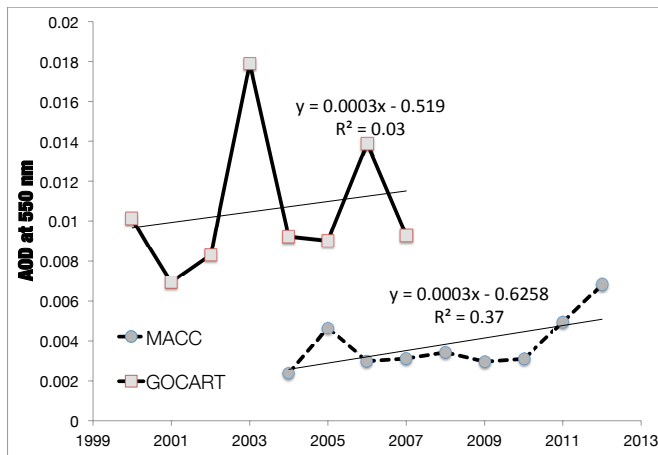
Marco T 1/2/16 10:

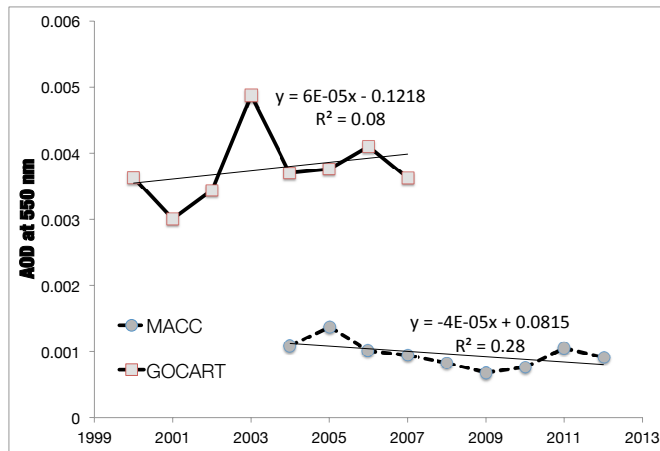
Deleted: Dark grey simulations, mild grey to NORESM.



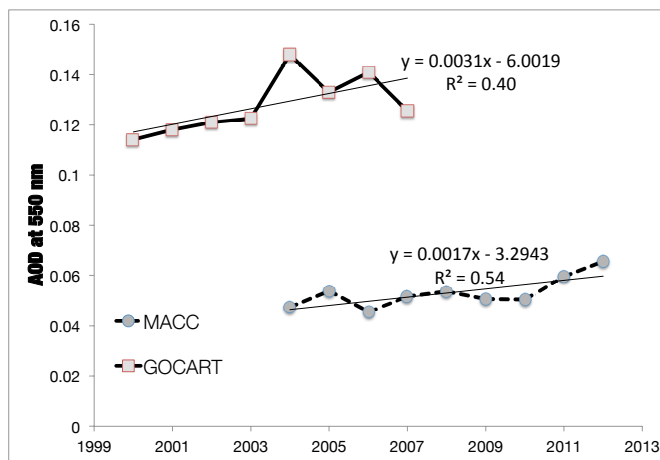
(a)

(b)





(c)



(d)

Figure 13 May – June averaged aerosol optical depth at 550 nm for a) dust, b) organic matter, c) black carbon and d) total obtained from the GOCART model and from the MACC model (as in Dumont et al., 2014) for the domain bounded by 75 to 80°N and 30 to 50° W. All trends are not statistically significant with the exception of the MACC outputs for Dust ($p < 0.01$) and Total Aerosol ($p < 0.05$).

1



Marco T 1/2/16 10:18

Deleted: Page Break ... [4]

Unknown

Formatted: Font:Italic, Font color: Auto

Unknown

Formatted: Font:Italic, Font color: Auto

1

	June				July				August				JJA			
Station	rmse	Rmse [%]	slope	# of years	rmse	rmsep	slope	# of years	rmse	rmsep	slope	# of years	rmse	rmsep	slope	# of years
Swiss	0.12	19.60	-0.22	11	0.02	3.86	1.12	9	0.04	6.92	1.00	8	0.02	2.73	1.06	7
CP	0.07	8.72	0.12	12	0.06	7.40	0.14	14	0.06	7.21	0.11	13	0.07	8.20	-0.02	11
Humboldt	0.08	10.38	-0.16	8	0.07	9.31	0.35	9	0.08	9.98	0.39	10	0.07	9.42	0.27	8
Summit	0.01	1.45	0.85	15	0.02	2.25	-0.25	16	0.01	1.71	-0.68	16	0.01	1.22	0.12	15
TunuN	0.05	6.72	-0.66	15	0.06	7.89	0.79	15	0.07	8.84	0.69	15	0.06	7.53	0.37	15
Dye-2	0.02	2.58	0.57	14	0.02	2.15	0.75	14	0.01	1.73	0.68	15	0.01	1.54	0.82	12
Jar1	0.06	8.45	0.68	13	0.10	23.80	0.68	15	0.15	43.55	0.22	14	0.07	14.24	0.66	12
Saddle	0.01	1.28	0.94	14	0.02	1.95	0.61	14	0.01	1.75	0.46	14	0.01	1.31	0.71	14
NASAE	0.03	4.23	0.46	14	0.05	5.97	0.14	14	0.04	5.11	0.24	14	0.04	4.97	0.24	14
NASA SE	0.02	2.76	0.59	13	0.02	2.32	0.67	13	0.02	2.14	0.36	14	0.02	2.23	0.56	13
JAR2	0.06	12.27	0.20	11	0.05	10.00	-0.10	12	0.06	11.96	-0.06	11	0.04	8.51	0.16	10
Mean	0.048	7.13			0.0455	6.99			0.05	9.2			0.038	5.62		

2 Table 1 Comparison between GLASS retrieved albedo and GC-NET in -situ albedo measurements, for monthly- and seasonally-
3 averaged albedos at twelve surface stations on the Greenland ice sheet.

	STATION		
	Thule 77°28'00"N, 69°13'50"W	Ittoqqortoormiit 70°29'07"N, 21°58'00"W	Kangerlussuaq 67°00'31"N, 50°41'21"W
Year			
2007	0.042±0.010	N/A	N/A
2008	0.040±0.017	N/A	0.051±0.012
2009	0.093±0.020	N/A	0.088±0.017
2010	0.052±0.011	0.052±0.005	0.049±0.007
2011	0.060±0.017	0.072±0.041	0.053±0.012
2012	0.065±0.011	0.044±0.009	0.072±0.020
2013	0.050±0.007	0.053±0.009	0.066±0.010

1
2 Table 2 June-July-August mean and standard deviation of measured aerosol optical depth
3 (AOD) at 550 nm at the three sites of Thule, Ittoqqortoormiit and Kangerlussuaq of the
4 AERONET network (AERONET web site, <http://aeronet.gsfc.nasa.gov>, 2013).

6

Marco T 1/2/16 10:22

Deleted: -

... [5]

Marco T 1/2/16 10:22

Formatted: Space Before: 6 pt, After: 0 pt

[2] The Graduate Center of the City University of New York

[3] Lamont Doherty Earth Observatory of Columbia University, New York, NY

Therefore, in the next section, we focus on assessing whether atmospheric aerosol levels over the GrIS have increased (as a proxy for whether the deposition of aerosol has increased) and we look for trends in forest fires in the two of the main source regions for aerosols over the GrIS.

Attributions: atmospheric deposition of impurities and number of forest fires

Atmospheric deposition of impurities

Ice core analyses of black carbon in the central regions of the GrIS have been used to study long-term variability and trends in pollution deposition (McConnell et al., 2007; Keegan et al., 2014). These records show that snow at these locations was significantly more polluted in the first half of the 20th century than presently. Both these records and in-situ measurements at Summit (Cachier and Pertuisot, 1994; Chylek et al., 1995; Hagler et al., 2007; Doherty et al, 2010) also indicate that in recent decades, the snow in central Greenland has been relatively clean, with concentrations smaller than 4 ng g⁻¹ for BC. This amount of BC could lower snow albedo by only 0.002 for $r=100\text{ }\mu\text{m}$, or 0.005 for $r=500\text{ }\mu\text{m}$ (Figure 5a of Dang et al., 2015). More recently, Polashenski et al. (2015) analysed BC and dust concentrations in 2012-2014 snowfall along a transect in northwest Greenland. They found similarly low concentrations of BC and concluded that albedo decreases in their study region are unlikely to be attributable to increases in BC or dust. Black carbon in snow has also been measured in-situ at single points in time at a few other locations; the only region with repeat measurements in a given location over decades is in the percolation zone of South Greenland. Snow sampled in 1983 at Dye-3 had a median of 2 ng g⁻¹ (Clarke and Noone, 1985). In 2008 and 2010, measurements 160 km away at Dye-2, using the same method, had medians of 4 ng g⁻¹ in spring and 1 ng g⁻¹ in summer (Table 9 of Doherty et al, 2010).

In the absence of in-situ measurements of impurity concentration trends over Greenland more broadly, we investigate trends in Atmospheric Optical Depth (AOD) from outputs of aerosol models and from ground-based measurements at several locations around the GrIS. AOD is a measure of the total extinction (omni-directional scattering plus absorption) of sunlight as it passes through the atmosphere, and is related to atmospheric aerosol abundance. Thus, it is a metric for the mass of aerosol available to be potentially deposited onto the GrIS surface. In the aerosol models, we are able to examine trends in total AOD as well as in aerosol components: BC, dust and organic matter. In addition, we examined trends in modelled deposition fluxes of these species to the GrIS.

For our analysis, we used model results from the Aerosol Comparisons between Observations and Models (AeroCom) project, an open international initiative aimed at understanding the global aerosol and its impact on climate (Samset et al., 2014; Myhre et al., 2013; Jiao et al., 2014; Tsigaridis et al., 2014). The project combines a large number

of observations and outputs from fourteen global models to test, document and compare state-of-the-art modelling of the global aerosol. We specifically show standardised (i.e., subtracting the mean and then dividing by the standard deviation) deposition fluxes of BC, dust and organic aerosols (OA) from the GISS modelE contribution to the AeroCom phase II series of model runs (<http://aerocom.met.no/aerocomhome.html>). The runs used here took as input the decadal emission data from the Coupled Model Intercomparison Project Phase 5 (CMIP5). Figure 6 and Figure 7 show modelled deposition fluxes at the two locations of Kangerlussuaq (Figure 6, 67°00'31"N, 50°41'21"W) and Summit (Figure 7, 72°34'47"N, 38°27'33"W) for the months of June, July and August and aerosol components (BC, dust and organic matter). These locations were selected as representative of the ablation zone (Kangerlussuaq) and the dry-snow zone (Summit). The analysis of the AeroCom outputs shows no statistically significant trend in the modelled fluxes for either location. Results of the analysis of fluxes over different areas point to similar conclusions. Similar results are obtained when considering the months of January, February and March, when aerosol concentration is expected to be higher. The results here presented complement other studies (e.g. Stone et al., 2014) indicating that, since the 1980s, atmospheric concentrations of BC measured at surface stations in the Arctic have decreased, with variations attributed to changes in both anthropogenic and natural aerosol and aerosol precursor emissions.

Mean summer values of AOD (550 nm) measured at three AERONET (<http://aeronet.gsfc.nasa.gov>) Greenland sites based in Thule (northwest Greenland; 77°28'00"N, 69°13'50"W), Ittoqqortoormiit (east-central Greenland; 70°29'07"N, 21°58'00"W), and Kangerlussuaq during the period 2007 – 2013 (with the starting year ranging between 2007 and 2009, depending on the site) are reported in Table 2, together with their standard deviations. None of the stations show statistically significant trends in AOD, consistently with the results of the analysis of the modelled deposition fluxes.

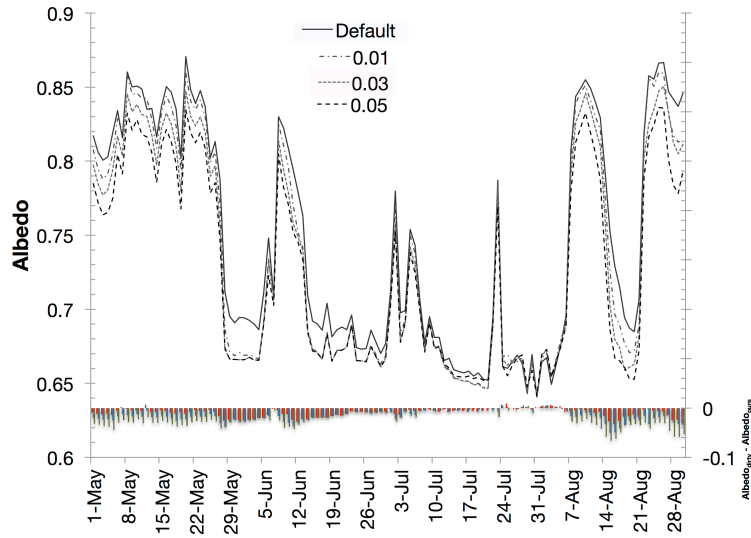
A recent study (Dumont et al., 2014) concluded that dust deposition has been increasing over much of the GrIS and that this is driving lowered albedo across the ice sheet. That conclusion was based on trends of an “impurity index”, which is the ratio of the logarithm of albedo in the 545-565 nm MODIS band (where impurities affect albedo) to the logarithm of albedo in the 841-876 nm band (where they do not). In the MODIS product used in Dumont et al. (2014) study, albedo values rely on removal of the effects of aerosols in the atmosphere. In the Dumont et al. (2014) study this correction was made using simulations of atmospheric aerosols by the Monitoring Atmospheric Composition and Climate (MACC) model. Their resulting “impurity index” shows positive trends, and these are attributed in part (up to 30%) to increases in atmospheric aerosol not accounted for by the model, and the remainder to increases in snow impurities. The latter is consistent with our findings herein: that GrIS darkening is in part attributable to an increase in the impurity content of surface snow. However, Dumont et al. (2014) assume that this increase in surface snow impurities is a result of enhanced deposition from the atmosphere. They do not account for the possibility that positive trends in impurity content may instead be a result of a warming-driven in-snow processes. Indeed, their own table shows variable AOD at AERONET stations in Greenland, but no trend over the period studies (2007 – 2012).

Drivers: number of forest fires over North America and Eurasia

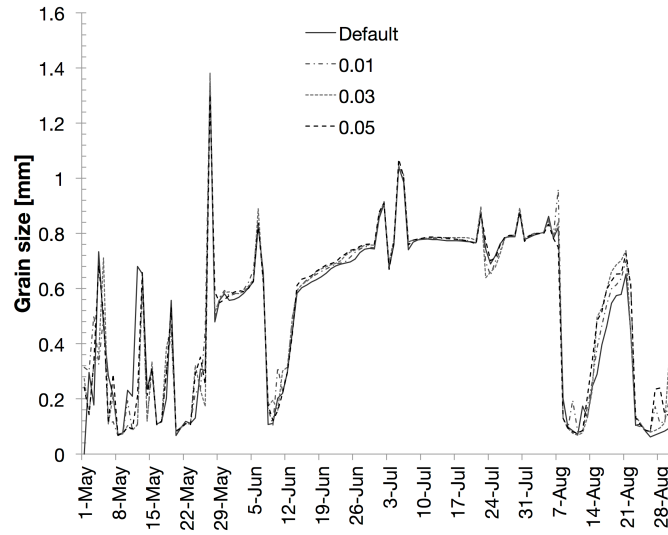
Biomass burning in North America and Siberia is a significant source of combustion aerosol (BC and associated organics) to the GrIS (Hegg et al., 2009, 2010). Therefore, we investigated trends in the number of active fires in these two source regions. To this aim, we used the MODIS monthly active fire products produced by the TERRA (MOD14CMH) and AQUA sensors (MYD14CMH) generated at 0.5° spatial resolution and distributed by the University of Maryland via anonymous ftp (http://www.fao.org/fileadmin/templates/gfims/docs/MODIS_Fire_Users_Guide_2.4.pdf, http://modis.gsfc.nasa.gov/data/dataproducts.php?MOD_NUMBER=14). The results of our analysis are summarised in *Figure 8*, showing the standardised (subtracting the mean and dividing by the standard deviation of the 2002 – 2012 baseline period) cumulative number of fires detected over North America (NA) and Eurasia (EU) by the MOD14CMH and MYD14CMH GCM climatology products between 2002 and 2012. The figure shows large inter-annual variability but no significant trend (at 90 % level) in the number of fires over the two areas between 2002 and 2012. The period between 2004 and 2011, when enhanced melting occurred over the GrIS, shows a negative trend (though also in this case not statistically significant). Notably, we were not able to find studies specifically looking at trends in boreal forest fire emissions. However, the results reported in Ichoku and Ellison (2014) and Xing et al. (2013, 2015) are consistent with our analysis of the number of fires over North America and Eurasia. In particular, Ichoku and Ellison (2014) point to the absence of trends in particulate matter emissions from forest fires between 2000 and 2012 across broad geographic regions, including those areas considered to be major sources of impurities for Greenland (North America, Europe and Eurasia). Moreover, Xing et al. (2013, 2015) indicate that direct anthropogenic emissions have also been decreasing across almost all of the mid- to high-latitude northern hemisphere. This

Light-absorbing impurities in snow affect albedo not only directly, but also indirectly by absorbing sunlight, warming the snowpack, and accelerating snow grain size growth. We started studying the magnitude of this “indirect effect” of impurities on snow grain size, and therefore albedo, by modifying the albedo scheme within MAR. Specifically, we reduced the visible component of the albedo, α_l in Eq. 2, by between 0.01 and 0.05 to simulate the effects of impurities. This was, in turn, used in Eq. 1 to compute the broadband albedo. The value of 0.05 was estimated as the maximum estimated albedo decrease for BC concentrations measured in the cold snow and percolation zones of the GIS. The value of -0.05 used in our simulations for each iteration of MAR likely overestimates the effect of impurities on grain size at the beginning of the melting season, but underestimates the effect during the melting season when impurities tend to concentrate at the snow surface (Doherty et al., 2013). Higher concentrations of impurities are present along the margins of the ice sheet because of their proximity to local sources of dust and the proliferation of algae and microorganisms on the ice surface, so the effect of impurities on grain size is likely larger there. Still the results of this synthetic experiment can provide an initial indication of the indirect effect of impurities on the evolution of the snowpack and its albedo. We specifically focused

for our experiment on an area of 100 x 100 km² centred at Swiss Camp, one of the Greenland Climate Network stations (Steffen and Box, 2001) for the summer of 2012. *Figure 12* shows daily broadband albedo simulated by MAR, with and without the imposed albedo reductions of 0.01, 0.03 and 0.05 in the visible albedo. The differences in broadband albedo between the default case (pure snow) and the cases simulating dirty snow are relatively constant and equal to the imposed albedo reduction, until the end of May, when substantial melting begins (e.g., Tedesco et al., 2013). After this, all cases show broadband albedo lowered by an amount as low as the imposed visible albedo reduction. The presence of new snowfall during the first week of June increases albedo temporarily, with the “dirty snow” case (albedo reduction of 0.05) showing the fastest return to reduced albedo after the new snowfall. This can be explained by the accelerated grain growth induced by the increased absorbed solar radiation (*Figure 12b*), which is due to the reduced albedo in the visible region (i.e. the presence of absorbing impurities). A similar behaviour is simulated for the precipitation events occurring during the second week of August, though in this case the minimum albedo values obtained in the different cases are dependent on the introduced negative albedo anomaly (i.e. snow impurity content). This is in contrast to the behaviour during the snowfall event in the month of July when there is persistent melting; here, all cases show similar albedo values. We performed a linear regression between the grain sizes simulated for clean snow and for snow with the three imposed reductions in visible-band simulating the presence of light-absorbing impurities. These regressions had slopes of 1.0099 ($R^2 = 0.92$, -0.01 bias), 1.0037 ($R^2 = 0.91$, -0.03 bias) and 1.0094 ($R^2 = 0.9$, -0.05 bias) when considering all grain sizes. The slope between grain sizes in dirty vs. clean snow increase to 1.0529 ($R^2 = 0.89$, -0.01 bias), 1.0656 ($R^2 = 0.9$, -, -0.03 bias) and 1.0676 ($R^2 = 0.89$, -0.05 bias) when considering only cases where grain size is less than 0.6 mm. This value was selected based on an analysis of the temporal evolution of grain size (*Figure 12b*) as characterising the presence of persistent melting. The percentage difference between simulated grain sizes in clean pure versus dirty snow (*Table 3*) indicates that grain sizes are typically only about 1 % larger for dirty snow typical of the GIS dry snow and percolation zones, though these differences can be as high as 15 – 20 % during the period of snow metamorphosis and melting following new snowfall.



(a)



(b)

Figure 12 a) Daily broadband albedo and b) grain size simulated by MAR over a 100 x 100 km² area centred at Swiss Camp obtained when MAR simulated visible-band albedo is reduced by 0.01, 0.03 and 0.05 to simulate the effects of light-absorbing impurities in snow. The default value refers to the albedo calculated for impurity-free snow (Eq. 2). Bars at the bottom of plot a) (right-hand y-axis) gives the difference between the albedo of pure snow (“default”) and that when visible albedo is reduced (i.e., dirty snow).

Grain size difference [%]	$\Delta\alpha$		
	-0.01	-0.03	-0.05
Mean	1.01	1.22	1.12
Standard deviation	1.88	3.22	2.42
Maximum absolute difference	20.3	22.1	16.3

Table 3 Mean, standard deviation and maximum absolute difference of the difference between grain size in the case of pure snow and in the case of snow with impurities that reduce visible-band albedo by 0.01, 0.03 and 0.05. The difference is expressed as a percentage relative to the grain size value obtained in the case of pure snow.